



universität
wien

DISSERTATION

Titel der Dissertation

Roles of Wapl in cell cycle progression and chromosome
segregation

angestrebter akademischer Grad

Doktor/in der Naturwissenschaften (Dr. rer.nat.)

Verfasserin / Verfasser:	Antonio Tedeschi
Matrikel-Nummer:	0648446
Dissertationsgebiet (lt. Studienblatt):	Molekulare Biologie
Betreuerin / Betreuer:	Dr. Jan-Michael Peters

Wien, im 11. Jän. 2010

Abstract.....	3
Zusammenfassung	5
1. Introduction	8
1.1 The cell cycle	8
1.2 Cell cycle progression	10
1.3 Importance of sister chromatid cohesion in chromosome segregation.....	11
1.4 The cohesin complex	12
1.5 Cohesin regulation during the cell cycle.....	17
1.6 Wapl.....	23
1.7 Aims of this study	27
2. The prophase pathway of cohesin dissociation is required for proper chromosome segregation during mitosis.....	28
2.1 Generation of conditional and null Wapl alleles.....	28
2.2 Wapl is essential for mouse embryonic development	30
2.3 The resolution of sister chromatid arms in primary embryonic fibroblasts depends on Wapl	31
2.4 Wapl is required for proliferation of primary embryonic fibroblasts.....	34
2.5 Wapl regulates the dissociation of cohesin from prophase to metaphase...	37
2.6 Wapl is required for proper chromosome segregation but not for cohesin removal at the metaphase-anaphase transition	42

2.7 Separase is required to remove cohesin at the metaphase-anaphase transition in *Wapl* knockout primary embryonic fibroblasts..... 46

2.8 Partial *Scc1* depletion rescues the chromosome segregation defects in *Wapl* knockout primary embryonic fibroblasts 52

3. *Wapl* is required for cohesin dissociation from DNA and cell cycle progression during interphase 55

3.1 Cohesin axial structures in interphase *Wapl* knockout primary embryonic fibroblasts..... 55

3.2 *Wapl* regulates the amount of chromatin-bound cohesin in interphase primary fibroblasts..... 60

3.3 Identification of cohesin-binding sites in *Wapl* knockout primary fibroblasts 63

3.4 *Wapl* depletion causes partial condensation of chromatin in interphase primary embryonic fibroblasts 67

3.5 The cohesin vermicelli are not the consequence of incorrect mitotic divisions
69

3.6 *Wapl* is required for the G1-S progression of primary mouse fibroblasts 72

4. Discussion 79

5. References..... 90

Materials and Methods..... 97

Curriculum Vitae 102

Publications..... 103

Acknowledgments 104

Abstract

Chromosome segregation during mitosis depends on sister chromatid cohesion, which is mediated by the cohesin complex. Cohesion enables the biorientation of chromosomes on the mitotic spindle, but once biorientation has been achieved, cohesion has to be dissolved to allow the separation of sister chromatids in anaphase. In vertebrate cells, the majority of cohesin is removed from chromosome arms in prophase and prometaphase by a mechanism called the prophase pathway of cohesin dissociation. This pathway depends on a cohesin associated protein, called Wapl. When all chromosomes are bioriented on the metaphase plate, the protease separase cleaves the remaining cohesin complexes on chromosomes, in particular at centromeres, thus allowing chromosome segregation. Cohesin cleavage by separase is essential for mitosis because primary mouse embryonic fibroblasts (pMEFs) lacking Separase fail to segregate chromosomes.

Despite the fact that the prophase pathway has been studied for many years it remains unknown if this mechanism is essential for mitosis, or if the prophase pathway is simply redundant with the separase pathway. To address this question and to obtain insight into the functions of the prophase pathway I generated a *Wapl* conditional knockout (cko) mouse. I found that deletion of the *Wapl* gene causes embryonic lethality, suggesting that the prophase pathway is essential for viability. In pMEFs lacking *Wapl* we observed that sister chromatids remain abnormally tightly associated with each other until metaphase, but then can be separated in anaphase. However, in most anaphase cells numerous thick chromosome bridges are observed, resulting in incomplete cell division during cytokinesis. In pMEFs lacking *Wapl* cohesin remains associated with

chromosome arms up until metaphase, but in anaphase cohesin is removed from chromosomes, suggesting that Separase is sufficient to remove the bulk of cohesin from chromosomes. I confirmed this notion by analyzing pMEFs from *Wapl* *Separase* double cko mice. In these cells, cohesin cannot be removed from chromosomes at all, and both chromosome arms and centromeres remain tightly associated with each other. To test if the excess of cohesin on mitotic chromosomes is the cause of the chromosome bridges I partially depleted cohesin by *Scc1* RNA interference in *Wapl* knockout pMEFs. This resulted in a partial rescue of chromosome segregation defects suggesting that the persistence of cohesin on mitotic chromosomes is the cause of these abnormalities. I therefore conclude that the prophase pathway of cohesin dissociation is required for proper chromosome segregation during mammalian mitosis.

In addition, I characterized *Wapl*'s requirement for cell cycle progression in interphase. Inactivation of *Wapl* in pMEFs arrested in G0 phase strongly inhibited cell proliferation. Under these conditions, *Wapl* knockout cells rarely started S phase, suggesting that they are delayed or arrested in G0/G1 phase. Although the cause of this arrest is not yet clear, I found a dramatic increase of levels of chromatin-bound cohesin and of cohesin binding sites on DNA. The cohesin pattern in interphase *Wapl* knockout cells was also different than in control cells. Cohesin followed elongated structures that co-localized with DNA. These cohesin structures reminded me of thin worms and I therefore called them *vermicelli* (the Italian word for little worms). In addition I observed a more compacted interphase chromatin in *Wapl* knockout pMEFs. Future experiments will address the relationship between the cohesin vermicelli and chromatin structure.

Zusammenfassung

In der mitotischen Zellteilung hängt die Segregation der Chromosomen von der Kohäsion der Schwesterchromatiden ab, die durch den Proteinkomplex Cohesin hergestellt wird. Die Chromosomenkohäsion ermöglicht die bipolare Orientierung der Chromosomen auf der mitotischen Spindel; doch sobald diese Anordnung der Chromosomen in der Metaphase erreicht wird, muss die Kohäsion gelöst werden, damit die Schwesterchromatiden in der Anaphase getrennt werden können. In den Zellen von Wirbeltieren wird der Großteil der Cohesinmoleküle bereits während der Prophase und der Prometaphase von den Chromosomenarmen entfernt. Dieser Mechanismus wird „Prophase Pathway“ der Cohesin-Dissoziation genannt und benötigt das Cohesin-assoziierte Protein Wapl. In der Metaphase, wenn alle Chromosomen bipolar an der Äquatorialplatte ausgerichtet sind, spaltet die Protease Separase die – besonders an den Zentromeren – verbliebenen Cohesinkomplexe und bewirkt dadurch die Segregation der Chromosomen. Die Spaltung von Cohesin durch Separase ist essentiell in der Mitose, da primäre Mausfibroblasten (pMEFs) ohne Separase Chromosomen nicht segregieren können.

Obwohl der „Prophase Pathway“ bereits seit vielen Jahren bekannt ist und untersucht wird, ist ungewiss, ob er für die Zellteilung essentiell oder mit Cohesin-Spaltung in der Anaphase durch Separase redundant ist. Um diese Frage zu beantworten und um die Funktionsweise des „Prophase Pathway“ besser zu verstehen, generierte ich eine konditionale „Knock-out“ Maus für Wapl. Wir machten die Entdeckung, dass die Deletion des Wapl-Gens bereits für den Embryo lethal ist. Dies deutet darauf hin, dass der „Prophase Pathway“ für die Entwicklung der Maus essentiell ist. In primären embryonalen Fibroblasten der Maus (pMEFs) ohne Wapl konnten wir beobachten, dass Schwesterchromatiden bis zur Metaphase

ungewöhnlich eng miteinander assoziiert sind, in der Anaphase aber getrennt werden. Allerdings bemerkten wir in den meisten Zellen in der Anaphase zahlreiche Chromosomenbrücken, die in der Zytokinese unvollständige Zellteilung zur Folge haben. In pMEFs ohne Wapl bleibt Cohesin bis zur Metaphase mit den Chromosomenarmen assoziiert; in der Anaphase wird Cohesin aber von den Chromosomen entfernt. Dies weist darauf hin, dass Separase ausreicht, um alle Cohesinmoleküle zu spalten. Ich bestätigte diese Hypothese, indem ich pMEFs von Wapl-Separase Doppel-„Knock-out“-Mäusen analysierte: In diesen Zellen kann Cohesin überhaupt nicht von den Chromosomen entfernt werden, und sowohl Chromosomenarme als auch Zentromere bleiben eng miteinander verbunden. Um zu bestimmen, ob das Übermaß an Cohesinmolekülen – und nicht eine noch unbekannte, von Cohesin unabhängige Funktion von Wapl – die Chromosomenbrücken verursacht, verringerte ich die Menge an Cohesin in der Zelle durch RNA-Interferenz gegen Scc1 in Wapl „Knock-out“ Mäusen. Dies konnte die Segregationsdefekte mildern und deutet darauf hin, dass der Überschuss der Cohesinkomplexe der Grund für die beobachteten Abnormitäten ist. Deshalb vermute ich, dass der „Prophase Pathway“ der Cohesin-Dissoziation notwendig für die korrekte Chromosomensegregation in der Zellteilung von Säugern ist.

Zusätzlich bestimmte ich den Einfluss von Wapl auf das Fortschreiten des Zellzyklus in der Interphase: Ich etablierte ein Protokoll zur Inaktivierung von Wapl in G₀-arretierten pMEF-Zellen und beobachtete, dass die Deletion von Wapl eine starke Hemmung der Zellproliferation verursacht. Unter diesen Bedingungen konnten nur wenige Zellen die Replikationsphase erreichen, viele verharrten aber in der G₀/G₁-Phase. Zwar ist die Ursache dieses Arrests noch nicht klar, jedoch konnte ich eine dramatische Zunahme an Chromatin-gebundenem Cohesin und an Cohesin-

Bindestellen an der DNA feststellen. Das Muster der Cohesin-Lokalisation in Wapl „Knock-out“ Interphase-Zellen war auch verändert, verglichen mit Kontrollzellen. Die Cohesinmoleküle erscheinen als längliche Struktur, die mit der DNA co-lokalisiert. Diese Cohesinstruktur gleicht dünnen Fäden oder Würmern, weshalb ich diese Struktur *vermicelli* (das italienische Wort für kleine Würmer) taufte. Zusätzlich beobachtete ich eine sehr kompakte Interphase-Chromatinstruktur in Wapl „Knock-out“ pMEFs. Künftige Experimente sollen helfen, den Zusammenhang von Cohesin-*vermicelli* und veränderter Chromatinstruktur zu verstehen.

1. Introduction

1.1 The cell cycle

Cell reproduction is a fundamental process for the development and the function of each living organism. For instance, an adult human organism is the result of many cell divisions from a single cell. However, uncontrolled cell divisions can be fatal for the organism, therefore cell reproduction must be tightly regulated.

The cell cycle is defined as the sequence of events that leads to the eukaryotic cell reproduction (reviewed in Morgan, 2007). The two main phases of the cell cycle are interphase, when cell's components are duplicated, and mitosis (M phase) when the duplicated components are equally distributed into two daughter cells (Figure 1).

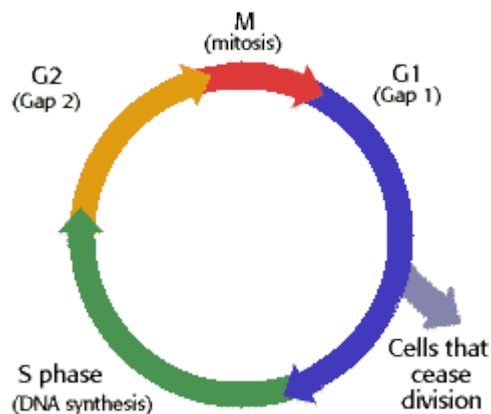


Figure 1: Schematic drawing of the cell cycle.

Interphase can be further divided into three phases: G1 phase (for gap 1), S phase (for synthesis) and G2 phase (for gap 2). During the so called gap phases, G1 and G2, many cellular components are duplicated. However, only in S phase is the DNA replicated, and as a result the chromosomes are

duplicated. At the end of S phase, each chromosome is composed of two tightly linked copies, referred to as sister chromatids.

M phase consists of two major events: nuclear division (mitosis) and cell division (cytokinesis). Mitosis is further divided into five stages in vertebrate cells: prophase, prometaphase, metaphase, anaphase and telophase (Figure 2).

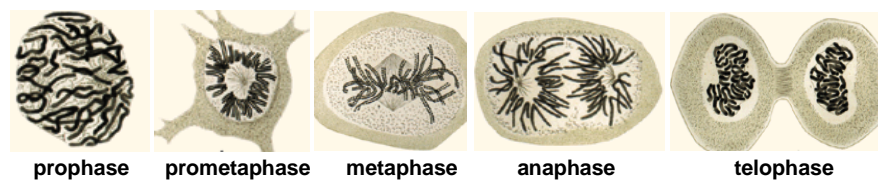


Figure 2: Schematic drawing of mitotic phases (Flemming 1882)

During prophase, the chromosomes undergo condensation and become visible under the microscope as individual rods. Prometaphase starts when the nuclear envelope breaks down and the mitotic spindle, a bipolar array of microtubules, forms around the sister chromatids. Each pair of sister chromatids become attached to microtubules from opposite poles, a configuration known as biorientation. Metaphase is achieved when all chromosomes biorient and thereby align at the centre of the spindle (metaphase plate). Anaphase occurs when sister chromatids are separated and segregated to opposite poles of the spindle. During telophase, the mitotic spindle disassembles and the nuclear envelope re-forms around the chromosomes at the two opposite poles. Chromosomes also start to decondense. The two daughter cells are then separated by the ingression of the cell membrane at the site of cell division, a process called cytokinesis.

During the next G1 phase, the cell either starts a new cycle or enters in a non dividing state, referred to as G0 (G zero).

1.2 Cell cycle progression

Successful cell reproduction is achieved only if the cell cycle events happen in the correct order. For example, chromosome segregation starts only after DNA replication is complete, otherwise the cell progeny receive incomplete genetic information.

Cell cycle progression is triggered by a combination of phosphorylation and degradation, which ensure the unidirectionality of the cycle. The main cell cycle kinases are Cdks (cyclin dependent kinases), which phosphorylate several proteins involved in DNA replication and mitotic division (reviewed in Morgan, 1997). In order to become active, Cdks require the binding of regulatory proteins called cyclins (reviewed in Murray, 2004). Cyclin levels oscillate during the cell cycle, with different cyclins active during different cell cycle stages. This results in the formation of distinct cyclin-Cdk complexes which promote different cell cycle events. For example, the mitotic cyclin B is only present from late G2, when chromosomes are already duplicated, to anaphase, when it is degraded.

The degradation of cyclins is therefore essential for cell cycle progression. Degradation of interphase cyclins is triggered by the E3 ubiquitin ligase SCF (Skp1/cullin/F-box protein) (reviewed in Cardozo and Pagano, 2004); whereas the APC/C (Anaphase promoting complex/Cyclosome) is active during M phase (reviewed in Peters, 2006). The mitotic cyclin B is one of the main

targets of the APC/C. Its degradation results in Cdk1 inactivation and therefore mitotic exit.

Cells have also evolved sophisticated control mechanisms, called checkpoints, to inhibit a later event if the earlier one is not complete (reviewed in Morgan, 2007). Cdks and other factors are the targets of the checkpoints. For example, the spindle assembly checkpoint (SAC) inhibits the APC/C complex activity if mitotic spindle formation is delayed (reviewed in Musacchio and Salmon, 2007). This prevents premature sister chromatid separation before anaphase and therefore incorrect genome transmission.

1.3 Importance of sister chromatid cohesion in chromosome segregation

The logic of chromosome segregation is to segregate each sister chromatid of a pair to opposite poles of the cell (Section 1.1). After completion of cytokinesis, this results in the formation of two genetically identical daughter cells. It is therefore crucial that the two sister chromatids of each chromosome are physically connected to each other when the cell approaches the metaphase-anaphase transition. The linkage between the two sister chromatids, referred to as cohesion, allows chromosome biorientation in early mitosis. Indeed, sister chromatid cohesion offers resistance to the mitotic spindle pulling forces stabilizing bipolar attachments over improper ones and therefore contributes to chromosome alignment at the metaphase plate (reviewed in Pinsky and Biggins, 2005). Sister chromatids that have lost cohesion before biorientation could be segregated in the same cell. Aneuploid cells (cells with an abnormal number of chromosomes) are usually eliminated

in the human organism by compromising its viability during embryogenesis. However, in the event that the aneuploid cells are able to survive, it could lead to the development of tumors in adult humans (reviewed in Weaver and Cleveland, 2006).

Sister chromatid cohesion must be established as soon as chromosomes are replicated in S phase in order for the sister chromatids to be accurately segregated. It was first suggested that DNA catenation, the intertwining of sister DNA molecules that occurs when replication forks meet, could be the mechanism that holds sister chromatids together and its resolution by topoisomerase enzymes would allow sister separation (reviewed in Murray and Szostak, 1985). Although DNA catenation can account for some cohesion between sister DNA molecules, genetic screens identified gene products not involved in DNA catenation but which still caused precocious sister chromatid separation (Guacci et al., 1997; Michaelis et al., 1997). This suggested that sister chromatid cohesion is a distinct event from DNA catenation and that protein factors exist to keep sister chromatids together soon after replication.

1.4 The cohesin complex

There are many pieces of evidence both in yeast (reviewed in Nasmyth and Haering, 2005) and in animal cells (reviewed in Peters et al., 2008) that sister chromatid cohesion is mediated by the cohesin complex. In addition to its function in chromosome segregation the cohesin complex has a fundamental role in DNA damage repair (reviewed in Watrin and Peters, 2006) and in gene expression (reviewed in Wendt and Peters, 2009).

Architecture of the cohesin core complex

The cohesin core complex is composed of four subunits, namely Smc1, Smc3, Scc1 and Scc3 (Guacci et al., 1997; Losada et al., 1998; Losada et al., 2000; Michaelis et al., 1997; Sumara et al., 2000; Toth et al., 1999). Smc1 and Smc3 are members of the Structural Maintenance of Chromosomes (Smc) family which is conserved from bacteria to humans (Hirano, 2006; Michaelis et al., 1997; Strunnikov et al., 1993). Smc proteins have a unique domain organization: two nucleotide-binding motifs, one at the N-terminus, known as Walker A, and one at the C-terminus, known as Walker B, are separated by a long region with alpha helical structure and a globular hinge domain at the center. Electron microscopy and biochemical studies showed that Smc proteins fold back on themselves through antiparallel coiled-coil interactions (Haering et al., 2002; Hirano and Hirano, 2002; Melby et al., 1998). This results in the formation of a globular ATPase 'head' at one end and a globular 'hinge' domain at the other. Smc1 and Smc3 tightly associate at their hinge domain whereas their ATPase heads are bound to the C-terminal domain and the N-terminal domain of Scc1, respectively (Haering et al., 2002). Scc1 belongs to a protein family known as kleisin (from the Greek word "to close", kleisimo), which functions in bridging the Smc heterodimers (Schleiffer et al., 2003). In eukaryotic cells, there are two additional Smc heterodimers (reviewed in Hirano, 2006): Smc2-Smc4, which is part of the condensin complex and is implicated in chromosome assembly and segregation, and the Smc5-Smc6, which is implicated in DNA repair and checkpoint response.

The Smc1-Smc3-Scc1 arrangement results in a tripartite ring structure with an outer diameter of 50 nm (Figure 3) (Haering et al., 2002). Moreover, electron

microscopic studies strongly support this cohesin ring structure (Anderson et al., 2002).

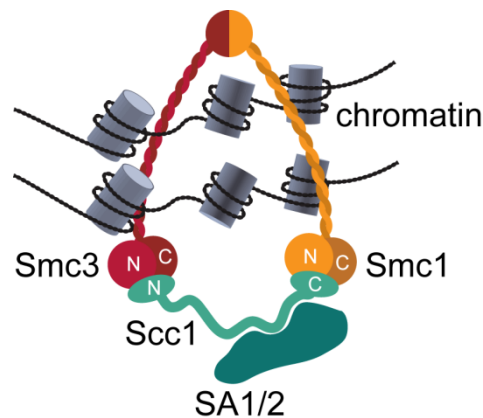


Figure 3: A model of the cohesin complex. See the text for the details (adapted from Peters et al. 2008)

The fourth subunit, known as Scc3, binds to the C-terminus of Scc1 (Haering et al., 2002). In vertebrate cells, two closely related homologues of Scc3, SA1 and SA2, exist. They bind to cohesin in a mutually exclusive manner (Losada et al., 2000; Sumara et al., 2000). Cohesin^{SA1} and cohesin^{SA2} are differentially required for telomere and centromere cohesion, respectively (Canudas and Smith, 2009).

Cohesin associated proteins

Three additional proteins bind cohesin in a sub-stoichiometric manner. One of these proteins is the evolutionarily conserved Pds5 protein which associates with the cohesin complex in all species studied so far (Dorsett et al., 2005; Hartman et al., 2000; Losada et al., 2005; Panizza et al., 2000; Stead et al., 2003; Sumara et al., 2000; Tanaka et al., 2001; Wang et al., 2002). In vertebrates there are two Pds5 isoforms, Pds5A and Pds5B, which associate with cohesin in a mutually exclusive manner (Losada, Yokochi et al. 2005).

Pds5 can interact with the cohesin subunit Scc1 and can also form a sub-complex with another cohesin-associated protein called Wapl (Ben-Shahar et al., 2008; Gandhi et al., 2006; Kueng et al., 2006; Rowland et al., 2009; Shintomi and Hirano, 2009; Sutani et al., 2009).

Wapl is highly conserved among metazoan species, and it has recently been shown that the budding yeast Rad61 protein, distantly related to vertebrate Wapl, interacts with cohesin (Ben-Shahar et al., 2008; Rowland et al., 2009; Sutani et al., 2009). Therefore Rad61 is also called Wpl1.

A third protein, called sororin has been identified only in vertebrates (Rankin et al., 2005; Schmitz et al., 2007). It is still unknown how sororin interacts with cohesin.

How and where cohesin interacts with DNA

Because the cohesin core complex forms a gigantic ring-like structure, it has been proposed that it might mediate sister chromatid cohesion by trapping both sister chromatids inside its ring (Gruber et al., 2003; Haering et al., 2002). The cohesin ring model is supported by several observations in yeast (reviewed in Nasmyth and Haering, 2009). For example, proteolytic cleavage of either Scc1 or Smc3 by TEV protease triggers cohesin dissociation from DNA and loss of sister chromatid cohesion (Gruber et al., 2003; Uhlmann et al., 2000). Moreover, in vitro experiments using yeast minichromosomes showed that either Scc1 cleavage or linearization of the DNA abolishes cohesion (Ivanov and Nasmyth, 2005, 2007). Cohesion between minichromosomes is also lost after protein denaturation but not if cohesin subunits are covalently connected to each other via chemical cross-linking in

vitro (Haering et al., 2008). Importantly, Scc1 is cleaved in eukaryotic cells at the metaphase-anaphase transition triggering cohesin dissociation from chromosomes and sister chromatid separation (Section 1.5).

In eukaryotic genomes cohesin binds at both centromeres and chromosome arms. The cohesin population at the centromeres is particularly important because the mitotic spindle exerts its pulling forces directly at the kinetocores, the specialized protein structures built at centromeres to attach microtubules. In yeast cohesin is more enriched at the centromeres than on chromosome arms, whereas the situation is less clear in mammalian cells (reviewed in Peters et al., 2008). In yeast, cohesin attachment regions on chromosome arms do not show any DNA sequence specificity but most of them are found in intergenic regions at sites of convergent transcription (Blat and Kleckner, 1999; Glynn et al., 2004; Lengronne et al., 2004). One interpretation of this observation is that the transcription machinery is able to push away cohesin during gene transcription. However, the situation is different in mammalian cells, where cohesin binding sites are enriched in regions adjacent to genes (Parelho et al., 2008; Wendt et al., 2008), suggesting a role for cohesin in gene regulation. Indeed, in mammalian cells most cohesin binding sites are identical to the binding sites of the transcriptional insulator protein CTCF, and cohesin is required for the insulator function of CTCF at some of these sites (Parelho et al., 2008; Rubio et al., 2008; Stedman et al., 2008; Wendt et al., 2008). It remains to be clarified how cohesin contributes in mechanistic terms to gene regulation (reviewed in Wendt and Peters, 2009).

1.5 Cohesin regulation during the cell cycle

It was first observed in yeast that cohesin associates with DNA from late G1, shortly before chromosomes are duplicated in S phase, until the metaphase-anaphase transition when cohesion between sister DNAs is broken to allow proper segregation (Michaelis et al., 1997). Cohesin has therefore to be loaded onto DNA in G1 phase, establish cohesion between sister chromatids in S phase and be removed from chromosomes at the metaphase-anaphase transition (Figure 4). These processes are tightly regulated and many aspects of their regulation are still a mystery.

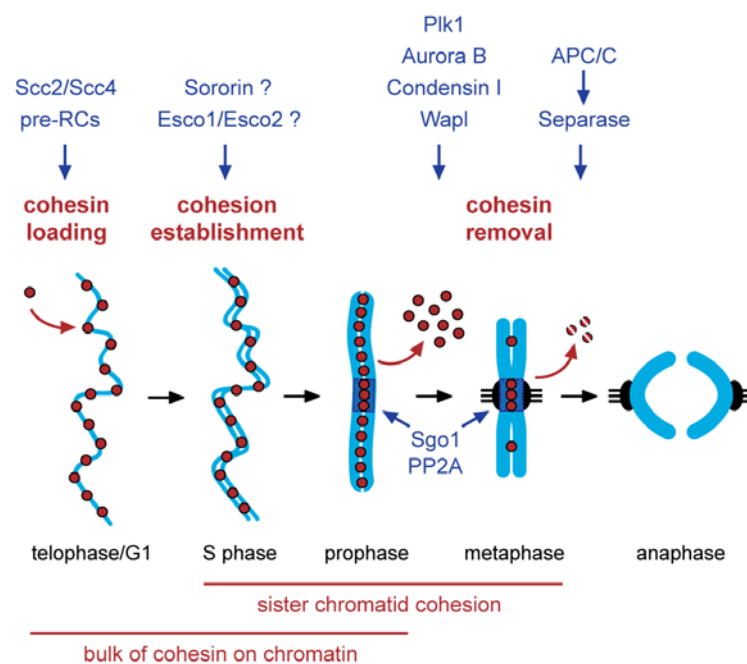


Figure 4: Illustration of the different stages of the cohesion cycle and their regulation in vertebrate cells. The red circles indicate cohesin. See the text for the details (from Peters et al. 2008).

Cohesin loading

In yeast, cohesin is loaded onto DNA in late G1 (Guacci et al., 1997; Michaelis et al., 1997), whereas in vertebrate cells, cohesin is loaded already in telophase (Darwiche et al., 1999; Gerlich et al., 2006; Losada et al., 1998; Sumara et al., 2000). Cohesin loading onto DNA depends on the Scc2/Scc4 complex, which has been identified in various organisms (Bernard et al., 2006; Ciosk et al., 2000; Furuya et al., 1998; Gillespie and Hirano, 2004; Rollins et al., 2004; Takahashi et al., 2004; Watrin et al., 2006). The Scc2/Scc4 complex might directly recruit cohesin to the DNA and promote its loading by possible stimulating cohesin's ATPase activity. This might in turn result in the opening of the cohesin hinge domain to allow DNA entrapment inside the ring (reviewed in Peters et al., 2008). In *Xenopus* egg extracts Scc2/Scc4 recruitment onto DNA further depends on the formation of prereplicative complexes (pre-RCs) on DNA (Gillespie and Hirano, 2004; Takahashi et al., 2008; Takahashi et al., 2004). This is not the case in yeast (Uhlmann and Nasmyth 1998) and it is not known whether pre-RCs are required for the recruitment of Scc2/Scc4 and cohesin complexes in mammalian cells.

Cohesion establishment

Although cohesin binds DNA in G1 phase, sister chromatid cohesion is established during DNA replication in S phase (few exceptions are known, reviewed in Uhlmann, 2009). In mammalian cells cohesin binds to DNA dynamically in G1 phase (Gerlich et al., 2006). After DNA replication half of chromatin-bound cohesin is stably bound and some of this cohesin pool holds sister chromatids together until the metaphase-anaphase transition (Gerlich et

al., 2006). Evidence that after DNA replication cohesin is stably bound to chromatin has been obtained also in yeast (Bernard et al., 2008; Haering et al., 2004). How does cohesin become cohesive during S phase? In budding yeast the acetyltransferase Eco1 associates with DNA replication forks and acetylates the cohesin subunit Smc3 coupling DNA replication with the establishment of sister chromatid cohesion (Ivanov et al., 2002; Lengronne et al., 2006; Moldovan et al., 2006; Skibbens et al., 1999; Toth et al., 1999; Unal et al., 2008). A similar situation might exist in human cells where two Eco1 orthologs, called Esco1 and Esco2, exist (Hou and Zou, 2005; Zhang et al., 2008). Interestingly, mutations in Scc3, Pds5 or Wpl1 can suppress Eco1 lethality and rescue to some extent the cohesion defects caused by Eco1 deletion (Ben-Shahar et al., 2008; Rowland et al., 2009; Sutani et al., 2009). It is unclear how, at the molecular level, Smc3 acetylation and the Scc3-Pds5-Wpl1 complex contribute to the establishment of sister chromatid cohesion (Peters and Bhaskara, 2009).

The vertebrate protein sororin might also be involved in cohesion establishment in S phase or in cohesion maintenance in G2 (Schmitz et al., 2007). In fission yeast Pds5 is involved in cohesion maintenance in G2 phase, although its role in cohesion is less clear in vertebrate cells (Losada et al., 2005; Zhang et al., 2007).

Cohesin removal in early mitosis: the prophase pathway

In vertebrate cells the bulk of cohesin is removed already in prophase; i.e. long before sister chromatids separate (Darwiche et al., 1999; Losada et al., 1998; Sumara et al., 2000). This so-called prophase pathway removes most,

but not all, cohesin from chromosome arms (Gimenez-Abian et al., 2004; Waizenegger et al., 2000). Furthermore, centromeric cohesin is not removed by the prophase pathway.

How is cohesin removed from chromosomes in early mitosis? It was observed that cohesin dissociation in prophase is independent of both APC/C activity (Sumara et al., 2000) and Scc1 cleavage, which is required later in anaphase for sister separation (Waizenegger et al., 2000). Subsequent studies identified several proteins involved in the prophase pathway of cohesin dissociation. One of these proteins is the mitotic kinase Plk1 which phosphorylates the cohesin subunits Scc1 and SA1/2 (Gimenez-Abian et al., 2004; Lenart et al., 2007; Losada et al., 2002; Sumara et al., 2002). Expression of a non-phosphorylatable SA2, but not of a non-phosphorylatable Scc1, in cultured human cells impairs dissociation of cohesin from chromosome arms in prophase and prometaphase (Hauf et al., 2005). In addition, cohesin phosphorylation by Plk1 reduces cohesin's ability to bind DNA (Sumara et al., 2002). However, SA2 phosphorylation is not sufficient for cohesin dissociation in early mitosis (see below).

The mitotic kinase Aurora B also plays a role in the prophase pathway (Gimenez-Abian et al., 2004; Losada et al., 2002). Aurora B does not phosphorylate cohesin but might contribute to cohesin dissociation in early mitosis by recruiting the condensin I complex to DNA (Lipp et al., 2007). Indeed, proper loading of condensin I in prometaphase is needed for cohesin removal from chromosome arms, although the molecular mechanism is still unknown (Hirota et al., 2004).

Inactivation of Plk1, Aurora B or condensin I and expression of non-phosphorylatable SA2 prevents only some cohesin dissociation from chromosome arms, suggesting that one or more additional factors are required for the complete removal of cohesin in early mitosis. Indeed, inactivation of the Wapl protein has a dramatic effect on cohesin dissociation in prophase (Gandhi et al., 2006; Kueng et al., 2006), suggesting a key role of Wapl in the prophase pathway (Section 1.6). A recent study using *Xenopus* egg extracts showed that Pds5 is also required for cohesin release in early mitosis, likely by interacting with Wapl (Shintomi and Hirano, 2009).

Functions of the prophase pathway

The physiological function of the prophase pathway of cohesin removal in vertebrate cells is currently unknown. Different hypotheses, not mutually exclusive, have been suggested (reviewed in Peters et al., 2008).

The observation that chromosome condensation occurs when cohesin is removed from DNA in prophase suggested that the latter could be a prerequisite for the former event. This could also explain why in yeast, where little mitotic chromosome condensation occurs (Guacci et al., 1994), the prophase pathway is absent. However, no major condensation defects have been observed after the inactivation of the prophase pathway.

It has also been shown that the inactivation of the prophase pathway impairs sister chromatid resolution along chromosome arms (Gandhi et al., 2006; Gimenez-Abian et al., 2004; Hauf et al., 2005; Hirota et al., 2004; Kueng et al., 2006; Losada et al., 2002). A similar phenotype is observed after inactivation of topoisomerase II (Losada et al., 2002; Porter and Farr, 2004), suggesting

that removal of cohesin could help in the decatenation of sister DNAs. However, no segregation defects, which would be expected following inhibition of topoisomerase II activity, have been reported after the inactivation of the prophase pathway.

Another possibility is that the release of cohesin in prophase is required because separase would not be able to cleave all cohesin at the metaphase-anaphase transition. However, even Wapl inactivation does not induce segregation defects, suggesting that separase can cleave all the cohesin on chromosomes.

It could also be possible that the prophase pathway is required so that not all the cohesin is cleaved by separase. This preserves the bulk of cohesin that can be re-loaded in telophase. This might be essential for cohesin function in gene-regulation during G1 (Wendt et al., 2008).

Protection of centromeric cohesion from the prophase pathway

The Sgo1 protein protects centromeric cohesin from the prophase pathway of cohesin dissociation (Kitajima et al., 2005; McGuinness et al., 2005; Salic et al., 2004; Tang et al., 2004). Sgo1 inactivation results in cohesin release from centromeres and premature sister chromatid separation in early mitosis.

How does Sgo1 achieve this task? It was shown that premature sister separation in Sgo1-depleted human cells can be rescued by the expression of non-phosphorylatable SA2, suggesting that Sgo1 counteracts cohesin phosphorylation at centromeres (McGuinness et al., 2005). Indeed, Sgo1 interacts with the protein phosphatase complex PP2A and Sgo1-PP2A can dephosphorylate SA2 in vitro (Kitajima et al., 2006; Riedel et al., 2006; Tang

et al., 2006). Other proteins have also been shown to be involved in centromeric cohesion protection (reviewed in Peters et al., 2008).

Cohesin removal at the metaphase-anaphase transition

Cohesion between sisters is maintained until all chromosomes are bioriented at the metaphase plate. Only then is the spindle assembly checkpoint inactivated and the APC/C becomes active thus targeting several proteins for degradation (Section 1.2). These APC/C substrates include securin and cyclin B, both of which are required for Separase inhibition in vertebrate cells (Gorr et al., 2005; Hornig et al., 2002; Huang et al., 2008; Huang et al., 2005; Stemmann et al., 2001; Waizenegger et al., 2002).

Separase is a protease that, once active, cleaves the cohesin subunit Scc1 (Uhlmann et al., 1999; Waizenegger et al., 2000). Scc1 cleavage is thought to open the cohesin ring, allowing the two sisters to be pulled to opposite poles of the cell. In yeast it was shown that Scc1 cleavage in metaphase is sufficient to initiate sister chromatid separation (Uhlmann et al., 2000). Importantly, expression of non-cleavable Scc1 or deletion of separase leads to severe defects in chromosome segregation in both yeast and mammalian cells (Hauf, 2001; Kumada et al., 2006; Uhlmann et al., 1999; Wirth et al., 2006).

1.6 Wapl

The Wapl protein was initially found to be involved in heterochromatin formation and chromosome segregation in *Drosophila melanogaster* (Dobie et al., 2001; Perrimon et al., 1985; Verni et al., 2000). The molecular function of Wapl became much clearer later when it was found to physically interact with

the cohesin complex (Gandhi et al., 2006; Kueng et al., 2006). Wapl associates with cohesin throughout the cell cycle although not as stably as the core cohesin subunits, and like cohesin, localizes to chromatin from telophase until prophase of the next mitosis.

Wapl is highly conserved among metazoan species, especially in its C-terminal half, which is predicted to be predominantly α -helical. However, the N-terminal half of vertebrate Wapl contains three FGF motifs, one of which is required for interaction with Pds5, and the other two for its interaction with Scc1-SA1 (Shintomi and Hirano, 2009).

Wapl inactivation in *Drosophila* and budding yeast results in mild cohesion defects (Verni et al., 2000; Warren et al., 2004). However, in fission yeast and in vertebrate cells Wapl is required for the dissociation of cohesin from DNA (Bernard et al., 2008; Hirano, 2006; Kueng et al., 2006; Shintomi and Hirano, 2009).

Wapl inactivation by RNA interference (RNAi) in cultured human HeLa cells severely impaired sister chromatid resolution along chromosome arms in early mitosis (Gandhi et al., 2006; Kueng et al., 2006). Analysis of chromosome morphology by spread and Giemsa staining showed typical X-shape chromosomes in control cells but not in Wapl depleted cells, where the two sisters of each chromosome were still tightly associated. The lack of sister chromatid resolution in Wapl-depleted cells was a consequence of excess cohesin on mitotic chromosomes, and could be rescued by partial Scc1 depletion by RNAi. Remarkably, endogenous cohesin could be detected on mitotic chromosomes by immunofluorescence microscopy after Wapl depletion by RNAi. Inactivation of other regulators of the prophase pathway

also results in cohesin enrichment on chromosomes, but this cohesin could be detected only after expression of a tagged cohesin subunit (Section 1.5). Wapl is therefore the main regulator of the prophase pathway of cohesin dissociation.

How does Wapl promote cohesin dissociation from chromosomes in early mitosis? It has been shown that Wapl does not prevent the activity and the localization of any other component of the prophase pathway (Kueng et al., 2006). In fact, the cohesin subunit SA2 is phosphorylated although cohesin still cannot be released from chromosomes in Wapl depleted cells. It is more plausible that Wapl promotes cohesin dissociation through its direct interactions with the cohesin complex, as suggested by recent experiments using *Xenopus* extracts (Shintomi and Hirano, 2009).

Interestingly, Wapl activity is not restricted to mitosis (Bernard et al., 2008; Kueng et al., 2006). After DNA replication in mammalian cells there are two cohesin sub-populations: one that is stably bound to DNA, and another that associates dynamically with chromatin (Section 1.5). However, Wapl depletion by RNAi results in an increase in residence time of the dynamically bound cohesin pool in G2 phase of cultured HeLa cells. This suggests that the ability of cohesin to interact dynamically is facilitated by Wapl even in G2 phase of the cell cycle.

What are the consequences of Wapl inactivation by RNAi in mammalian cells? Wapl depleted cells delay progression through mitosis but chromosome segregation occurs in a proper manner (Gandhi et al., 2006; Kueng et al., 2006). In addition, no major defects were observed in interphase except for a G2/M delay (S Kueng and JM Peters, unpublished results) and a change in

nuclear morphology (Gandhi et al., 2006). However, Wapl is an essential gene in the mouse and in *Drosophila* (Oikawa et al., 2004; Verni et al., 2000), suggesting that the prophase pathway of cohesin dissociation might have an important function during the development of an organism.

1.7 Aims of this study

The prophase pathway of cohesin dissociation removes most of cohesin from chromosomes during early mitosis but its functions are still a mystery (Section 1.5). To broaden our understanding of the prophase pathway we decided to take a genetic approach to conditionally inactivate the *Wapl* gene in the mouse.

To achieve this, I aim to generate a *Wapl* conditional knockout (cko) mouse and to determine the requirement of *Wapl* during mouse development.

I then aim to derive *Wapl* cko primary fibroblasts (pMEFs) and test their progression through cell cycle after *Wapl* deletion. In particular, I aim to focus on chromosome morphology during mitotic progression and especially on chromosome segregation at the metaphase-anaphase transition.

I also aim to cross *Wapl* cko mice with *Separase* cko mice in order to inactivate the two main regulators for cohesin dissociation in mitosis and study the effects of their co-deletion during mitotic progression.

In addition, I aim to investigate whether *Wapl* inactivation has consequences for cell cycle progression during interphase in pMEFs.

2. The prophase pathway of cohesin dissociation is required for proper chromosome segregation during mitosis

2.1 Generation of conditional and null *Wapl* alleles

Taking advantage of homologous recombination in mouse ES cells, exons 3 and 4 of *Wapl* locus were flanked with *LoxP* recombination sites in order to create a *Wapl* floxed allele, *Wapl*^F (Figure 5A and Materials and Methods).

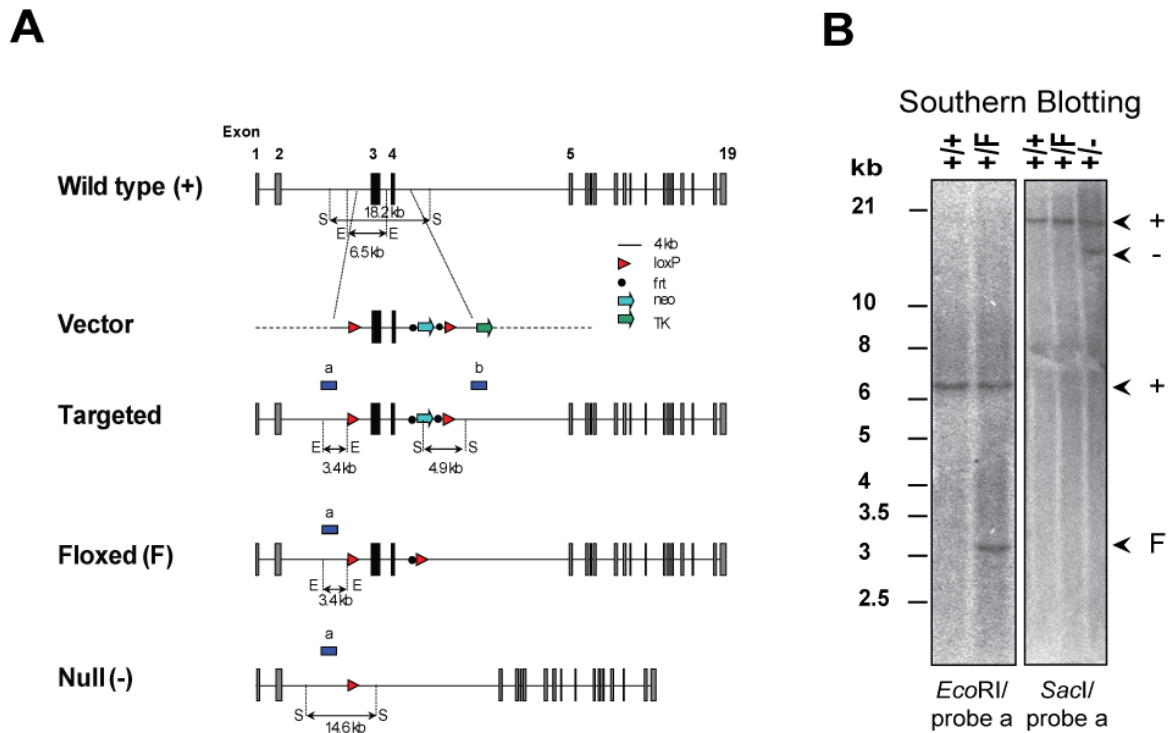


Figure 5: Generation of conditional and null *Wapl* allele

(A) Schematic representation of: the *Wapl* genomic locus; the targeting vector showing the neo-TK cassette and *LoxP* sites; the structure of the correctly targeted allele; the conditional allele (F for floxed); and the null allele (-). Also shown are the *EcoRI* (E) and the *SacI* (S) restriction fragments detected by probe a. Probe b was used as an independent probe for positive ES cell clones (data not shown).

(B) Southern blotting of *EcoRI*-digested tail DNA and *SacI*-digested tail DNA probed with probe a to confirm the genotypes.

Deletion of exons 3 and 4 by Cre-mediated recombination leads to a frame shift, thus generating stop codons in all three open reading frames.

Mice harboring the floxed allele were then crossed with a Cre-deleter strain to create a *null* allele, *Wapl*^{-/-}. I confirmed the genotypes by Southern blotting (Figure 5B) and by PCR (see Material and Methods).

I then prepared primary mouse embryonic fibroblasts (pMEFs) from 13.5-day *Wapl*^{F/F} embryos and infected them with an Adenovirus expressing Cre (AdCre) to test *Wapl* depletion.

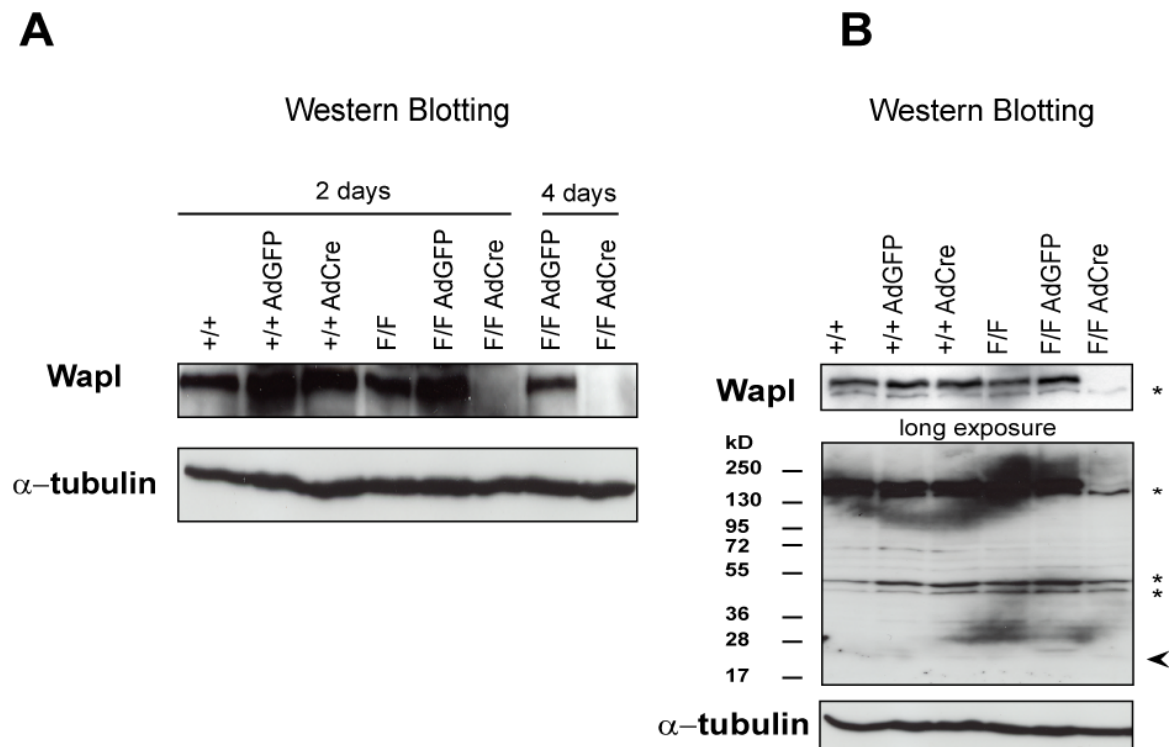


Figure 6: Characterization of *Wapl*^{F/F} primary embryonic fibroblasts

- (A) Western blotting of wild-type (+/+) and *Wapl*^{F/F} (F/F) pMEFs, either non-infected or infected with either AdGFP or AdCre, then probed to detect *Wapl* and α -tubulin.
- (B) Western blotting using the same sample as in (A) but then probed with an antibody against the protein product of exons 1 and 2 of *Wapl*. (*) indicates non-specific bands. The row-head indicates the predicted size of the *Wapl* truncated protein product.

Control *Wapl*^{+/+} pMEFs were also prepared from the same litter. Western blotting analysis, using an antibody against the *Wapl* C-terminal region, showed that *Wapl* protein was efficiently depleted below immunoblotting detection levels after AdCre infection but not after infection with a control Adenovirus expressing GFP (AdGFP, Figure 6A). Moreover, AdCre did not affect the level of *Wapl* protein in control *Wapl*^{+/+} pMEFs (Figure 6A). Untreated *Wapl*^{F/F} pMEFs had *Wapl* protein levels comparable to those of untreated *Wapl*^{+/+} pMEFs, suggesting that the *floxed* allele is as functional as the wild-type allele. Importantly, using an antibody against the very N-terminal region of *Wapl*, we confirmed that not even a truncated *Wapl* protein was present in *Wapl*^{Δ/Δ} cells (Figure 6B). I concluded that *Wapl*^Δ is indeed a *null* allele.

2.2 *Wapl* is essential for mouse embryonic development

To determine if the *Wapl* gene is essential for mouse development *Wapl*^{+/-} mice were intercrossed. Genotype analysis by PCR showed that no homozygous *Wapl*^{-/-} mice were born out of 73 live births. *Wapl*^{+/-} mice were born at the expected frequencies (Table IA), grew to adulthood, and appeared to be healthy. These data imply that *Wapl* is an essential gene during mouse embryogenesis and that a single copy of the gene is sufficient for embryonic development. We also intercrossed *Wapl*^{+F} mice (Table IB). Homozygous *Wapl*^{F/F} mice were born approximately at the expected frequencies (Table IB)

and did not show any apparent abnormalities, implying that the *Wapl* floxed allele is possibly as functional as the wild-type.

Table I A. Deletion of *Wapl* is embryonic lethal

Day of embryonic development	<i>Wapl</i>^{+/+}	<i>Wapl</i>^{+/-}	<i>Wapl</i>^{-/-}	Total
p21	50 (68.5%)	23 (31.5 %)	0 (0%)	73 (100%)

From intercrosses between *Wapl*^{+/-} mice, no *Wapl*^{-/-} mice were born in a total of 73 live births. p, postnatal days.

Table I B. *Wapl* F/F are born at the expected frequencies

Day of embryonic development	<i>Wapl</i>^{+/+}	<i>Wapl</i>^{+/-}	<i>Wapl</i>^{F/F}	Total
p21	17 (25.4%)	28 (41.8 %)	22 (32.8%)	67 (100%)

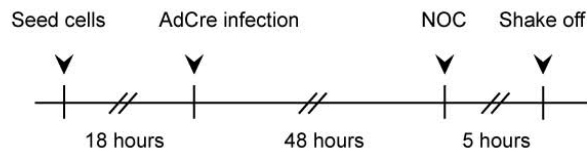
From intercrosses between *Wapl*^{+/-} mice, *Wapl*^{F/F} mice were born approximately at the expected frequencies. p, postnatal days.

2.3 The resolution of sister chromatid arms in primary embryonic fibroblasts depends on *Wapl*

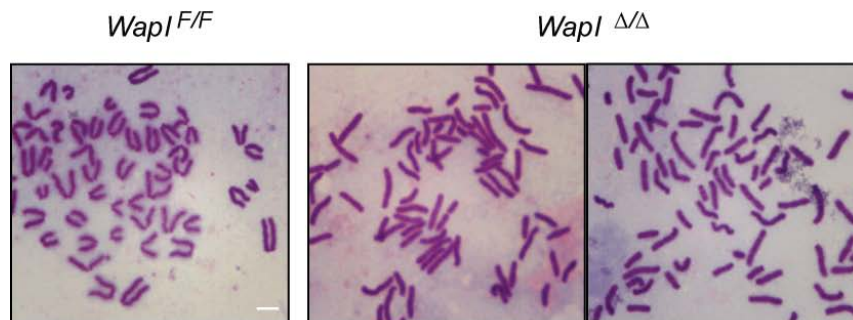
It has previously been shown that *Wapl* is required for dissociation of cohesin from chromosomes arms during prophase in cultured HeLa cells, a transformed cell line (Gandhi et al., 2006; Kueng et al., 2006). Cohesin

dissociation results in the resolution of sister chromatid arms, which come apart in early mitosis. I therefore asked if Wapl has a similar function in pMEFs. *Wapl*^{F/F} cells were seeded at 30% confluency and, 18 hours afterwards, either infected with AdCre virus or treated with infection medium without virus (Figure 7A). Forty-eight hours afterwards both control *Wapl*^{F/F} and *Wapl*^{Δ/Δ} knockout cells were treated for five hours with nocodazole to enrich for mitotic cells. I then collected mitotic cells by shake-off and analyzed their chromosomes by spreading and Giemsa staining (Figure 7B). Since nocodazole is a microtubule depolymerizing agent, the cells were arrested in a prometaphase-like state due to the action of the spindle assembly checkpoint. In these non-physiological conditions, sister chromatid arms, but not centromeres, come apart completely, allowing us to assay for cohesion defects. However, during a physiological mitosis the sister chromatids come only partially apart. Chromosomes from control *Wapl*^{F/F} pMEFs showed a typical acrocentric V-shape (68% of the cells, figure 7B, 7Ca) with the sisters connected at centromeres, at one end, and separated along the arms. A considerable fraction of control cells (24%) showed chromosomes with only partially-resolved arms (Figure 7Cb). This likely represents a cell population that entered mitosis during the last hours of nocodazole treatment and therefore did not have enough time to completely resolve cohesion along the arms. I also observed a small fraction of cells (5%) with unresolved chromosome arms (Figure 7Cc) and another small fraction (4%) with single or very condensed chromatids (Figure 7Cf,g). However, I found that in 60% of *Wapl*^{Δ/Δ} cells, sister chromatids are tightly associated with each other along

A



B



C

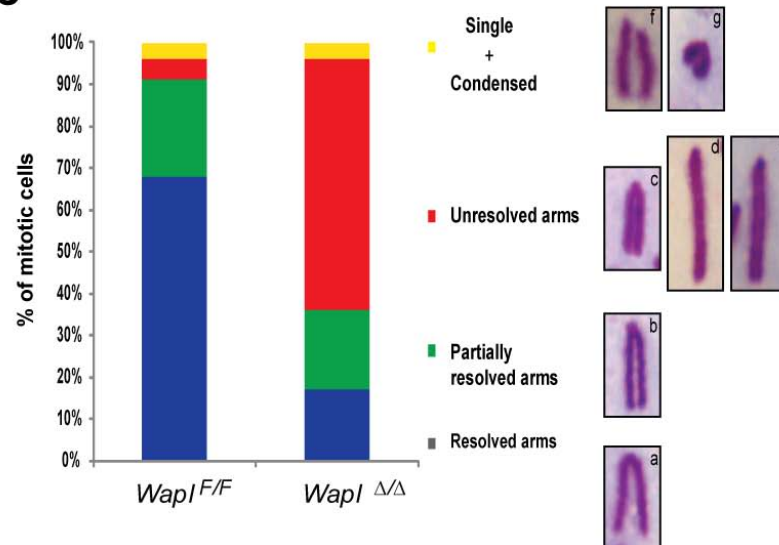


Figure 7: Wapl is required for sister-chromatid resolution in pMEFs

- (A) Schematic overview of viral infection and harvesting procedure.
 (B) Mitotic cells were collected by shake-off after 5 hours of nocodazole treatment and analyzed by hypotonic spreading and Giemsa staining. Size bar, 5 μ m.
 (C) Prometaphases obtained as in (B) were classified according to their chromosome morphology (n=100).

the entire chromosome axis (Figure 7B, 7Cd and e). Only 17% of *Wapl*^{Δ/Δ} cells showed completely resolved chromosome arms and, similarly to control, 19% showed partially resolved arms (Figure 7C). I also noticed that in *Wapl*^{Δ/Δ} cells chromosomes with unresolved arms are longer than those in control cells (compare Figure 7Cc, typical example of unresolved arms for control cells, with Figure 7Cd and e, only observed in *Wapl* knockout cells). These results show that Wapl is required for sister-chromatid resolution during early mitosis also in pMEFs.

2.4 Wapl is required for proliferation of primary embryonic fibroblasts

High levels of Cre protein induce growth arrest and chromosomal abnormalities (reviewed in Schmidt-Supprian and Rajewsky, 2007). This situation complicates the interpretation of cell cycle phenotypes that are observed after Cre-mediated deletion of floxed genes. To study Wapl function in proliferating cells *Wapl* strains were therefore crossed with *R26cre-ER^{T2}* mice (Seibler et al., 2003). These mice harbor a *cre-ER^{T2}* knock-in allele under the control of endogenous *Rosa26* promoter. The Cre recombinase is fused to the mutated ligand binding domain of the human estrogen receptor (*ER^{T2}*), which responds to the artificial ligand 4-hydroxy-tamoxifen (4-OHT). In the absence of 4-OHT, the Cre-ER^{T2} protein is retained in the cytoplasm; upon binding of 4-OHT, it translocates into the nucleus where it mediates recombination of genomic LoxP sites. The Cre-ER^{T2} inducible system has three main advantages. First, Cre-ER^{T2} protein is present at a low level because it is under the control of the endogenous *Rosa26* promoter. Second,

Cre activity can be further modulated using a suitable 4-OHT concentration. Third, Cre-ER^{T2} activity can be turned off by removing the 4-OHT and therefore causing the protein to be translocated into the cytoplasm. I then isolated *Wapl*^{-F} *R26cre-ER^{T2}* and *Wapl*^{+F} *R26cre-ER^{T2}* pMEFs and asked if *Wapl* is required for cell proliferation. After splitting, both cell lines were cultured for three days to 100% confluency and contact inhibition (Figure 8A). Subsequently, I serum starved the cells to synchronize them in G0, and added 4-OHT at a final concentration of 500 nM for 2 days. Finally, both cell lines were split in fresh medium to trigger proliferation and harvested every 24 hours for 5 days (Figure 8A). Importantly, this protocol allows me to distinguish between the first mitosis and the following ones. I first analyzed *Wapl* depletion efficiency by Western blotting. *Wapl*^{+F} cultures treated with 4-OHT (*Wapl*^{+Δ}) did not show a detectable decrease of *Wapl* protein over time (Figure 8B). In contrast, *Wapl*^{-F} cultures treated with 4-OHT (*Wapl*^{-Δ}) showed a significant decrease of *Wapl* protein at the first time-points, from T0 to 48 hours after G0 release, and no detectable *Wapl* was present from 72 hours to 96 hours (Figure 8B). I concluded that the 4-OHT inducible *R26cre-ER^{T2}* system is suitable to efficiently delete the *Wapl* gene. I then assayed the ability of *Wapl*^{-Δ} cells to proliferate. Control *Wapl*^{+Δ} cultures proliferated normally, doubling their cell number every 24 hours for the first four days after G0 release (Figure 8A). They stopped proliferating at 120 hours because the cells become contact inhibited. In contrast, treating *Wapl*^{-F} cultures with 4-

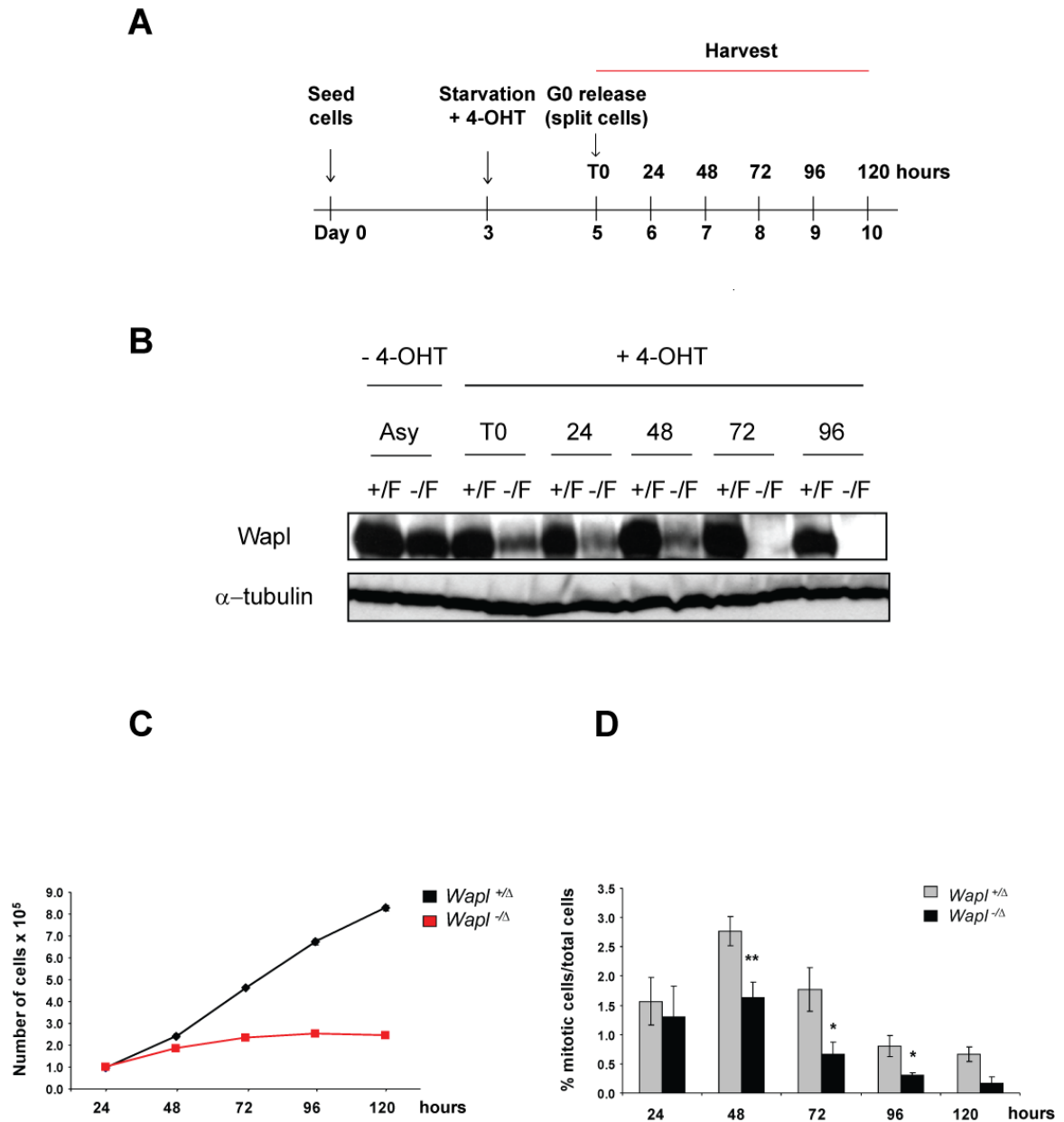


Figure 8: Wapl inactivation using 4-OHT

- (A) $Wapl^{+/F}$ R26cre-ER^{T2} and $Wapl^{-/F}$ R26cre-ER^{T2} pMEFs were plated and cultured for three days then treated with 0.5 nM 4-OHT for 2 days. On day 5 the cultures were expanded, the 4-OHT removed, and the cells analyzed at subsequent time-points.
- (B) $Wapl^{+/F}$ R26cre-ER^{T2} (+/F) and $Wapl^{-/F}$ R26cre-ER^{T2} (-/F) pMEFs from (A) analyzed by Western blotting. Asy, asynchronous cells.
- (C) Plot showing reduction of proliferation following $Wapl$ inactivation. $Wapl^{+/Δ}$ indicates $Wapl^{+/F}$ R26cre-ER^{T2} pMEFs treated with 4-OHT; $Wapl^{-/Δ}$ indicates $Wapl^{-/F}$ R26cre-ER^{T2} treated with 4-OHT.
- (D) Mitotic index (MI) is consistently lower in $Wapl^{-/Δ}$ cultures compared to control $Wapl^{+/Δ}$ cultures. Quantitative results were obtained from three experiments. A total of 3000 cells were scored for each time-point. (*) Significant ($P < 0.01$) or (**) highly significant ($P < 0.001$) differences between control and $Wapl^{-/Δ}$ cultures were evaluated using Student's T-test.

OHT had a potent antiproliferative effect (Figure 8C). *Wapl*^{-Δ} cultures proliferated for the first three days, although the cell number doubled only once in this period of time, but they stopped proliferating from 72 hours to 120 hours. Consistent with this result, the mitotic index (MI, number of mitotic cells/total cells) dramatically decreased in *Wapl*^{-Δ} cultures (Figure 8D). I scored mitotic cells by DNA morphology using DAPI and staining for the mitotic phosphorylation of serine 10 on histone H3 (H3S10ph). Control *Wapl*^{+Δ} cultures reached the first mitosis 24 hours after G0 release (Figure 8D). The peak of mitotic cells appeared at 48 hours, the second mitotic division, and as the cultures became more confluent the MI decreased over time. I did not observe any difference in the MI at 24 hours between control and *Wapl*^{-Δ} cultures. However, from 48 hours the MI significantly decreased in *Wapl*^{-Δ} cultures compared to control ones. I did not observe floating cells, an indication of apoptosis, even when *Wapl*^{-Δ} cells were left for 5 weeks in culture. Taken together, these results demonstrate that *Wapl* is required for normal proliferation of pMEFs.

2.5 *Wapl* regulates the dissociation of cohesin from prophase to metaphase

I next analyzed cohesin localization by immunofluorescence microscopy (IFM) in mitotic pMEFs deficient for *Wapl*. It has previously been shown that high amounts of cohesin can be detected on chromosomes in prophase and prometaphase HeLa cells after *Wapl* depletion by RNAi. However, *Wapl*-

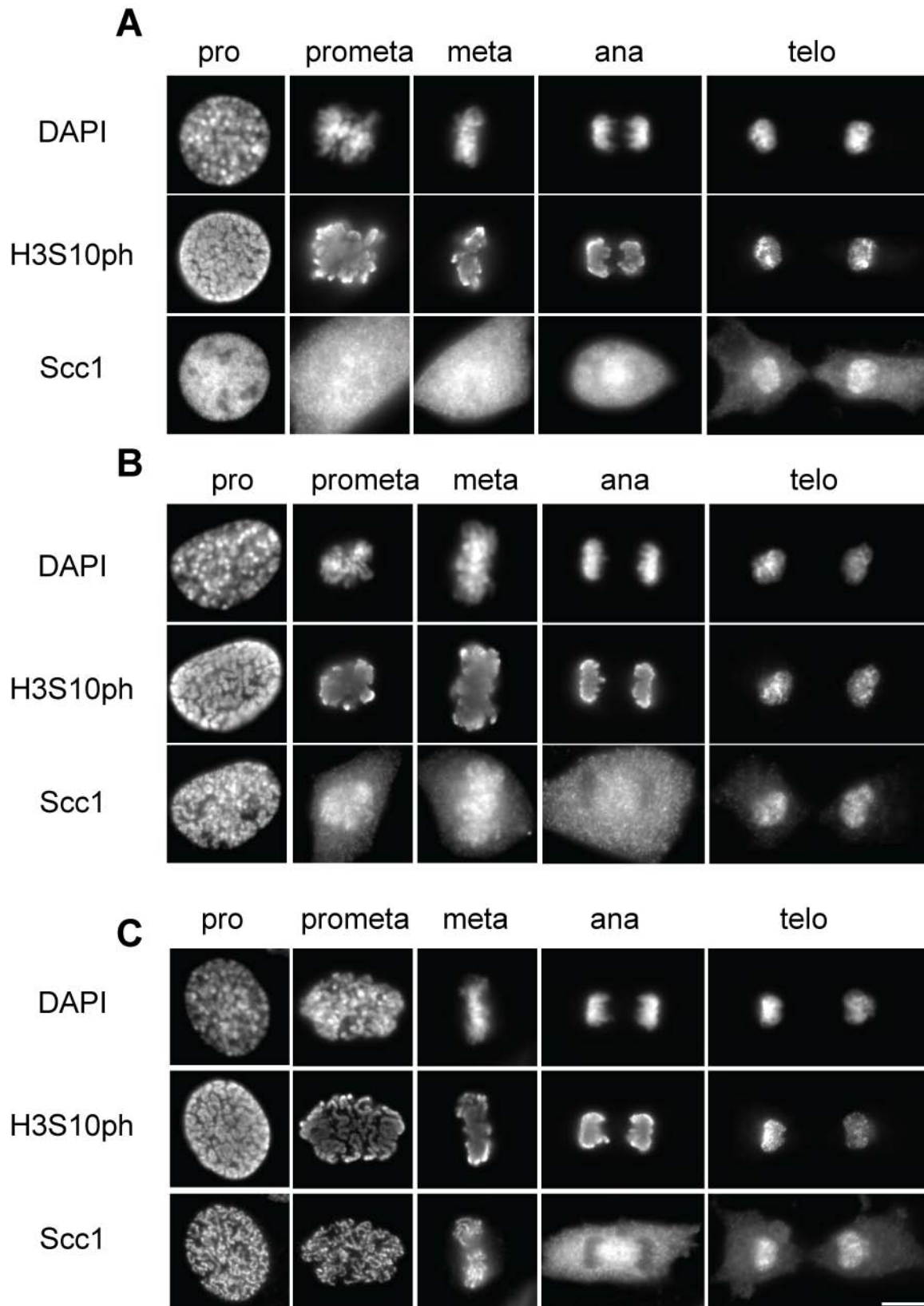


Figure 9: Wapl regulates the dissociation of cohesin from prophase to metaphase
 Immunofluorescence analysis with the indicated antibodies. A) control *Wapl*^{+Δ} cells 72 hours after G0 release; B) *Wapl*^{-Δ} cells 24 hours after G0 release; C) *Wapl*^{-Δ} cells 72 hours after G0 release. Bar, 10 μm.

depleted HeLa cells reached metaphase with strikingly less cohesin on chromosomes compared to early mitotic stages (Kueng et al., 2006). It remained unclear if residual amounts of Wapl caused partial dissociation of cohesin in these cells between prophase and metaphase, or if cohesin can also slowly dissociate from mitotic chromosomes in the absence of Wapl. To address this question I fixed control *Wapl*^{+/ Δ} and *Wapl*^{-/ Δ} pMEFs in 4% paraformaldehyde and stained the total cohesin pool with antibodies against Scc1, Smc3 and SA1/2. Figure 9A shows control mitotic cells stained with a Scc1 antibody. Most of cohesin is soluble during mitosis because the prophase pathway removes it from chromosomes in early stages (Figure 9A). Therefore Scc1 staining appeared diffuse and excluded from the DNA, particularly after the nuclear envelope had broken-down in prometaphase (Figure 9A). However, cohesin behavior in *Wapl*^{-/ Δ} cells was strikingly different. At the early time-point of 24 hours, 41% of total prophase, prometaphase and metaphase cells from *Wapl*^{-/ Δ} cultures showed the Scc1 signal in part co-localizing with the DNA signal, and in part in the cytoplasm (Figure 9A and Figure 10).

Only few cells (9%, Figure 10) had a strong and clear Scc1 signal exclusively along the chromosome (Figure 9A). Strikingly, the percentage of cells in which the Scc1 signal co-localized exclusively with the DNA signal increased over time (from 50% at 48 hours to 65% at 72 hours, Figure 10). Remarkably, metaphase cells, especially at 72 hours (Figure 9A), showed chromosomal Scc1 signal which was as strong as in prophase and prometaphase cells.

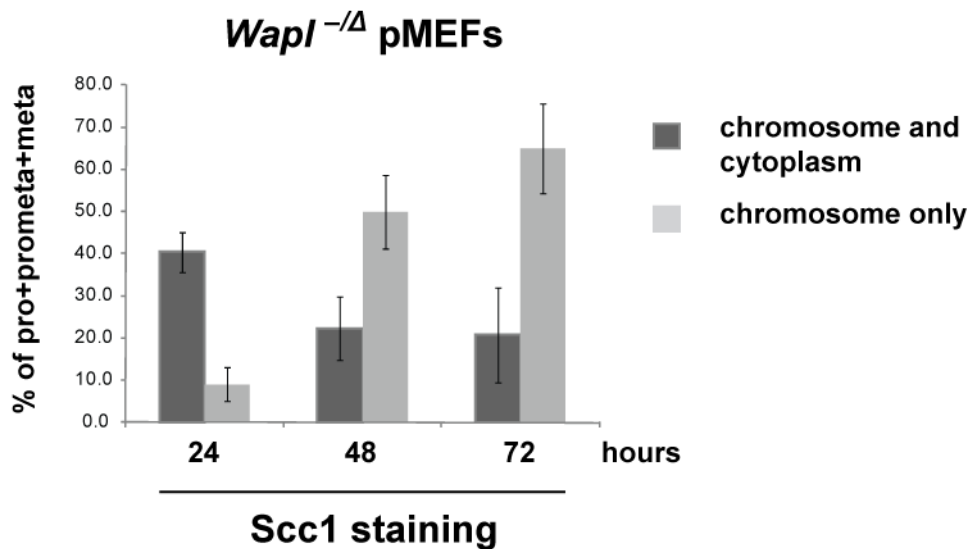


Figure 10: *Wapl* regulates the dissociation of cohesin from prophase to metaphase

Wapl^{-/ Δ} prophase (pro), prometaphase (prometa) and metaphase (meta) cells in Figure 9 were classified according to Scc1 localization. Quantitative results were obtained from three experiments (n>150 for cell type and each time-point).

Only few mitotic cells could be found in *Wapl* knockout cultures from 72-120 hours, thus not allowing a statistical analysis. When I pre-extracted the cells with detergent to remove the soluble cohesin pool before paraformaldehyde fixation, I could still observe a high amount of cohesin co-localizing with the DNA signal, suggesting that cohesin is stably bound to chromosomes after *Wapl* inactivation (data not shown; only few mitotic cells could be recovered because pMEFs detach easily from coverslips during treatment with the detergent that was used for pre-extraction). Importantly, in control *Wapl*^{+/ Δ} cells and in *Wapl*^{-/ F} cells not treated with 4-OHT, the Scc1 signal was never found localizing along the chromosomes as in *Wapl* knockout cells (data not shown). Similar results were obtained using antibodies against Smc3 (Figure 11A and 11D) and SA1/2 (Figure 11B and 11C).

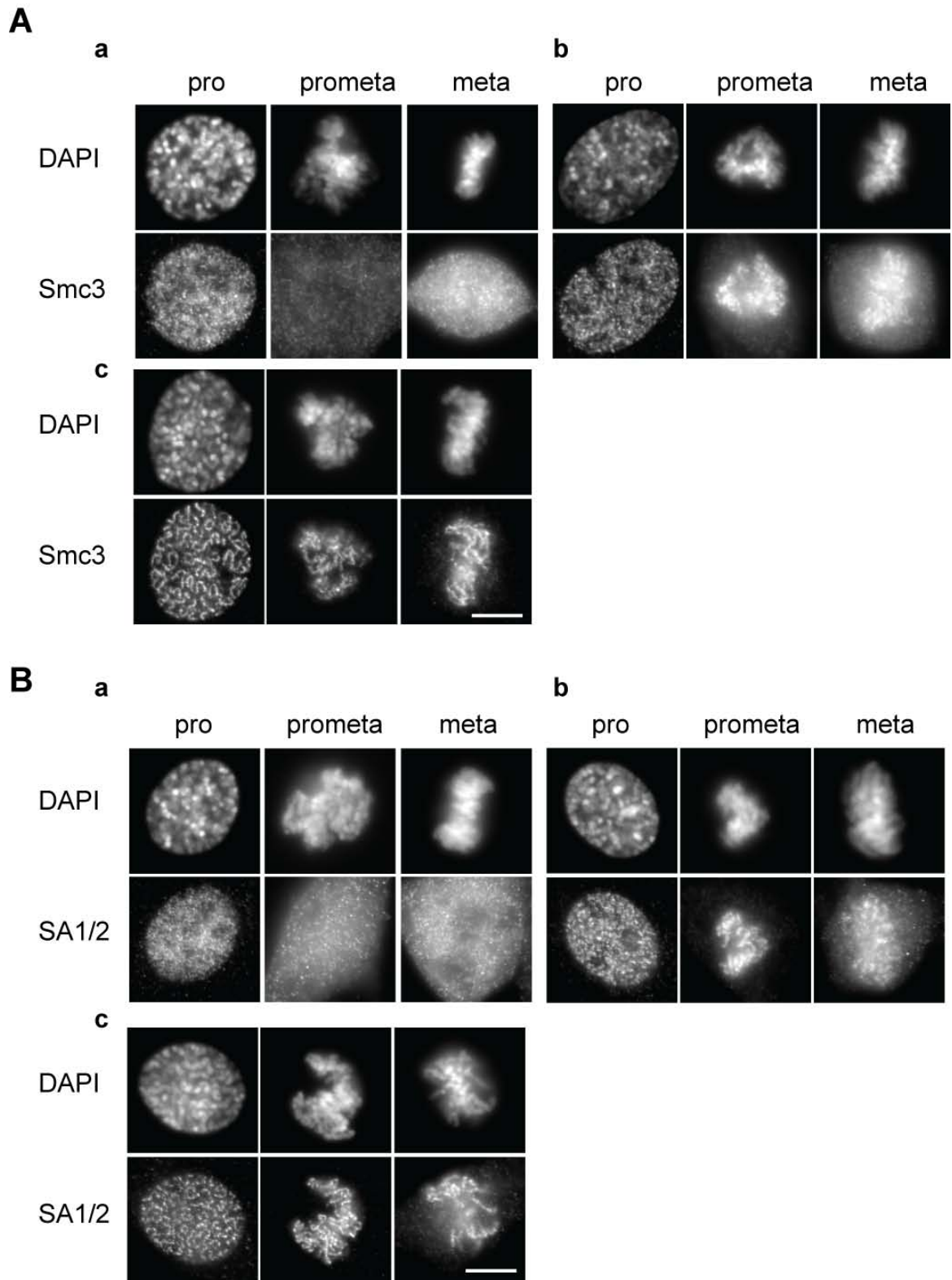


Figure 11: Wapl regulates the dissociation of cohesin from prophase to metaphase

(A) Smc3 staining: a) control *Wapl*^{+Δ} cells 72 hours after G0 release; b) *Wapl*^{-Δ} cells 24 hours after G0 release; c) *Wapl*^{-Δ} cells 72 hours after G0 release;

(B) SA1/2 staining: a) control *Wapl*^{+Δ} cells 72 hours after G0 release; b) *Wapl*^{-Δ} cells 24 hours after G0 release; c) *Wapl*^{-Δ} cells 72 hours after G0 release; Bar, 10 μm.

I concluded that *Wapl* depletion severely affects dissociation of cohesin from prophase to metaphase in pMEFs. The previously observed partial removal of cohesin from metaphase chromosomes in HeLa cells transfected with *Wapl* siRNA (Kueng et al., 2006) may therefore have been due to residual amount of *Wapl*.

2.6 *Wapl* is required for proper chromosome segregation but not for cohesin removal at the metaphase-anaphase transition

I next wanted to know if the failure of cohesin removal in *Wapl* deficient cells affects mitotic progression. Mitotic stages were classified according to DNA morphology and H3S10ph staining (Figure 9). At every time-point analyzed, I found a slight increase of prophase cells in *Wapl*^{-Δ} cultures, statistically significant at 72 hours, compared to control cells (Figure 12A). However, comparable percentages of anaphases and telophases were found in both control and *Wapl* knockout cultures (Figure 12A). *Wapl* depletion therefore delays cells in prophase but does not affect progression into anaphase, consistent with RNAi experiments (Kueng et al., 2006). We also observed that in *Wapl*^{-Δ} anaphases the bulk of cohesin was excluded from chromosomes, a situation remarkably different from metaphase (compare metaphase and anaphase in Figures 9B and C). Taken together, these observations suggest that *Wapl* knockout cells delay in early mitosis but they progress into

anaphase removing the bulk of cohesin from chromosomes.

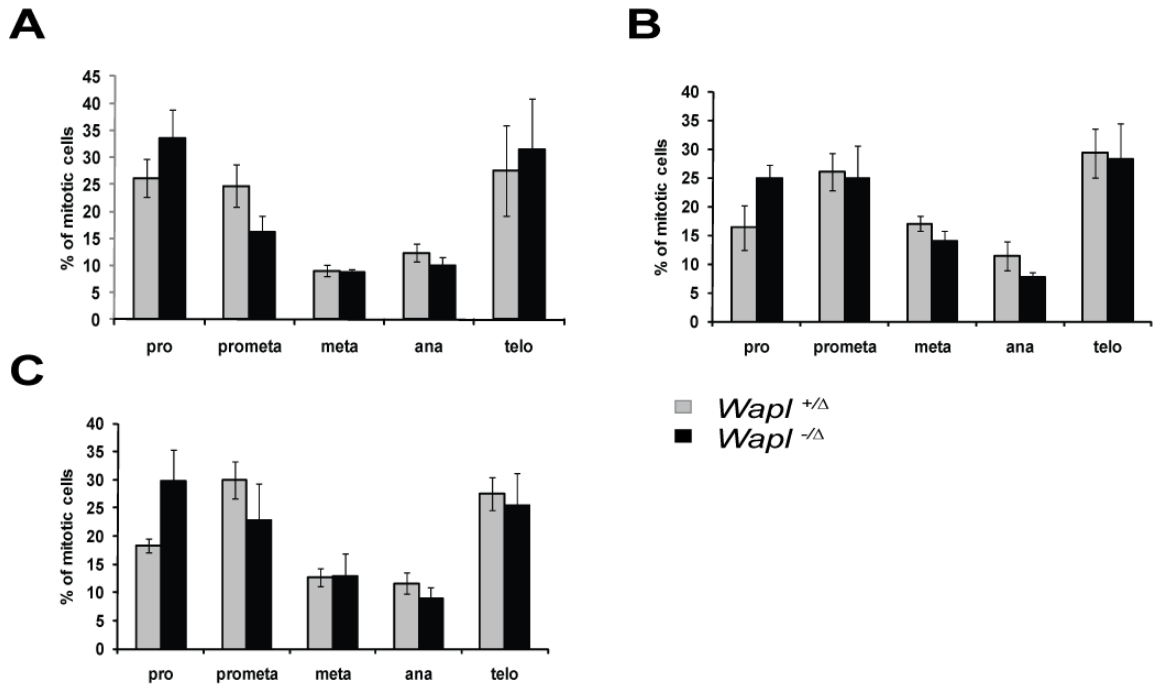


Figure 12: Mitotic progression

Mitotic cell stages were defined according to DNA morphology and H3S10ph staining (figure 9) in control *Wapl*^{+Δ} and *Wapl*^{-Δ} cultures at: A) 24 hours from G0 release; B) 48 hours from G0 release and C) 72 hours from G0 release (pro: prophase; prometa: prometaphase; meta: metaphase; ana: anaphase; telo: telophase). 3000 interphase cells per cell type and time-point were scored.

Previous studies in cultured HeLa cells showed that *Wapl* depletion by RNAi did not affect chromosome segregation during mitosis (Gandhi et al., 2006; Kueng et al., 2006). I then looked at chromosome segregation in *Wapl*^{-Δ} anaphases. Most control cells showed normal chromosome segregation in anaphase and telophase, with the two main chromosome sets pulled apart to opposite poles (Figure 9). Surprisingly, most *Wapl*^{-Δ} anaphases and telophases were abnormal with fine chromosome bridges between the two main chromosome sets (Figure 13B).

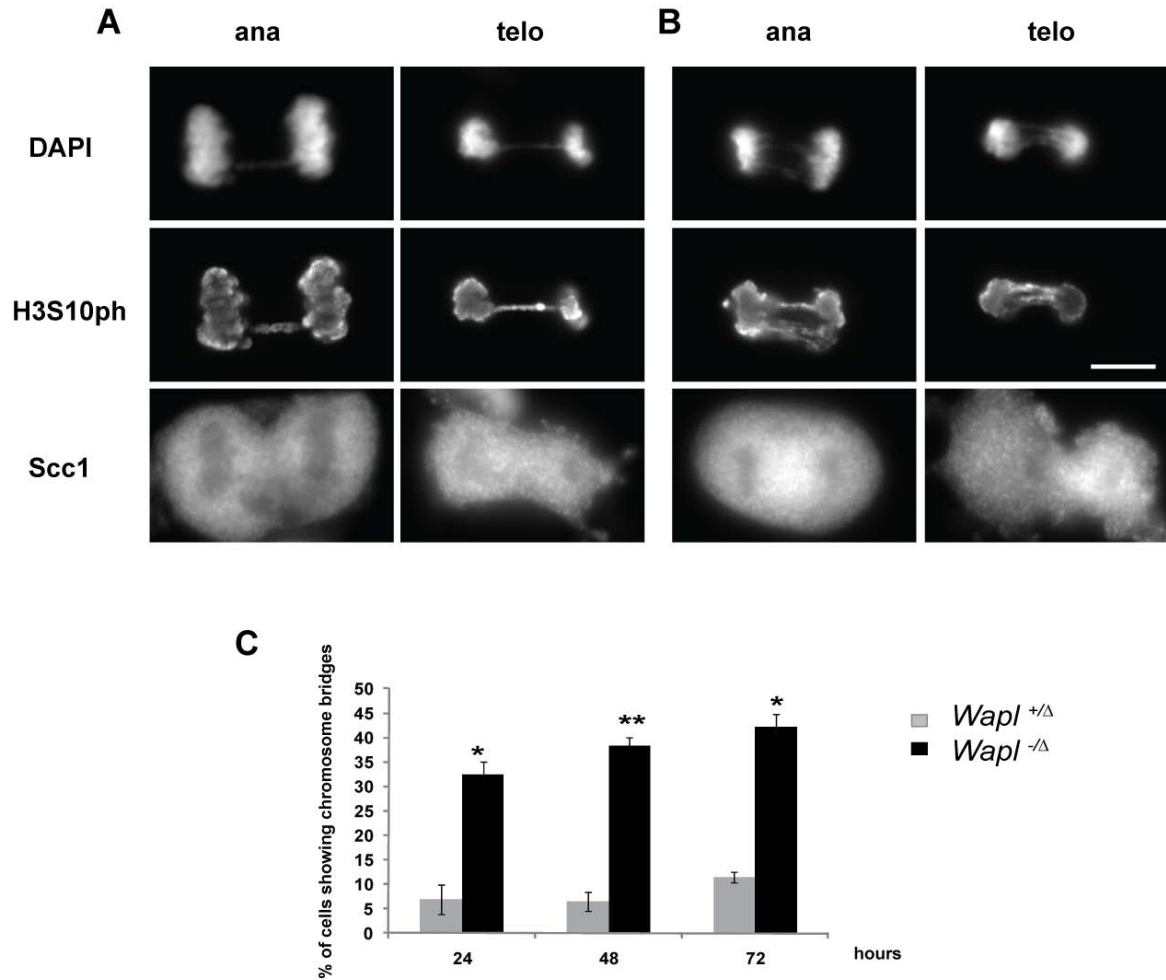


Figure 13: Wapl is required for proper chromosome segregation

(A) Shown are anaphase and telophase cells (stained as in figure 9) with chromosome bridges from A) control *Wapl*^{+Δ} cultures and B) *Wapl*^{-Δ} cultures;

(B) Chromosome bridges were scored in *Wapl*^{+Δ} and *Wapl*^{-Δ} cultures. Quantitative results were obtained from three experiments. More than 90 cells were scored for each time-point and cell type. Significant (*) ($P < 0.01$) or (**) highly significant ($P < 0.001$) differences between control and *Wapl*^{-Δ} cultures were evaluated using the Student's T-test. Bar, 10 μ m.

Also in these abnormal anaphases the bulk of cohesin was removed from chromosomes, although I cannot exclude the possibility that small amounts of cohesin were still present on the chromosome bridges. Some chromosome bridges were also observed in control cells but at lower frequency (Figure 13C) and these bridges were typically thinner than those in *Wapl* deficient cells (compare abnormal anaphases from control cultures in Figure 13A with abnormal anaphases from *Wapl* knockout cultures in Figure 13B). The

chromosome bridges in control *Wapl*^{+/ Δ} anaphases were possible the result of unspecific recombination mediated by the Cre enzyme because they were not observed in *Wapl*^{+/ F} cells not treated with 4-OHT (data not shown). In order to monitor the activity of the Cre-ER^{T2} enzyme in control *Wapl*^{+/ F} cells I confirmed by PCR the appearance of the Δ allele after 4-OHT treatment (data not shown). *Wapl*^{-/ Δ} abnormal anaphases increased over time (figure 13C) and concomitantly the chromosome bridges became more severe: at 72 hours almost 50% of abnormal cells showed two or more chromosome bridges compared to 20% at 24 hours. In addition, I observed a significant increase over time in the number of binucleated interphase cells in *Wapl*^{-/ Δ} cultures (Figure 14). At 24 hours, when cells showed to enter the first mitosis, control and *Wapl* knockout cultures still contained comparable numbers of binucleated cells but at later time-points significantly more binucleated cells were found in *Wapl*^{-/ Δ} than in *Wapl*^{+/ Δ} cultures (Figure 14B). This suggests that the binucleated cells in *Wapl* knockout cultures were the consequence of abnormal mitotic divisions. In most binucleated *Wapl* knockout cells the two nuclei were located next to each other (Figure 14A, upper panel ii) but in many cases it was possible to observe a single chromosome bridge connecting the two nuclei (Figure 14A, lower panel iii and iv). These observations indicate

that Wapl is essential for proper chromosome segregation in pMEFs.

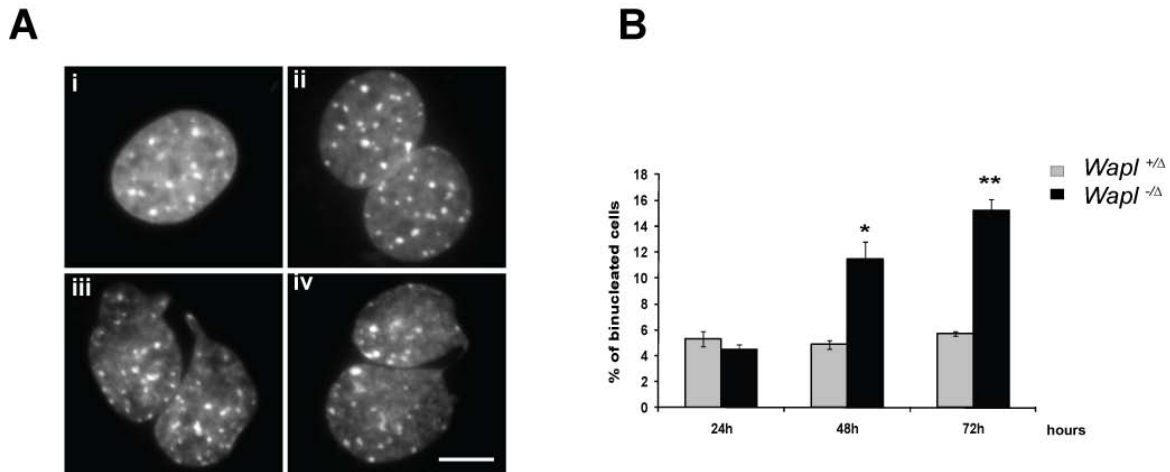


Figure 14: Wapl is required for proper chromosome segregation

(A) Shown are examples of normal interphase cells (DNA stained with DAPI) from control culture (i) or binucleated cells common to control and *Wapl*^{-Δ} cultures (ii) or binucleated cells found only in *Wapl*^{-Δ} cultures (iii, iv).

(B) The graph shows the percentage of binucleated cells. 3000 interphase cells per cell type and time-point have been scored. Significant ($P < 0.01$) or (**) highly significant ($P < 0.001$) differences between control and *Wapl*^{-Δ} cultures were evaluated using the Student's T-test test. Bar, 10 μ m.

2.7 Separase is required to remove cohesin at the metaphase-anaphase transition in Wapl knockout primary embryonic fibroblasts

I speculated that the excess of cohesin in *Wapl* knockout cells was removed from the chromosomes by Separase at the metaphase-anaphase transition. To address this issue I decided to cross *Wapl* cko mice with *Separase* cko mice (Wirth et al., 2006). I then isolated *Wapl*^{-F} *Separase*^{-F} *R26cre-ER*^{T2} pMEFs. It has previously been shown that Separase inactivation in MEFs prevents cohesin removal from centromeres and sister chromatids separation in anaphase (Kumada et al., 2006; Wirth et al., 2006). After one DNA replication cycle in the absence of Separase, spreads of mitotic chromosomes show diplochromosomes, in which two sets of sister chromatids remain

attached at their centromeres but resolved along the arms. I then analyzed the morphology of mitotic chromosomes from *Wapl Separase* double knockout cells and from control cells by spreading and Giemsa staining, 48 hours after AdCre infection (the same conditions described in Figure 3 were followed). Following infection with AdCre, 88% of control wild-type cells showed completely or partially resolved sister chromatids, a small percentage (4%) of cells with unresolved arms and no cells with diplochromosomes (Figure 15). In *Separase* knockout cells, 19% showed diplochromosomes and only 1% of cells contained unresolved arms (Figure 15). In contrast, 75% of all *Wapl* knockout cells contained chromosomes with unresolved arms, and no cells with diplochromosomes were observed (Figure 15). However, when double *Wapl Separase* knockout cells were observed, 46% showed diplochromosomes with unresolved arms, i.e. a combination of *Wapl* and *Separase* knockout phenotypes (Figure 15). I also found that 26% of the cells contained unresolved arms only and that 9% of cells contained only diplochromosomes (Figure 15). An explanation for the higher percentage of diplochromosomes in the double knockout compared to the single *Separase* knockout could be that *Wapl* is required to remove some cohesin from the centromeres, or in the proximity of centromeres, during mitosis. Therefore in those cells where *Separase* is only partially depleted *Wapl* inactivation could enhance defects in sister chromatid separation. I also observed in the double *Wapl Separase* knockout, very rarely, quadruplochromosomes, which are the result of two rounds of DNA replication in the absence of *Separase*, with unresolved chromosome arms (Figure 15A, last panel).

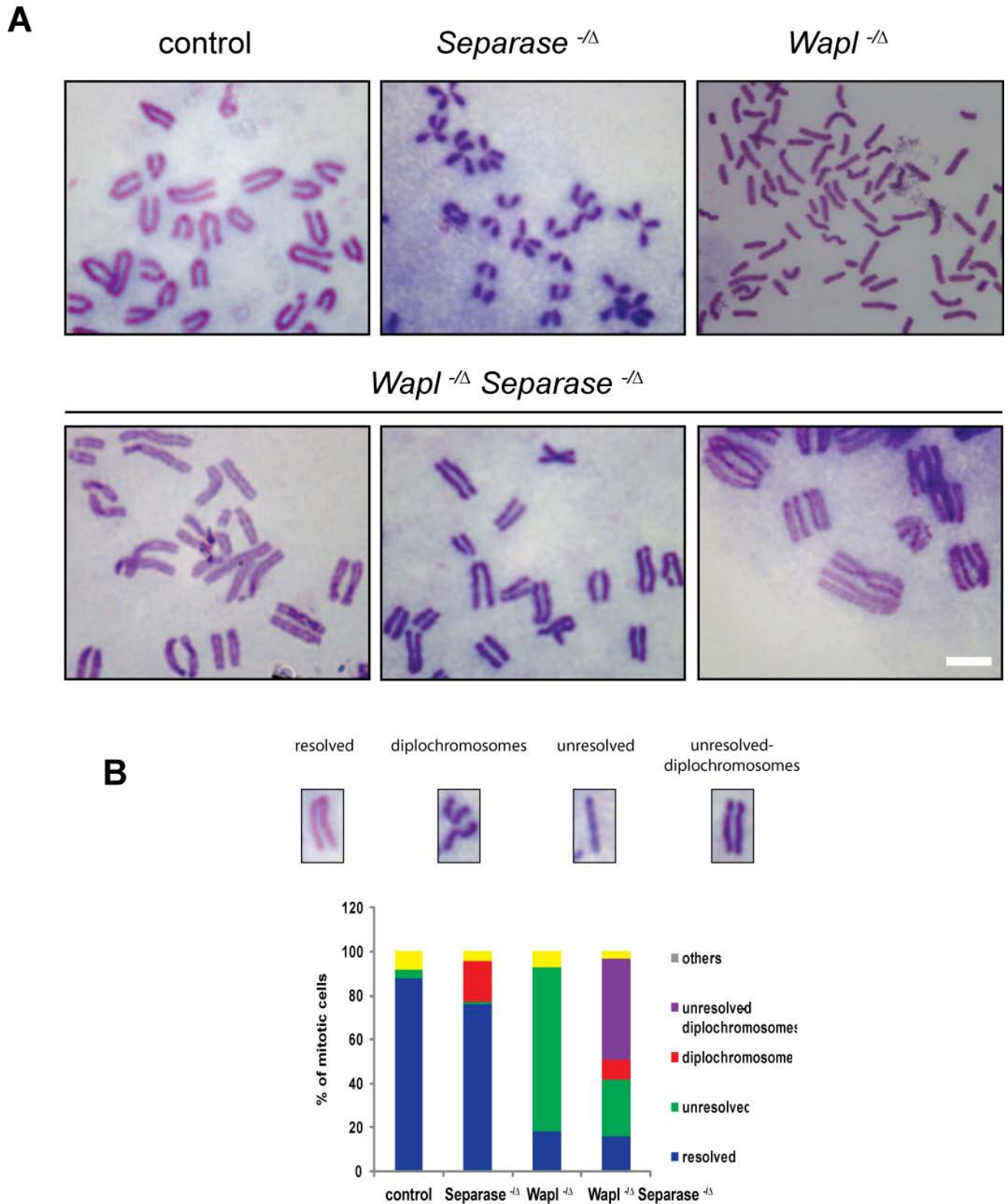


Figure 15: Chromosome morphology in *Wapl* *Separase* knockout prometaphases
 (A) Prometaphase chromosomes from control wild-type, *Separase*^{-Δ}, *Wapl*^{-Δ} or *Wapl*^{-Δ} *Separase*^{-Δ} pMEFs were analyzed by spread and Giemsa staining;
 (B) Prometaphases obtained as in (A) were classified according to their chromosome morphology (n=100). Bar, 5 μm.

These results confirm that the prophase pathway and the Separase pathway are distinct in their functions (Hauf et al., 2001; Waizenegger et al., 2000): the first is required for cohesin dissociation from chromosomes arms and the second for cohesin removal from centromeres.

Although Separase is required for sister chromatids separation in anaphase, it is dispensable for mitotic exit and cytokinesis (Kumada et al., 2006; Wirth et al., 2006). *Separase* knockout cultures show an increase of cells with metaphase chromosome morphology according to DNA morphology. However it has been shown that many of these metaphases are lacking cyclin B1, indicating that the APC/C had been activated and the cells had exited mitosis. Many of these metaphase-like cells later decondense their chromosomes and give rise to interphase cells with double the normal content of DNA. I next analyzed *Wapl Separase* knockout mitotic cells by immunofluorescence microscopy. For this purpose I inactivated Wapl and Separase using 4-OHT according to the scheme in figure 8A and analyzed the cells 36 and 48 hours after G0 starvation. According to DAPI and H3S10ph staining I found an increase of metaphase cells in *Separase*^{-Δ} cultures, as expected, and in *Wapl*^{-Δ} *Separase*^{-Δ} cultures compared to control wt and *Wapl*^{-Δ} cultures (data not shown). In order to analyze if these cells are in metaphase or represent cells that have entered an anaphase-like state without having been able to segregate sister chromatids, I stained them with DAPI and with antibodies against Scc1 and Aurora B. Aurora B normally relocates from the centromeres in metaphase to the midzone in anaphase. However, in *Separase* knockout cells, which exit mitosis without separating sister chromatids, Aurora B staining appears diffuse in the cytoplasm, likely because

the midzone has not been formed, or Aurora B is enriched in the cortical region of the ingressing cleavage furrow (Wirth et al., 2006). In a control culture all metaphases analyzed (classified according to DNA morphology), showed an Aurora B signal that co-localized with the chromosomes, mainly at the centromeric regions, while Scc1 signal was located in the cytoplasm (Figure 16). As previously reported, in *Separase*^{-Δ} cultures many metaphases showed Aurora B as well as Scc1 staining in the cytoplasm (Figure 16A; 26% of metaphases at 36 hours and 30% at 48 hours, see Figures 16B,C). In *Wapl*^{-Δ} metaphases I observed many metaphases with Aurora B and Scc1 signal localizing on the chromosomes, in agreement with my previous observations (Figure 16A; 74% of metaphases at 36 hours and 78 % at 48 hours, see Figures 16B, C). Strikingly, only in *Wapl*^{-Δ} *Separase*^{-Δ} metaphases I found cells with Aurora B staining in the cytoplasm and a strong Scc1 signal on the chromosomes (Figure 16A; 40% of metaphases at 36 hours and 43 % at 48 hours, see Figure 16B,C). These data suggest that *Wapl* *Separase* double knockout cells enter an anaphase-like state in which sister chromatids cannot be separated due the absence of *Separase*, and in which cohesin also persists on chromosomes arms, due to the absence of *Wapl*.

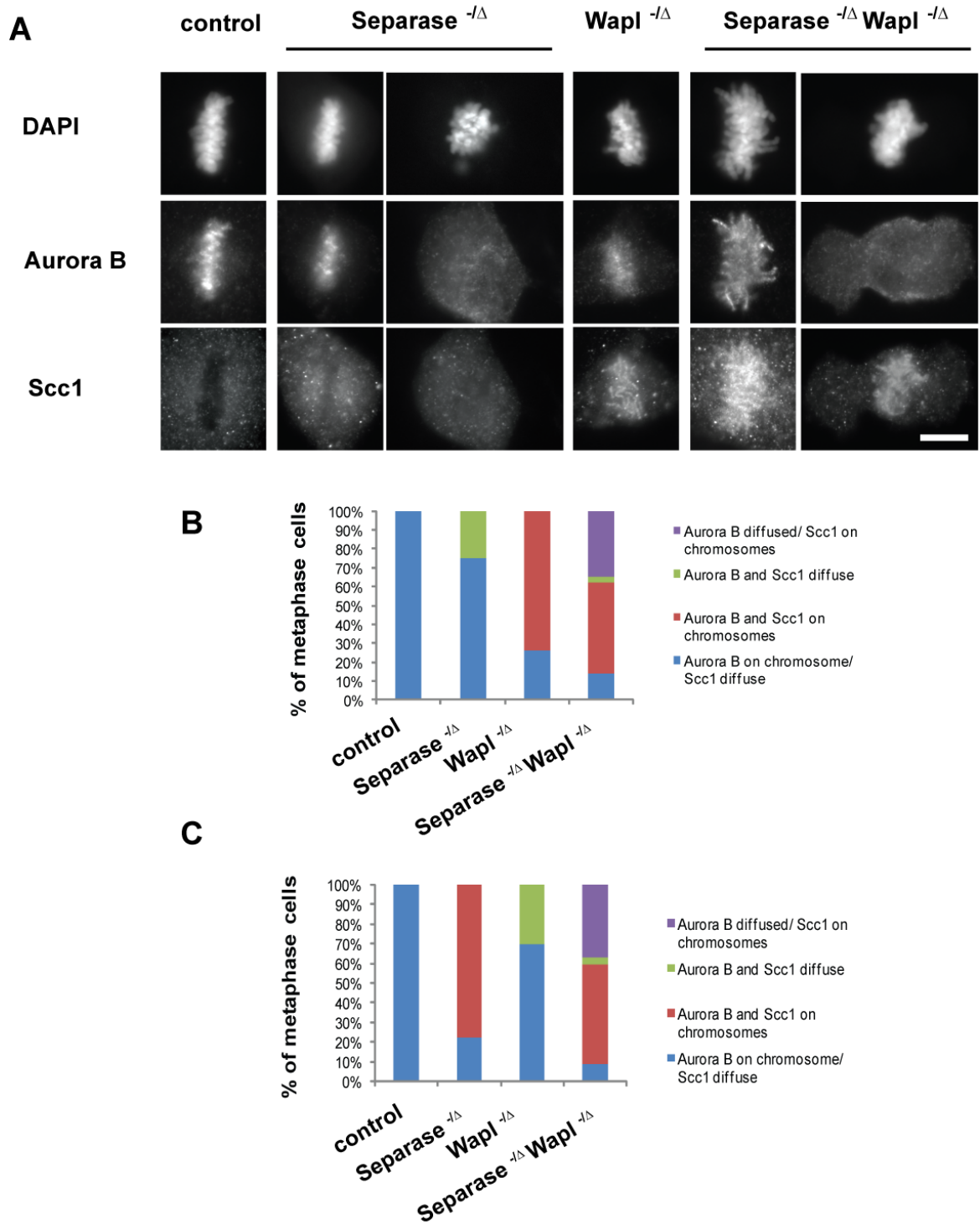


Figure 16: Analysis of *Wapl* *Separase* knockout pMEFs

(A) Control wild-type, *Separase*^{-Δ}, *Wapl*^{-Δ} or *Wapl*^{-Δ} *Separase*^{-Δ} pMEFs were cultured as in (8A). On day 5 the cultures were expanded, the 4-OHT removed, and the cells analyzed by immunofluorescence at 36 and 48 hours after G0 release. Immunostaining was performed using anti-Aurora B and anti-Sccl antibodies. DNA was stained with DAPI. Metaphase cells, classified according to DNA morphology, are shown. Bar, 10 μm.

(B) Metaphase cells in (A) are classified according to Aurora B and Sccl localization 36 hours and

(C) 48 hours after Go release (n=100)

2.8 Partial Scc1 depletion rescues the chromosome segregation defects in Wapl knockout primary embryonic fibroblasts

To test if chromosome bridges in *Wapl* knockout cells are caused by an excess of cohesin on chromosomes, I decided to partially deplete cohesin by RNA interference (RNAi) and ask whether chromosome segregation defects can be decreased. To this end, I deleted *Wapl* according to the scheme in Figure 17A, and 12 hours after release from G0 starvation I transfected *Wapl* knockout cells either with a control GL2 siRNA or with an Scc1 siRNA. Different Scc1 siRNA concentrations (10 nM, 50 nM and 100 nM) were used to find conditions that allow only a partial depletion of the Scc1 protein. I wanted to deplete cohesin only partially because complete loss of cohesin could cause defects in cohesion, DNA damage repair and gene regulation that could interfere with cell cycle progression. Cells were harvested and analyzed by IFM at 36 hours and 48 hours after release from G0 starvation, i.e. 24 and 36 hours after siRNA transfection, respectively (Figure 17A). When I stained for Scc1 I could observe that in *Wapl*-depleted cells transfected with GL2 siRNA the Scc1 signal was as expected enriched on chromosomes at both time-points (control panel in Figure 17B and Figure 17C, D). However *Wapl* knockout cells transfected with Scc1 siRNA showed a reduced Scc1 signal on chromosomes compared to control cells (panel 50 nM in Figure 17B and Figure 17C, D). The Scc1 depletion by RNAi was time- and dose-dependent, and I observed that at 48 hours there were many cells in which no Scc1 could be detected, especially at the highest siRNA concentration of 100 nM (panel 100 nM in Figure 17B and Figure 17C, D).

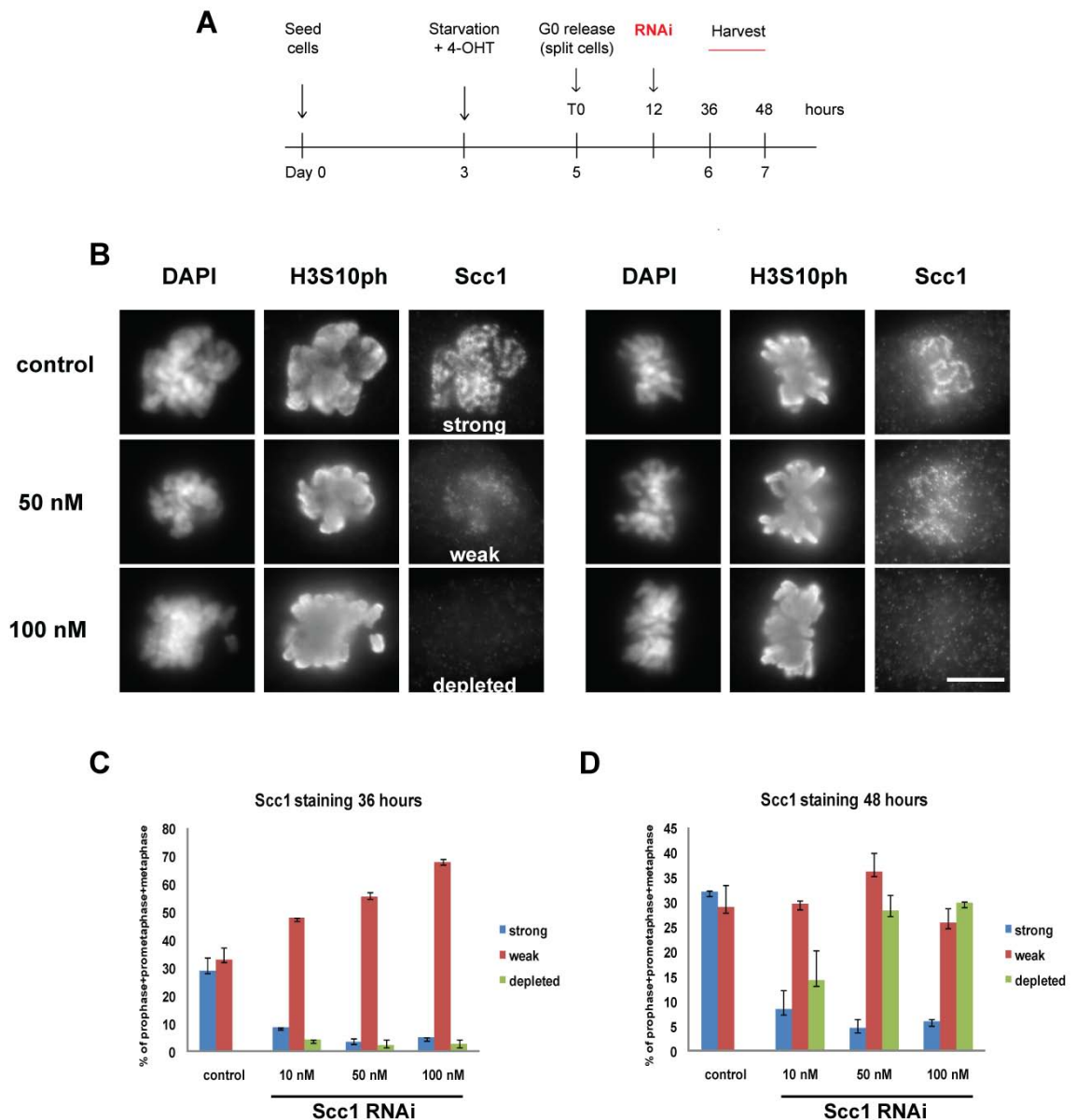


Figure 17 **Scc1** partial depletion reduces the chromosome segregation defects in *Wapl* knockout pMEFs

- (A) Schematic overview of *Wapl* inactivation combined with *Scc1* RNAi and harvesting time-points.
- (B) Shown are *Wapl*^{-/-} mitotic cells transfected with either 100 nM of GL2 siRNA (*control*) or 50 nM of *Scc1* siRNA (*50 nM*) or 100 nM of *Scc1* siRNA (*100 nM*). Immunostaining was performed using anti-H3S10ph and anti-*Scc1* antibodies. DNA was stained with DAPI. In the left panel prometaphases are shown; in the right panel metaphases are shown. Bar, 10 μ m.
- (C) Prophase, prometaphase and metaphase cells were classified according to *Scc1* staining (A) at 36 hours and
- (D) 48 hours after G0 release. More than 50 cells per cell type and time point have been scored from two experiments.

However, cultures transfected with Scc1 siRNA did not show any increase of mitotic index or accumulation of prometaphase cells (data not shown), suggesting that some cohesin was still present at the centromeres, even if it was not detectable by IFM. I conclude that I could partially deplete Scc1 in *Wapl* knockout cells.

I next analyzed control cultures and cultures treated with Scc1 siRNA for the presence of chromosome segregation defects by DAPI and H3S10ph staining. *Wapl* knockout cultures transfected with control siRNA showed a high incidence of chromosome bridges (Figure 18A, B). Strikingly, cultures transfected with Scc1 siRNA showed a significant reduction in the number of cells with chromosome bridges in anaphase and telophase (Figure 18A, B). These results are consistent with the hypothesis that the chromosome segregation defects in *Wapl* knockout cells are caused by defect in the prophase pathway.

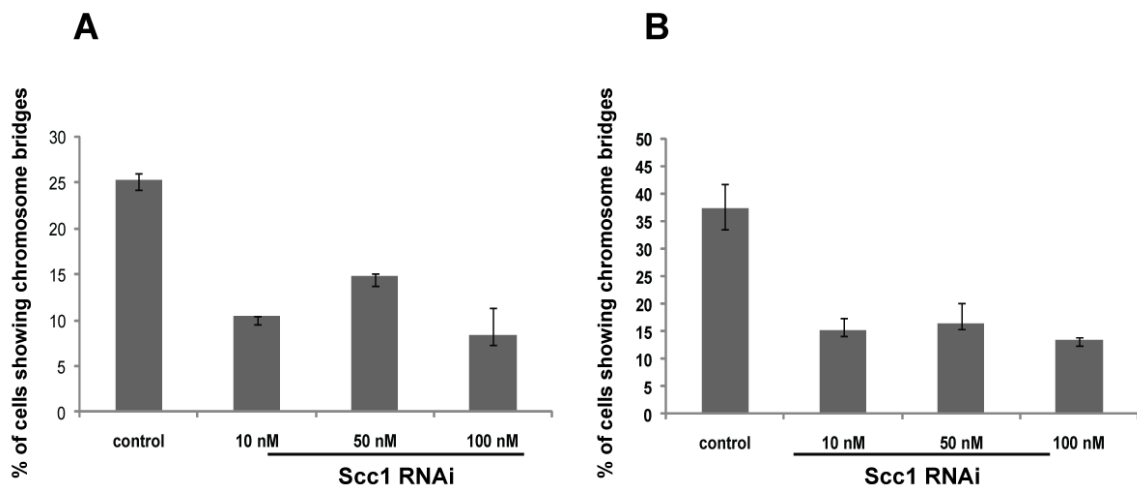


Figure 18: Scc1 partial depletion reduces the chromosome segregation defects in *Wapl* knockout primary embryonic fibroblasts

- (A) The percentage of cells showing chromosome bridges is shown at 36 hours and
- (B) 48 hours after G0 release. More than 50 cells per cell type and time point were scored from two experiments.

3. Wapl is required for cohesin dissociation from DNA and cell cycle progression during interphase

3.1 Cohesin axial structures in interphase Wapl knockout primary embryonic fibroblasts

FACS and immunofluorescence analysis showed that *Wapl* knockout cultures stopped proliferating and arrested in interphase (data not shown and Figure 8). Previous fluorescence recovery after photobleaching (FRAP) experiments indicated that Wapl knockdown by RNAi in HeLa cells increased the residence time of cohesin on chromatin during G2-phase (Kueng et al., 2006). Depletion of Wapl by RNAi also caused a modest increase of chromatin-bound cohesin during G2 phase (Kueng et al., 2006). Moreover, Wapl knockdown by RNAi delayed cell cycle progression (Kueng S and Peters JM, data not shown). I therefore decided to analyze cohesin localization by immunofluorescence in control *Wapl*^{+Δ} and *Wapl*^{-Δ} pMEFs obtained as in Figure 8A. The cells were fixed in 4% PFA and stained with DAPI and antibodies against the cohesin subunit Scc1 and Aurora B, which accumulates in the nucleus between late S phase and mitosis and therefore enables cells in G1 and early S phase (Aurora B negative) to be distinguished from cells in late S, G2 and prophase (Aurora B positive). As expected, control nuclei showed a diffused nucleoplasmic Scc1 staining, which was largely excluded from nucleoli and which did not differ between G1/early S and late S/G2 (Figure 19 Aa). In *Wapl*^{-Δ} cells, the Scc1 pattern was surprisingly different from that of the control (Figure 19Ab). The Scc1 signal was now mainly seen in highly elongated structures (Figure 19Ab).

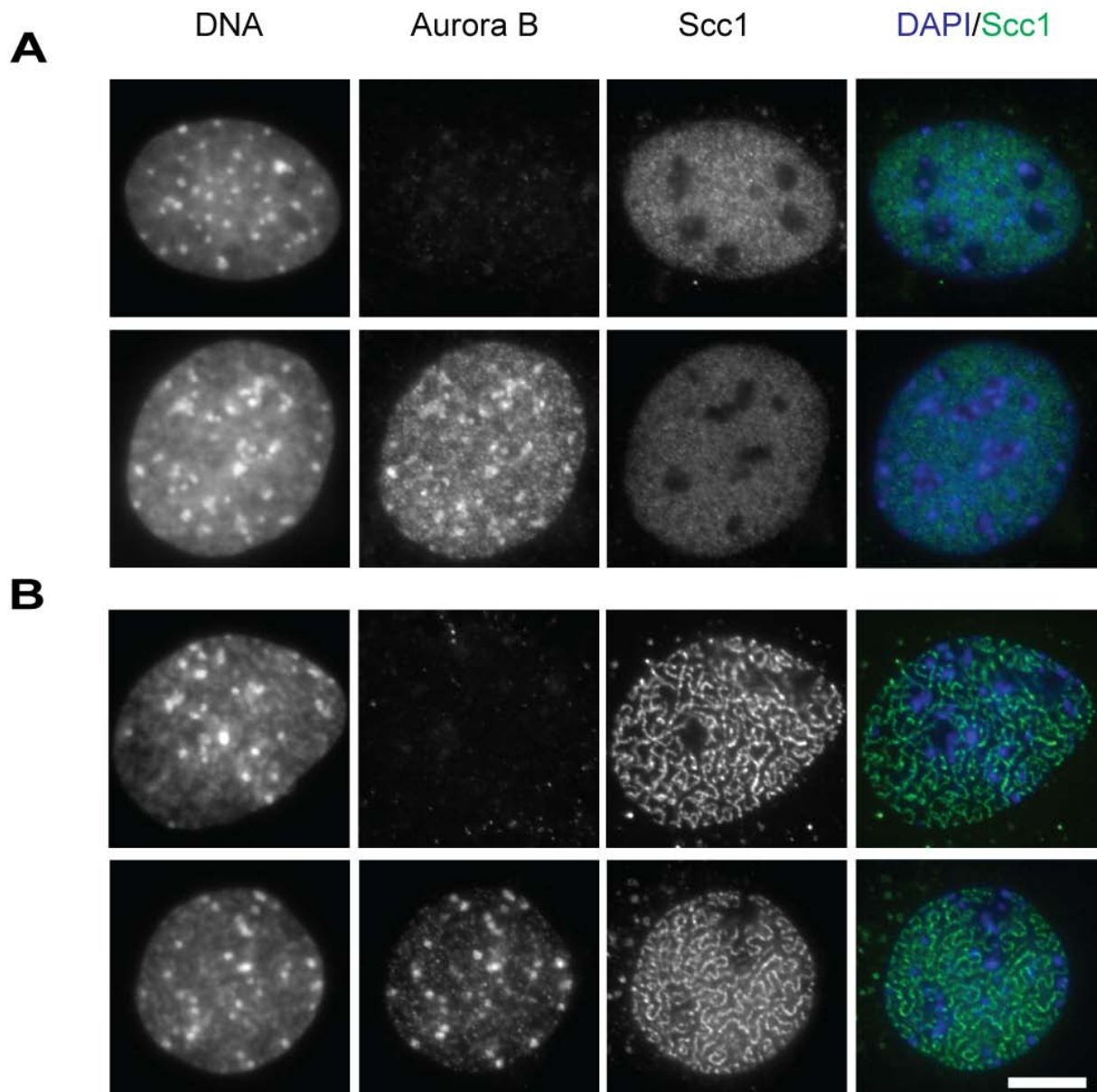


Figure 19: Cohesin vermicelli in *Wapl* knockout pMEFs

pMEFs were harvested at the time-points indicated in Figure 8A and fixed with paraformaldehyde (without pre-extraction). Immunostaining was performed using anti-Aurora B and anti-Scc1 antibodies. DNA was stained with DAPI.

- A) Scc1 staining pattern is shown in control *Wapl*^{+Δ} cells during G1/early S phase (upper panels, Aurora B negative staining) or in late S/G2 phase (lower panel, Aurora B positive staining);
- B) Scc1 staining pattern is shown in *Wapl*^{-Δ} cells during G1/early S phase (upper panels, Aurora B negative staining) or in late S/G2 phase (lower panel, Aurora B positive staining). Note that the Scc1 staining follows highly elongated structures in. I refer to those as cohesin vermicelli. Bar, 10 μm.

The shape of these structures resembled those of small worms. I therefore decided to call them “vermicelli”, after the Italian word for small worms. As judged by Aurora B staining the cohesin vermicelli appeared in both G1- early S and late

S-G2 cells (Figure 19Ab). The percentage of *Wapl*^{-Δ} cells with vermicelli increased dramatically from 4.3% at 24 hours to 79.1% at 120 hours (Figure 20). This correlated well with the efficiency of *Wapl* depletion: at the first time-points, when some *Wapl* protein was detectable by Western blotting (24 and 48 hours, Figure 8B), the incidence of the *vermicelli* phenotype was very low (Figure 20); when *Wapl* protein levels become undetectable (72 hours, Figure 8B) the vermicelli appeared at a higher frequency (Figure 20).

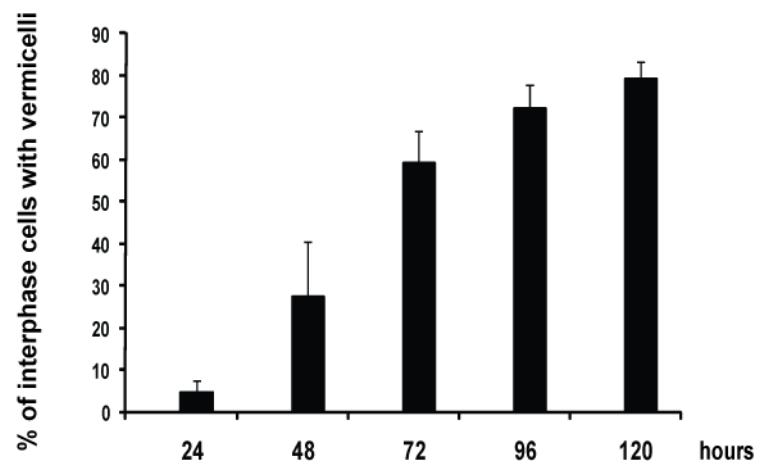


Figure 20: Cohesin vermicelli in *Wapl* knockout pMEFs

Plot showing the frequency of occurrence of the vermicelli phenotype in interphase *Wapl*^{-Δ} cells after G0 release (Figure 8A). A total of 1500 cells were scored for each time-point.

The vermicelli phenotype was never observed in control *Wapl*^{+Δ} cultures or in *Wapl*^{-F} cultures untreated with 4-OHT (data not shown). Similar results were obtained when I analyzed Smc3 and SA1/2 localization in pMEFs with or without removing the soluble cohesin pool by pre-extraction (Figure 21). Although the pre-extraction of interphase pMEFs with the detergent Triton X-100 caused the formation of nuclei with an irregular shape, it was possible to clearly distinguish the cohesin vermicelli in *Wapl*^{-Δ} cells (Figure 21Ac, d). Therefore in *Wapl*

knockout interphase pMEFs the cohesin pattern is dramatically changed.

A

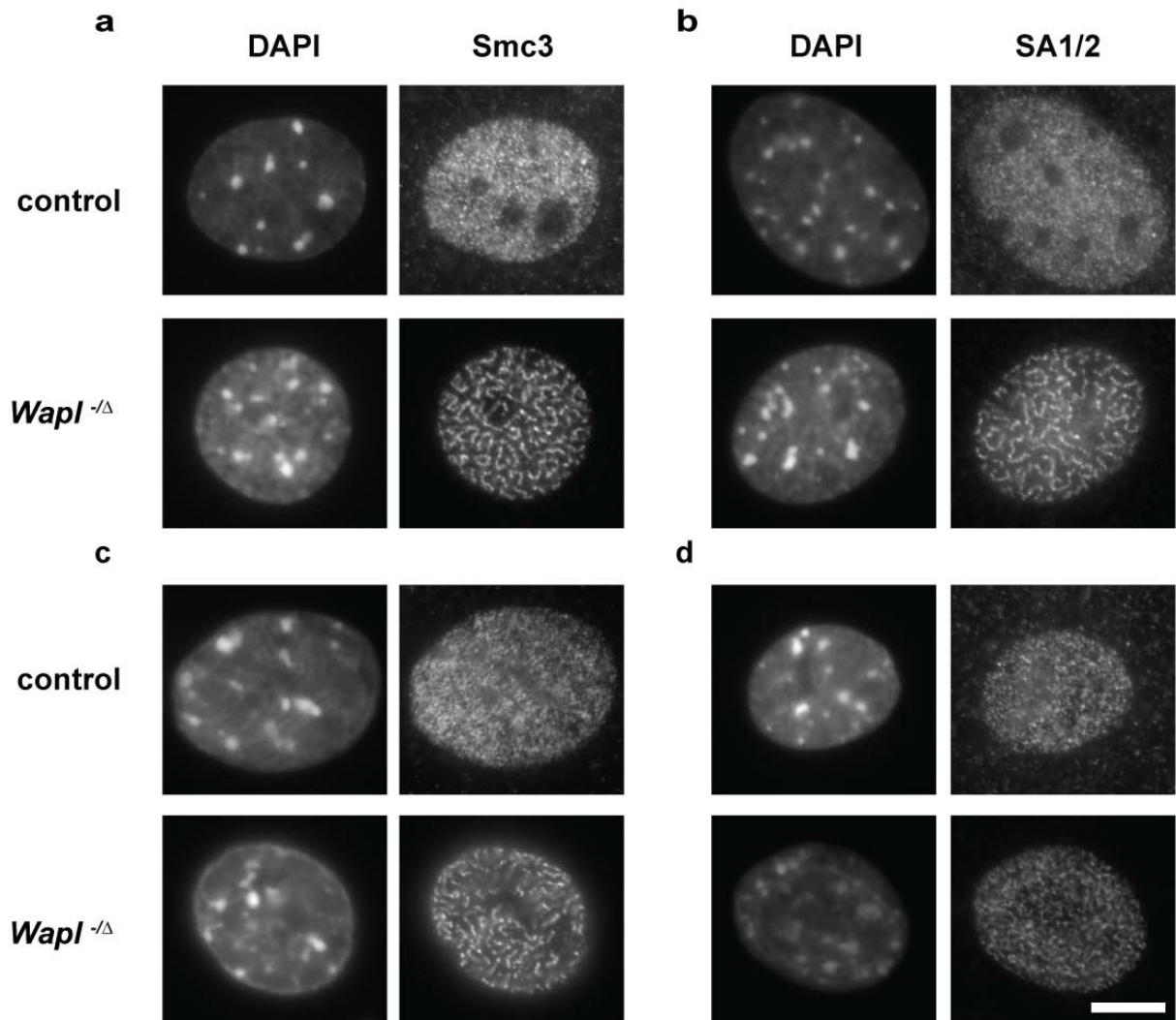


Figure 21: Cohesin vermicelli in *Wapl* knockout pMEFs

Examples of control *Wapl*^{+Δ} and *Wapl*^{-Δ} pMEFs stained with DAPI, to visualize the DNA, and with an antibody against the cohesin subunit Smc3 (a, c) or SA1/2 (b, d). The cells were harvested at 120 hours after G0 release (Figure 8A) and fixed directly with paraformaldehyde (a, b) or pre-extracted prior to fixation (c,d). Bar, 10 μm.

These observations show that cohesin localization is dramatically altered in interphase pMEFs lacking *Wapl*.

The cohesin *vermicelli* appeared reminiscent of axial structures in mitotic chromosomes that are formed by condensin complexes (Swedlow and Hirano, 2003). An intriguing possibility is that cohesin might form an axial structure in interphase chromosomes that is related to the condensin containing structure of

mitotic chromosomes. I therefore next asked whether a cohesin vermicello (i.e. a single worm-like structure) corresponded to one chromosome. Although I was so far unable to co-localize cohesin with centromeres and telomeres due to the lack of suitable antibodies, I made two informative observations. First, in mitotic *Wapl* knockout cells the cohesin staining appeared as a longitudinal axis from one end of each chromosome to the other (Figure 22A). This suggests that an interphase cohesin *vermicello* might also extend from telomere to telomere. Second, I mentioned above that in *Wapl Separase* knockout cells the bulk of cohesin cannot be removed at the metaphase-anaphase transition. However, these cells exit mitosis and decondense the DNA. When I observed these cells during mitotic exit in fixed samples, I could clearly see that each vermicello extended from telomere to telomere (Figure 22B). It is also interesting to note that each vermicello appears as a spiral during this stage (Figure 22B). These observations strongly support the hypothesis of one interphase chromosome containing one vermicello. The finding of the cohesin vermicelli was entirely unexpected because no such structures had been observed after RNAi-mediated depletion of *Wapl* (Gandhi et al., 2006; Kueng et al., 2006), possibly due to incomplete removal of *Wapl*. The formation of cohesin vermicelli after *Wapl* depletion suggests that *Wapl* might have a fundamental function in regulating cohesin-chromatin associations during interphase, and suggests that cohesin may play a role in global genome architecture.

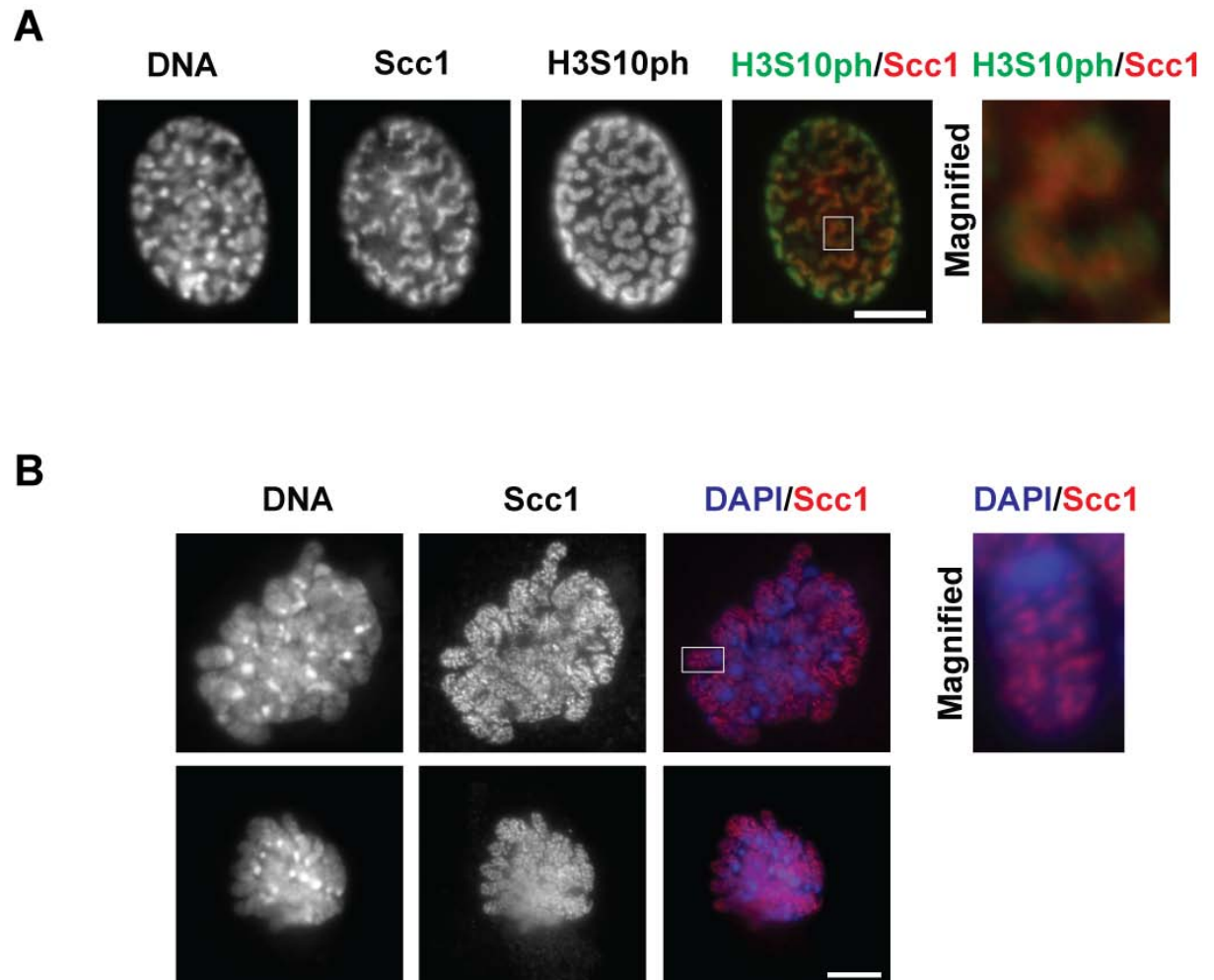


Figure 22: A cohesin vermicello might extend from the centromere to the telomere of a single chromosome

- (A) *Wapl*^{-Δ} pMEFs in prophase. Immunostaining was performed using anti-H3S10ph and anti-Scc1 antibodies. DNA was stained with DAPI. The chromosome selected in the merge picture H3S10ph/Scc1 is shown magnified on the side (magnified).
- (B) Examples of *Wapl*^{-Δ} *Separase*^{-Δ} pMEFs exiting from mitosis. Immunostaining was performed using an anti-Scc1 antibody, and DNA was stained with DAPI. The chromosome selected in the DNA/Scc1 merged picture is shown magnified on the side (magnified). Bars, 10 μm.

3.2 *Wapl* regulates the amount of chromatin-bound cohesin in interphase primary fibroblasts

The observation that the cohesin vermicelli were never found in control pMEFs raised the question of how *Wapl* inactivation resulted in their formation. It is

possible that the vermicelli are present also in pMEFs expressing Wapl but they cannot be visualized because cohesin binds dynamically to the DNA. A previous report showed that Wapl regulates the residence time of cohesin on DNA during interphase (Kueng et al., 2006). The cohesin vermicelli could then be explained with an increase of chromatin-bound cohesin after Wapl inactivation. Such an increase of chromatin-bound cohesin would make it possible to visualize the vermicelli by IFM. In order to test this possibility I compared chromatin-bound cohesin levels in control and *Wapl* knockout cells by quantitative immunofluorescence (qIF, see Materials and Methods). I decided to perform this analysis at 120 hours after G0 release (Figure 22A) because this time-point displayed the highest percentage of cells with vermicelli (Figure 20). Control *Wapl*^{+/ Δ} and *Wapl*^{-/ Δ} cells were pre-extracted with Triton X-100, to remove the soluble cohesin pool, fixed in 4% PFA and stained with DAPI and antibodies against Scc1 and Aurora B. The latter was again used as a cell cycle marker. The Scc1 signal was then quantified in pre-extracted G1/early S cells because *Wapl* knockout cultures had a very low percentage of late S/G2 cells (data not shown). Strikingly, I found a two-fold increase in Scc1 signal intensity after Wapl inactivation compared to control cultures (Figure 22B). In contrast, previous Wapl RNAi experiments had only shown an increase in chromatin-bound cohesin of approximately 1.25 fold compared to control G2 cells (Kueng et al., 2006). I next asked if *Wapl* deletion induced an increase of total cohesin level which could theoretically also explain the previous result. Decreasing amounts of total cell extract from control and *Wapl* knockout cultures were loaded and immunoblotted with antibodies against alpha-tubulin, used as loading control, and the cohesin subunit

Smc1.

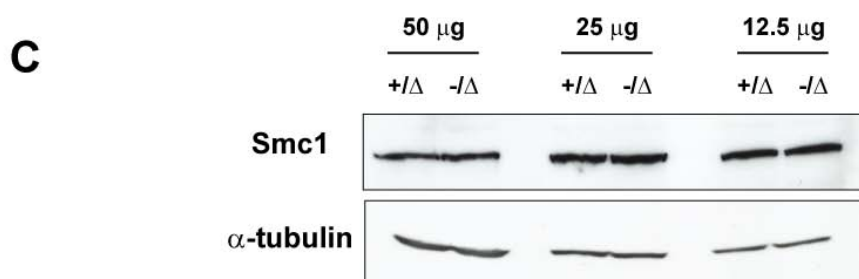
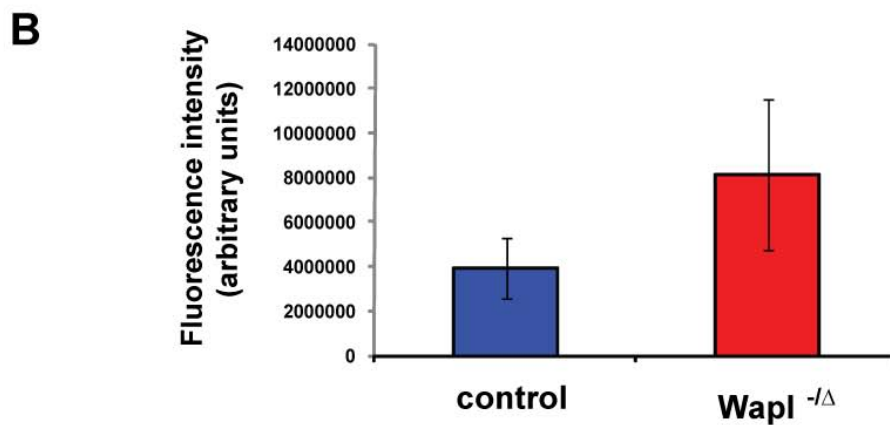
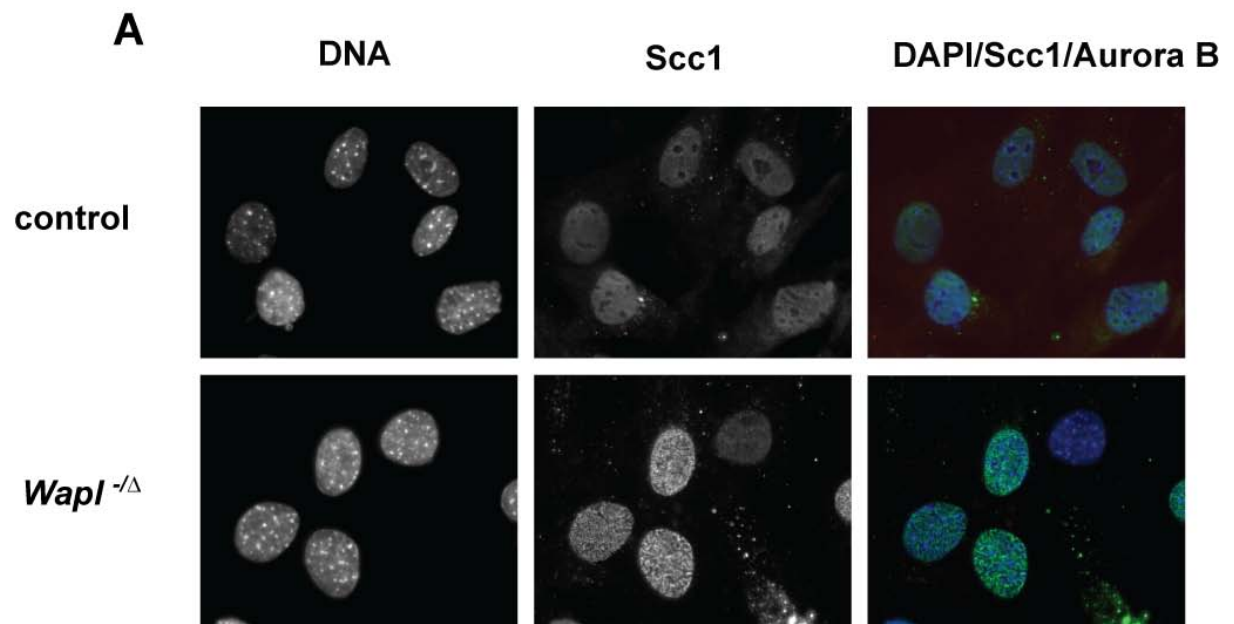


Figure 23: Increased amount of chromatin-bound cohesin in *Wapl* knockout pMEFs

- (A) Control *Wapl*^{+Δ} and *Wapl*^{-Δ} pMEFs were extracted with 0.1% Triton X-100 at 120 hours after G0 release (Figure 8A). The cells were stained for Sccl. DNA was stained with DAPI.
- (B) Sccl fluorescence intensities were quantified in cells obtained as in (A), using the ImageJ program. 25 cells per cell type were analyzed.
- (C) Western blots of control *Wapl*^{+Δ} pMEFs (+Δ) and *Wapl*^{-Δ} pMEFs (-Δ) probed to detect α-tubulin and Smc1. Total cell extracts were prepared from cultures harvested at 120 hours after G0 release (Figure 8A).

As shown in Figure 22C, no detectable differences were observed in Smc1 protein levels between control and *Wapl* depleted samples. *Wapl* deletion therefore caused a significant increase in cohesin binding to chromatin in interphase pMEFs. Based on FRAP experiments (Kueng et al., 2006) it is possible that this increase is caused by a defect in cohesin dissociation from DNA.

3.3 Identification of cohesin-binding sites in *Wapl* knockout primary fibroblasts

The cohesin-binding sites have been identified in the non-repetitive part of the entire human genome (Wendt et al., 2008) and in a small part (3%) of the mouse genome (Parelho et al., 2008). Because *Wapl* depletion caused an increase in cohesin on chromatin and allowed the visualization of axial vermicelli structures I then I tested whether the distribution of cohesin binding sites in the genome was changed in *Wapl* knockout pMEFs compared to control pMEFs. For this purpose, I performed Smc3 chromatin-immunoprecipitation (ChIP) experiments followed by Solexa-sequencing (Materials and Methods). I used *Wapl*^{+Δ} and *Wapl*^{-Δ} cultures at 120 hours after G0 release obtained as in Figure 8A. The *Wapl*^{-Δ} culture had a percentage of G1-early S cells (Aurora B negative cells) comparable to those in control *Wapl*^{+Δ} cultures (data not shown). Moreover, only the *Wapl*^{-Δ} cultures showed *vermicelli* (approximately 80% of the cells, data not shown). I identified 11,951 cohesin-binding sites in control *Wapl*^{+Δ} pMEFs.

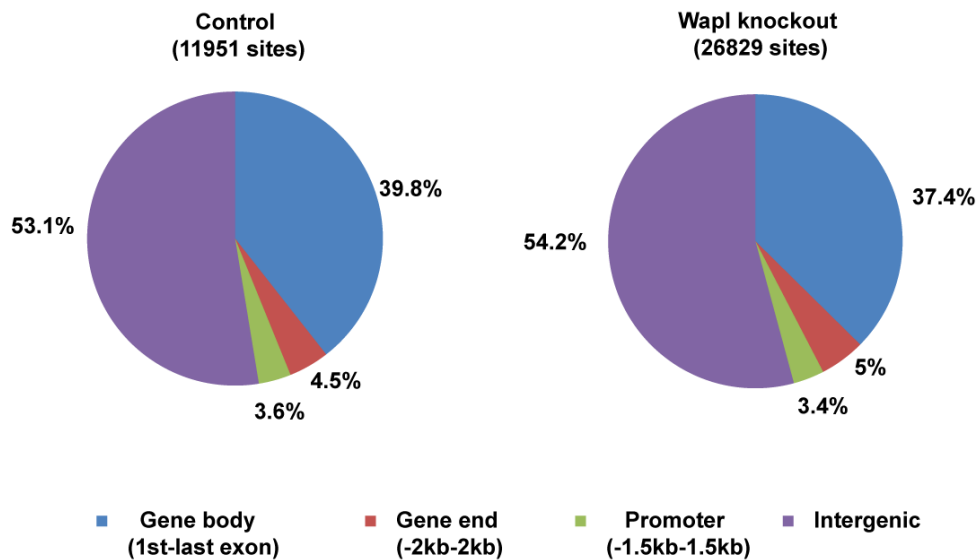


Figure 24: Distribution of cohesin binding sites within the mouse genome:

The Smc3 binding sites in control *Wapl*^{+Δ} pMEFs and *Wapl*^{-Δ} pMEFs were classified into four groups: gene body, gene end, promoter and intergenic.

This number is roughly similar to the 8,811 cohesin binding sites which have previously been identified by ChIP-chip experiments in the human genome (Wendt et al., 2008). The sites identified in control pMEFs are located in intergenic regions (53.1%), in gene bodies (38.8%), within 2 kb of gene ends (4.5%) or promoters (3.6%) (Figure 24). These results are also consistent with previously published data (Wendt et al., 2008). Moreover, I compared the cohesin-binding identified in this study with the published sites identified in 3% of the unique sequence content of the mouse genome (Parelho et al., 2008). I found that 23% of the sites I identified were also identified in mouse pre-B cells and 26% in mouse thymocytes indicating that our Smc3 ChIP-sequencing experiment identified bona fide cohesin-binding sites. When we analyzed *Wapl*^{-Δ} samples we found that the number of cohesin-binding sites dramatically increased from 11,951 to 26,829 (a 2.2-fold increase compared to control pMEFs). There were no obvious differences between *Wapl* deficient and expressing pMEFs with

respect to the distribution of cohesin binding sites in different genome region (Figure 24). I then asked how many sites were common between control *Wapl*^{+/ Δ} and *Wapl*^{-/ Δ} pMEFs. I found that *Wapl* knockout cells and control cells have 9,241 sites in common; 2770 sites were unique in the control; 17676 were unique in *Wapl* knockout cells. No major differences were observed in the genome distribution among these three classes of cohesin-binding sites.

A complete bioinformatics analysis of these data is still in progress, and furthermore I am planning to test the reproducibility of these results by repeating the ChIP-sequencing experiments. However, I made two interesting preliminary observations. First, when I compared common cohesin-binding sites I noticed that the peak-areas are greater after *Wapl* inactivation than in the control (Figure 25A). This suggests that there are not only more cohesin-binding sites after *Wapl* inactivation but that also more cohesin is bound to the sites that are also formed in control cells. Second, the comparison between my results and published results obtained using mouse pre-B cells and mouse thymocytes indicated that the distribution of the unique sites in *Wapl* knockout pMEFs is not random. Indeed I observed that many unique sites in *Wapl* knockout pMEFs are found also in mouse thymocytes or pre-B cells (Figure 25B). Taken together, these observations suggest that the number of potential cohesin binding sites in the mammalian genome is higher than previously reported. Moreover, the ability of cohesin to accumulate at these sites depends, at least in part, on *Wapl*.

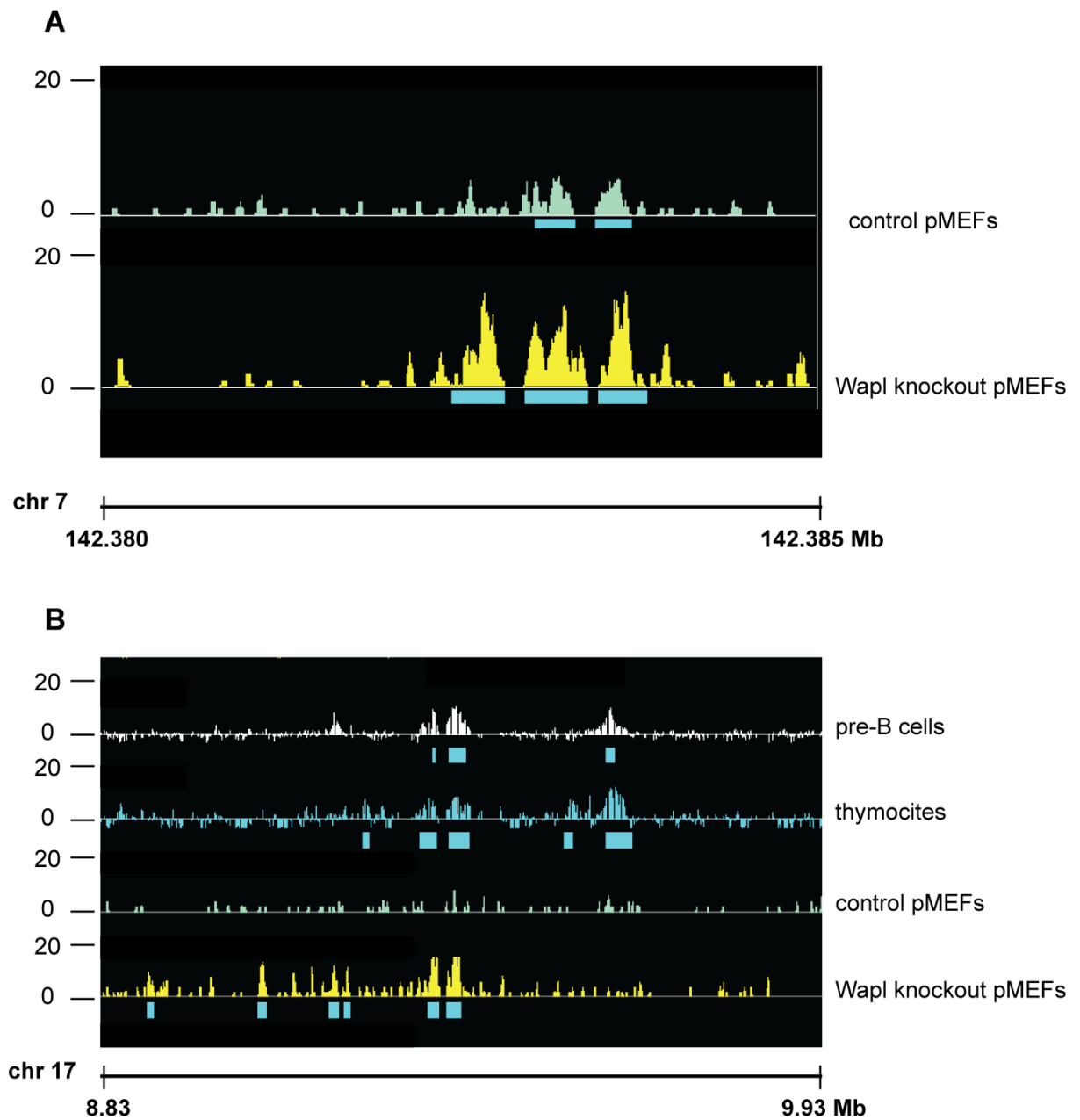


Figure 25: Identification of cohesin binding sites in the mouse genome by Chip-sequencing

- A) Comparison between cohesin binding sites in control *Wapl*^{+Δ} pMEFs and *Wapl*^{-Δ} pMEFs
 B) Comparison between cohesin binding sites in control *Wapl*^{+Δ} pMEFs, *Wapl*^{-Δ} pMEFs, pre-B cells and thymocytes. The data from pre-B cells and thymocytes were obtained by ChIP-chip (Parelho et al., 2008). Regions in which signals were significantly enriched are colored in light blue. The y axis displays tag density.

3.4 Wapl depletion causes partial condensation of chromatin in interphase primary embryonic fibroblasts

I noticed that in many cases the DNA, visualized by DAPI staining, appeared more condensed in interphase *Wapl* knockout pMEFs than in control cells (Figure 19, compare DNA in panel A with DNA in panel B). Although the DNA never appeared as condensed as in mitotic chromosomes, I could recognize axial chromatin structures that showed co-localization of the cohesin signal (Figure 19B). The cohesin complex is highly related to the condensin complex, which has been implicated in DNA condensation (Swedlow and Hirano, 2003). Moreover, cohesin and the insulator factor CTCF have been proposed to regulate gene expression through the formation of chromatin-loops (Hadjur et al., 2009; Mishiro et al., 2009; Nativio et al., 2009). I therefore considered the possibility that the high amount of cohesin in *Wapl* knockout pMEFs could induce an abnormal degree of chromatin condensation during interphase. In order to visualize chromatin structure in more detail, control and *Wapl* knockout cells were treated with an hypotonic solution before fixation followed by spreading and Giemsa staining (Figure 26). Both control *Wapl*^{+Δ} cultures and *Wapl*^{-Δ} cultures were harvested 120 hours after G0 release (Figure 8A). Very few mitotic cells can be observed at this time-point, and approximately 80% of cells in *Wapl*^{-Δ} cultures showed cohesin vermicelli (data not shown). Nuclei from the control culture were uniformly stained with Giemsa (Figure 26Aa and 26B).

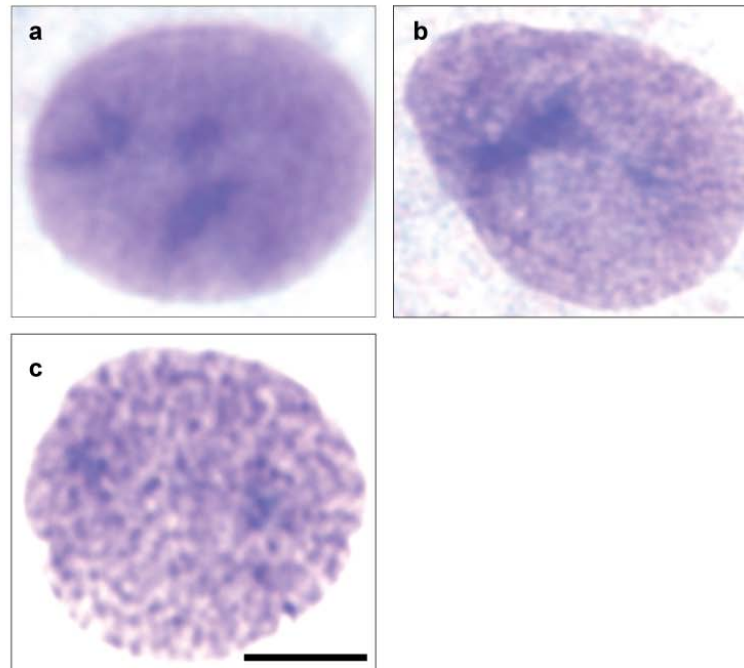
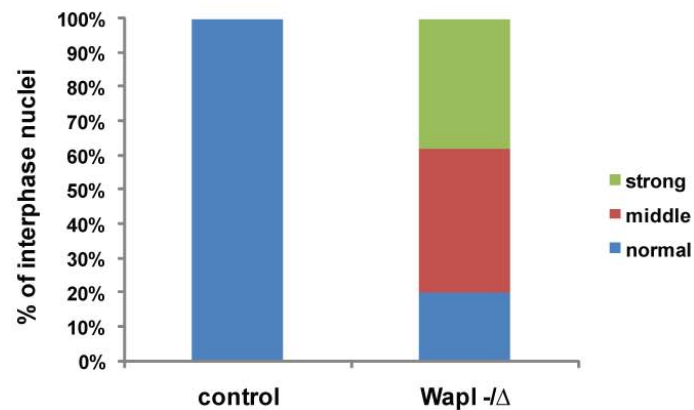
A**B**

Figure 26: *Wapl* knockout pMEFs show partial condensed chromatin in interphase

(A) Interphase cells were collected 120 hours after G0 release (described in Figure 8A) and analyzed by hypotonic spreading and Giemsa staining: a) normal nucleus from control *Wapl*^{+Δ} culture; b) nucleus with mild condensation defects from *Wapl*^{-Δ} culture; c) nucleus with severe condensation defects from *Wapl*^{-Δ} culture. Size bar, 10 μm.

(B) Interphase cells obtained as in (A) were classified according to their condensation state: normal (example in a), middle (example in b) or strong (example in c). (n=100).

However, the morphology of most nuclei from *Wapl*^{-Δ} cultures was strikingly different (Figure 26Ab, c). In 40% of cells the chromatin appeared more

compacted and arranged in elongated structures (Figure 26Ab and 25B); in 40% of cells milder changes in chromatin condensation were observed (Figure 26Ac and 26B); and 20% of cells showed a chromatin structure comparable to control cells (Figure 26Aa and 26B). Taken together, these observations suggest that high cohesin levels on DNA might induce partial condensation of chromatin already in interphase.

3.5 The cohesin vermicelli are not the consequence of incorrect mitotic divisions

I noticed that *Wapl* knockout cultures stopped proliferating when the vermicelli phenotype became predominant, between 48 and 72 hours (Figure 8C and Figure 20). One explanation for this anti-proliferative effect might be the high amount of chromatin-bound cohesin, which somehow inhibits cell proliferation. On the other hand, the anti-proliferative effect could also be the consequence of incorrect mitotic divisions, since in these experiments many *Wapl* knockout cells had undergone at least one mitosis, often in the presence of chromosome bridges. In order to distinguish between these two possibilities I developed a protocol to deplete Wapl protein in quiescent pMEFs, and I then analyzed the cells after they re-entered into the cell cycle. To this end, I extended the 4-OTH treatment in low serum medium from 2 days (Figure 8A) to 7 days (Figure 27A). After this time, the cells were split in fresh medium containing serum to trigger proliferation. I then collected control *Wapl*^{+Δ} and *Wapl*^{-Δ} cells for Western blotting and immunofluorescence analyses at the time-points indicated in Figure 27A. First, I prepared total protein extracts to blot against Wapl protein.

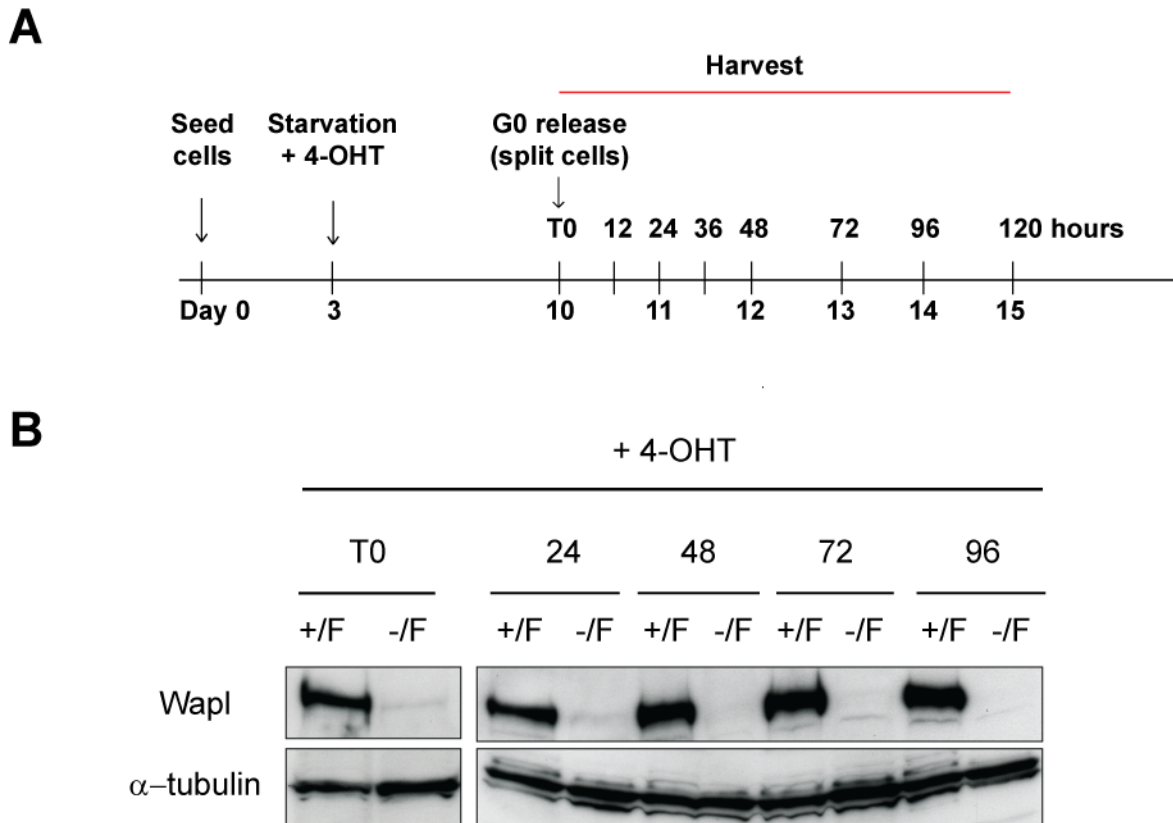


Figure 27: Wapl inactivation in quiescent pMEFs

(A) *Wapl*^{+/F} R26cre-ER^{T2} and *Wapl*^{-/F} R26cre-ER^{T2} pMEFs were seeded and cultured for three days then treated with 0.5 nM 4-OHT for 7 days. On day 10 the cultures were expanded, the 4-OHT removed, and the cells analyzed at subsequent time-points.

(B) Western blot of total cell extract of *Wapl*^{+/F} R26cre-ER^{T2} (+/F) and *Wapl*^{-/F} R26cre-ER^{T2} (-/F) pMEFs from (A), probed with anti Wapl antibody to show loss of expression of this protein, and with anti α -tubulin as a loading control.

Wapl was depleted below immunoblotting detection level already after 7 days of starvation (T0, Figure 27B; compare also with Figure 8B). I next asked if the cohesin vermicelli were present in *Wapl* knockout cultures. As shown in Figure 28, we observed cohesin vermicelli already at 12 hours after G0 release, when cells had not yet divided (see below). I could also distinguish cells with continuous strong vermicelli from cells with more discontinuous vermicelli, classified as “strong” and “middle” in Figure 28B, respectively.

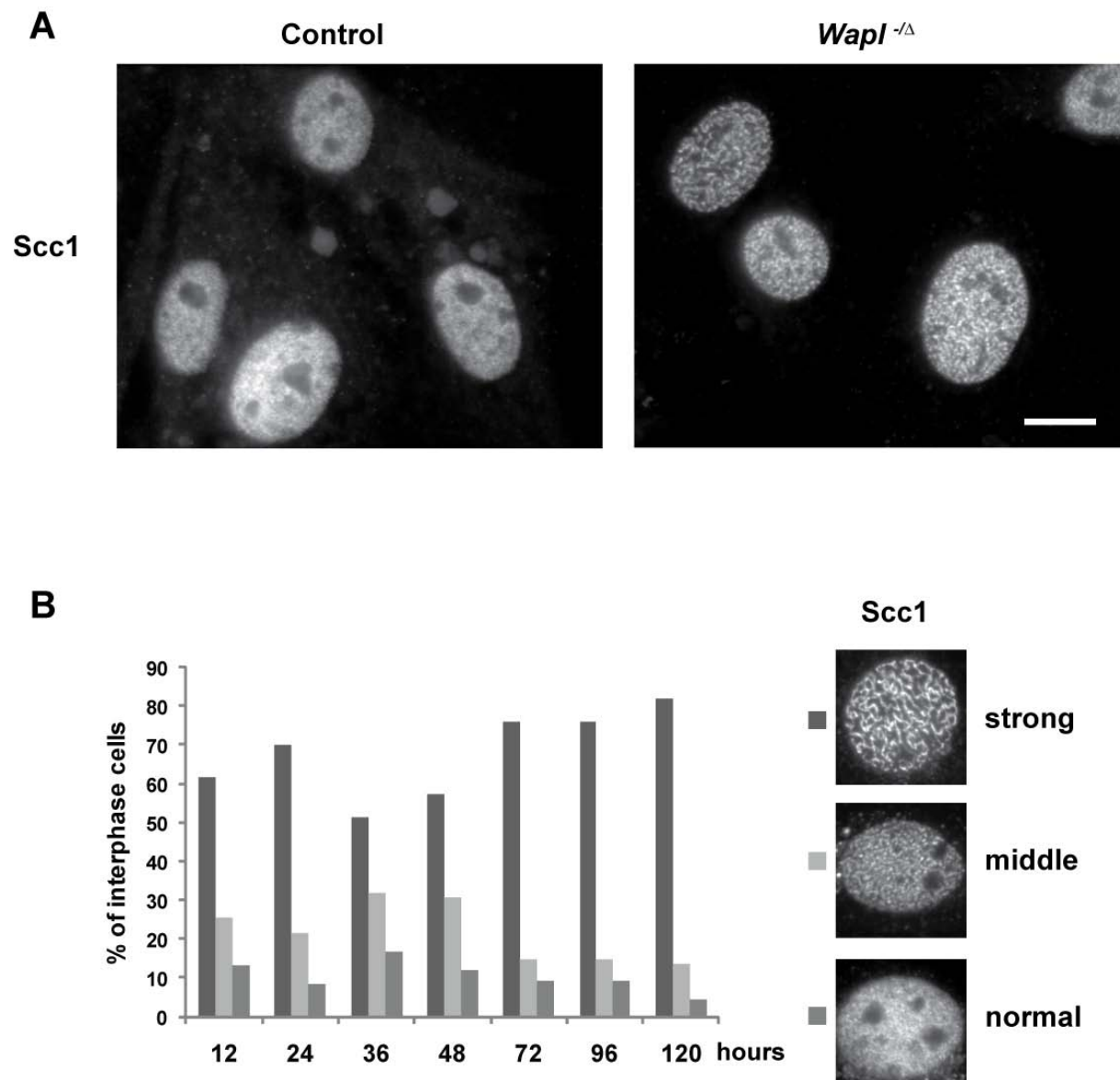


Figure 28: Cohesin vermicelli are not a consequence of incorrect mitotic divisions

(A) Control *Wapl*^{+Δ} pMEFs and *Wapl*^{-Δ} pMEFs obtained as in Figure 27A were stained with an anti-Scc1 antibody. DNA was stained with DAPI. Shown are examples at 12 hours after G0 release.

(B) Interphase *Wapl*^{-Δ} pMEFs obtained as in (A) were classified according to Scc1 pattern (n=500 per time-point). Bar 10 μm

It is possible that the cells with discontinuous *vermicelli* had still some Wapl protein left, although I could not directly address that due to the lack of suitable Wapl antibodies for IFM analysis. Cohesin vermicelli were never observed in control culture. This deletion protocol is therefore suitable to efficiently deplete

Wapl in non-cycling cells. Importantly, these observations indicate that the cohesin vermicelli are not an indirect consequence of incorrect mitotic divisions.

3.6 Wapl is required for the G1-S progression of primary mouse fibroblasts

Having developed a protocol to efficiently inactivate Wapl in quiescent cells (Figure 27), I next asked if *Wapl* knockout cultures could proliferate normally once they re-entered the cell cycle. Control *Wapl*^{+/ Δ} cultures divided every 24 hours as expected (Figure 29). However, *Wapl*^{-/ Δ} cultures did not increase their cell number during the 5 days that I kept them in culture (Figure 29).

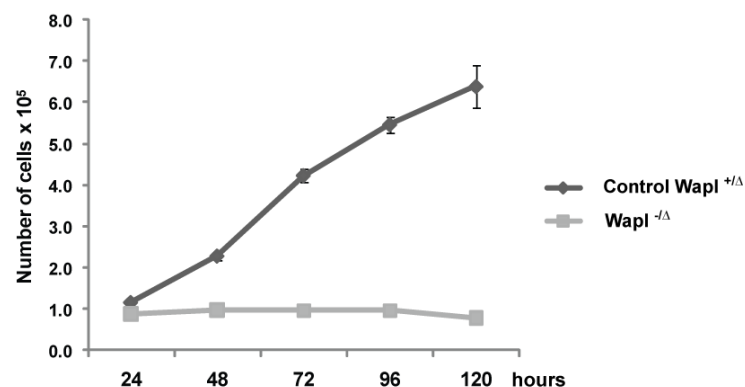
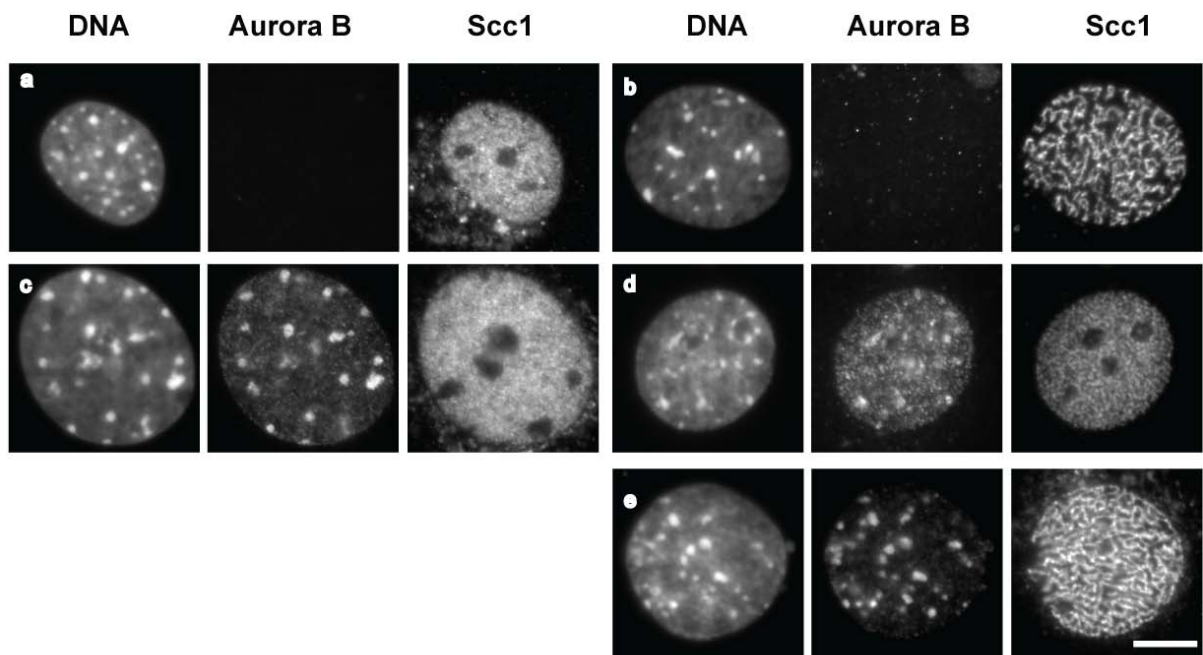
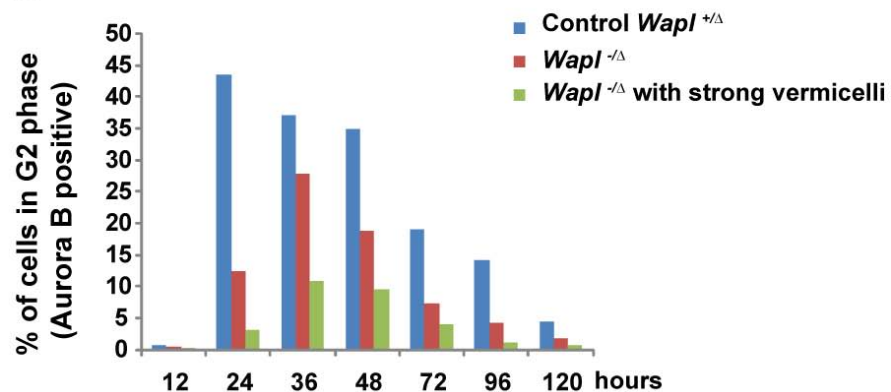


Figure 29: Wapl inactivation inhibits proliferation of pMEFs

Plot showing that cell proliferation is arrested following *Wapl* inactivation. *Wapl*^{+/ Δ} indicates *Wapl*^{+/ Δ} R26cre-ER^{T2} pMEFs treated with 4-OHT; *Wapl*^{-/ Δ} indicates *Wapl*^{-/ Δ} R26cre-ER^{T2} treated with 4-OHT.

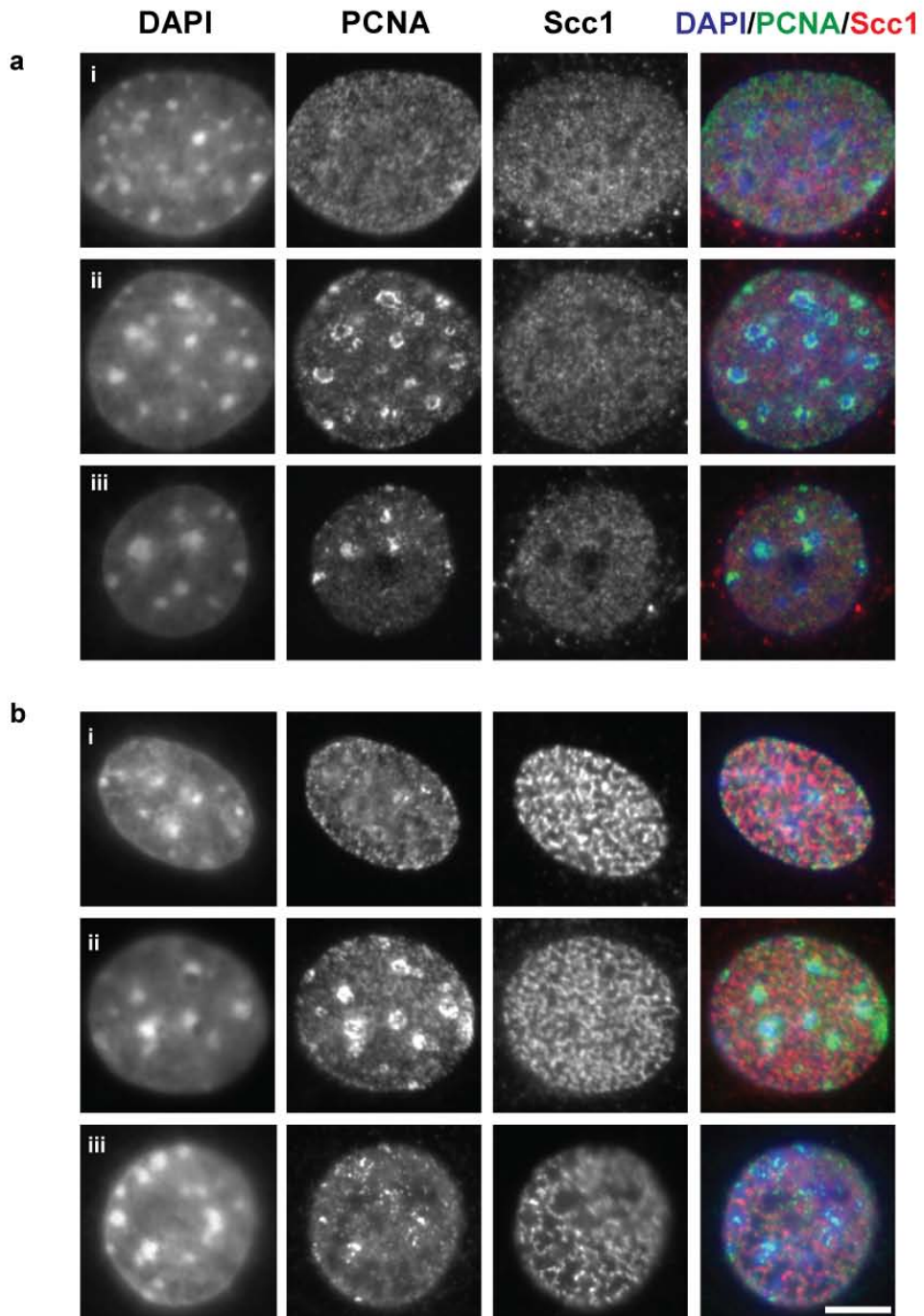
I could not observe any floating cells during that period of time, suggesting that *Wapl* knockout cells were arrested or delayed in the cell cycle, rather than dying. When I scored for mitotic cells by DNA morphology and H3S10ph staining we found very few mitotic cells in *Wapl* knockout culture compared to control one (data not shown). In order to characterize the cell cycle progression of *Wapl* knockout cultures in more detail, I analyzed specific cell cycle stage markers by

IFM. In the same experiment I used antibodies against the replication factor PCNA (Proliferating Cell Nuclear Antigen), Aurora B or BrdU (Bromodeoxyuridine) in combination with Scc1 staining and DAPI. First, I realized that *Wapl* knockout cultures had a low percentage of late S/G2 (Aurora B positive) cells (Figure 30). Interestingly, the percentage of late S/G2 cells was even lower if I considered only cells with continuous strong vermicelli (Figure 30Ae and 30B). This observation suggests that cells with higher amounts of chromatin-bound cohesin have more difficulties in progressing into late S/G2 phase. To distinguish whether *Wapl*^{-Δ} pMEFs arrested in S phase or in G1 phase I analyzed PCNA localization. PCNA is a sliding clamp protein essential for DNA replication. Figure 31Aa shows a typical PCNA staining pattern in control cells. As previously shown (reviewed in Morgan, 2007), PCNA staining appeared “dotty” in early S phase when the euchromatin is first replicated; later in middle S phase, PCNA clustered around heterochromatin; and during late S phase it co-localized with the heterochromatin. In *Wapl*^{-Δ} cultures I did not notice any obvious difference in the PCNA staining pattern compared to control cultures (compare Figure 31Aa with Figure 31Ab), but the frequencies with which these phases appeared were significantly changed following *Wapl* depletion. In control cells very few cells were in S-phase (PCNA positive) after 12 hours after G0 release (Figure 31B). The first peak of S-phase was observed at 24 hours (Figure 31B). In contrast, the percentage of S phase cells was very low in the *Wapl* knockout culture at each time-point examined (Figure 31B).

A**B****Figure 30: Wapl knockout pMEFs do not progress into G2 phase**

- (A) pMEFs obtained as in Figure 27A were stained with antibodies against Scc1 and Aurora B. DNA was stained with DAPI. Shown are: a) control *Wapl*^{+Δ} G1/early S cell (Aurora B negative staining); b) *Wapl*^{-Δ} G1/early S cell; c) control *Wapl*^{+Δ} late S/G2 cell (Aurora B positive staining); d) *Wapl*^{-Δ} late S/G2 cell with discontinuous cohesin vermicelli; e) *Wapl*^{-Δ} late S/G2 cell with continuous cohesin vermicelli. Bar, 10 μm.
- (B) Late S/G2 cells obtained in (A) were classified at different time-points. In “*Wapl*^{-Δ}” all late S/G2 cells (Aurora B positive staining) were included; in “*Wapl*^{-Δ} with strong vermicelli” only cells with continuous vermicelli (Ae) were included (n cells=500 per time-point).

A



B

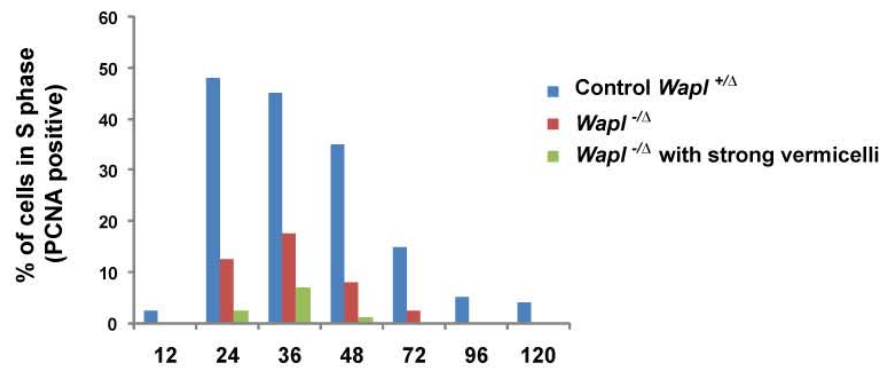


Figure 31: Wapl knockout pMEFs do not progress into S-phase

- (A) pMEFs obtained as described in Figure 27A were stained with antibodies against Scc1 and PCNA. DNA was stained with DAPI. a) control *Wapl*^{+Δ} cells in i) early S-phase, ii) middle S-phase and iii) late S-phase. b) *Wapl*^{-Δ} cells in i) early S-phase, ii) middle S-phase and iii) late S-phase. Bar, 10 μm.
- (B) Cells in S-phase obtained in (A) were classified at different time-points. In "*Wapl*^{-Δ}" all S-phase cells were included; In "*Wapl*^{-Δ} with strong vermicelli" only cells with continuous vermicelli were included (n cells=200 per time-point).

To confirm this result I treated control *Wapl*^{+Δ} and *Wapl*^{-Δ} cultures with BrdU for 30 minutes before harvesting them. BrdU is incorporated into newly synthesized DNA strands during S phase. I then stained with an anti-BrdU antibody. In control cells the BrdU pattern followed the PCNA pattern (compare Figure 31Aa with Figure 32Aa). Moreover, the percentage of BrdU positive cells in the control culture is similar to the percentage of PCNA positive cells (compare Figure 31B with Figure 32B). Strikingly, *Wapl* knockout cultures showed a very low percentage of BrdU positive cells at each time point analyzed (Figure 32B). In addition *Wapl*^{-Δ} cells showed a very poor incorporation of BrdU, independently of the replication stage (Figure 32Ab). I conclude that Wapl inactivation severely inhibits the transition from G1 to S phase in pMEFs.

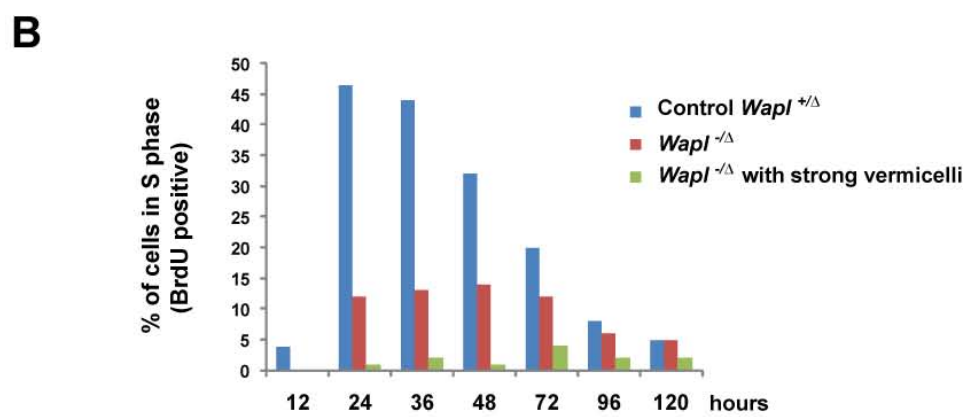
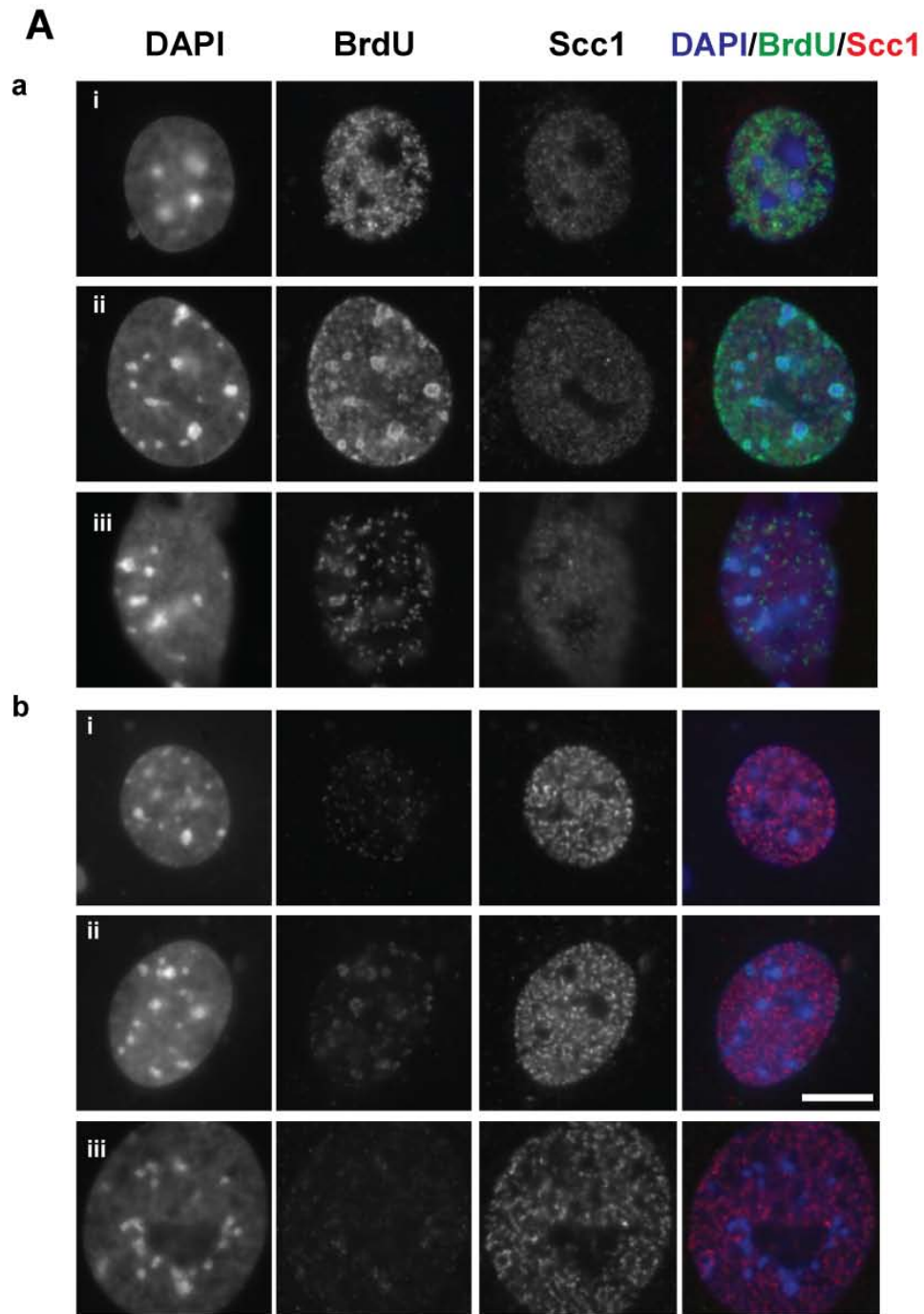


Figure 32: Low BrdU incorporation in Wapl knockout primary fibroblasts

- (A) pMEFs obtained as in figure 27A were treated with BrdU for 30 min before being harvested. Immunostaining was performed with antibodies against Scc1 and BrdU. DNA was stained with DAPI. a) control *Wapl*^{+/Δ} cells in i) early S-phase, ii) middle S-phase and iii) late S-phase. b) *Wapl*^{-Δ} cells in i) early S-phase, ii) middle S-phase and iii) late S-phase. Note that BrdU fluorescence intensity is lower in *Wapl*^{-Δ} pMEFs (b) than in control ones (a). Bar, 10 μm.
- (B) Cells in S-phase obtained in (A) were classified at different time-points. In "*Wapl*^{-Δ}" all S-phase cells were included; In "*Wapl*^{-Δ} with strong vermicelli" only cells with continuous vermicelli were included (n cells=200 per time-point).

4. Discussion

Equal genome distribution depends on cohesin cleavage by separase at the metaphase-anaphase transition (Hauf, 2001; Kumada et al., 2006; Uhlmann et al., 1999; Uhlmann et al., 2000; Wirth et al., 2006). This process is conserved from yeast to humans. However, in vertebrate cells most cohesin is removed from chromosome arms during prophase in a separase independent manner (Losada et al., 1998; Sumara et al., 2000; Waizenegger et al., 2000). Why vertebrate cells release the bulk of cohesin from chromosomes in early mitosis is still a mystery.

The major regulator of the prophase pathway of cohesin dissociation is the cohesin binding protein Wapl (Gandhi et al., 2006; Kueng et al., 2006). Despite the fact that Wapl depletion by RNAi in cultured human cells severely impairs cohesin dissociation during prophase, no major defects in chromosome segregation and cell cycle progression were observed after Wapl inactivation (Gandhi et al., 2006; Kueng et al., 2006).

It was therefore possible that the prophase pathway is redundant with the separase pathway, i.e. that Separase is required and sufficient to remove cohesin from mitotic chromosomes, whereas Wapl might not be essential for this process. However, it was also conceivable that chromosome segregation defects had not been observed in the previous RNAi experiments because Wapl had not been depleted completely under those conditions. Consistent with this possibility, it had been observed that the removal of cohesin from chromosomes was reduced, but not completely abolished, in cells transfected with Wapl siRNA (Kueng et al., 2006).

I therefore decide to generate a conditional *Wapl* knockout mouse, hoping that this would enable me to study chromosome segregation in the complete absence of *Wapl*.

Using primary embryonic mouse fibroblasts derived from these mice I showed for the first time that the prophase pathway of cohesin dissociation is essential for proper chromosome segregation. In addition, I found that *Wapl* is essential for early embryogenesis, and I discovered an essential role for *Wapl* during interphase cell cycle progression.

***Wapl* is essential for mouse embryonic development**

When I started this project no functional domains had been identified in the *Wapl* protein. It was known that the N-terminal half of the protein was required for *Wapl*'s association with cohesin, although the functional relevance of this association was unknown (Gandhi et al., 2006). It had also been reported that a constitutive *Wapl* knockout mouse lacking the highly conserved C-terminal half could not be obtained (Oikawa et al., 2004), possibly because such mice die during early embryogenesis (Dr. Oikawa, personal communication). I therefore decided to target in a conditional way the first exons (exons 3-4) in the *Wapl* mouse genomic locus, whose deletion eliminates most of the protein. The resulting *Wapl floxed* allele was germ-line transmitted and mice harboring this allele were born at the expected frequencies.

A *Wapl null* allele was obtained using a Cre-deleter mouse strain. *Wapl*^{-/-} mice were never recovered at the birth, confirming that *Wapl* is an essential gene during mouse development (Oikawa et al., 2004).

Western blotting analysis of total cell extract from pMEFs after *Wapl* deletion showed that neither full-length *Wapl* protein, nor a truncated protein corresponding to exons 1-2 could be detected. It is therefore unlikely that the production of a mutant polypeptide is the cause of the embryonic lethality of *Wapl null* mice. Moreover, the recent finding that the cohesin binding N-terminal half of *Wapl* is required for cohesin release from DNA in prophase (Shintomi and Hirano, 2009) further support the hypothesis that I generated a *Wapl null* allele.

Future experiments will be important to establish when and how *Wapl* knockout embryos die.

The prophase pathway is required for faithful chromosome segregation

Wapl deletion in pMEFs resulted in a striking enrichment of cohesin (Smc3, Scc1 and SA1/2) on chromosomes from prophase to metaphase. It has also to be noted that most if not all cohesin signal in *Wapl* knockout pMEFs was found to co-localize with mitotic chromosomes, with no apparently soluble cohesin present in the cytoplasm, at least at later time-points after *Wapl* inactivation. Although a direct comparison between HeLa cells and pMEFs cannot be done, these observations indicate that deletion of the *Wapl* gene in pMEFs leads to a more complete depletion of the *Wapl* protein than was previously possible by RNAi in HeLa cells. This notion is also supported by the observation that the accumulation of cohesin on chromatin after *Wapl* deletion in pMEFs was time dependent and correlated very well with *Wapl* depletion efficiency, as assessed by Western blotting.

The other striking phenotype that I observed in *Wapl* knockout pMEFs was the appearance of chromosome bridges between the two separating chromatid sets in anaphase. Both the severity and the incidence of chromosome bridges increased over time after *Wapl* inactivation, suggesting that low residual levels of *Wapl* might still be sufficient to sustain proper chromosome segregation. This might explain why *Wapl*-RNAi experiments did not show chromosome segregation defects (Gandhi et al., 2006; Kueng et al., 2006). Indeed, using a higher amount of *Wapl* siRNA than in previous studies, I was able, although not in a highly reproducible manner, to detect fine chromosome bridges also in HeLa cells undergoing anaphase (unpublished results).

The chromosome segregation abnormalities in *Wapl* knockout pMEFs were rescued to some extent by partial reduction of cellular cohesin levels by *Scc1* RNAi. These observations suggest that the excess of chromatin bound cohesin is the cause of improper chromosome segregation in *Wapl* knockout pMEFs and argue against a direct role of *Wapl*, unrelated to its effect on cohesin, during chromosome segregation. It has also to be noted that the *Wapl* knockout phenotype is different from the *Separase* knockout phenotype, where sister chromatids cannot be disjoined at their centromeres, resulting in the formation of polyploid cells (Kumada et al., 2006; Wirth et al., 2006). On the contrary, *Wapl* knockout cells could segregate their chromosomes, although not properly, eventually resulting in binucleated interphase cells often connected by a chromatin bridge.

How could the excess of chromatin-bound cohesin in *Wapl* knockout cells cause chromosome segregation defects? I considered two possibilities to explain this

phenotype. First, Separase might not be able to cleave all cohesin at the metaphase-anaphase transition in *Wapl* knockout pMEFs. The requirement for Separase activity is consistent with the finding that in *Wapl* knockout cells cohesin is largely excluded from chromosomes in anaphases, whereas *Wapl* Separase knockout cells exit mitosis with high level of cohesin on DNA. However, so far I was not able to detect any cohesin signal on chromosome bridges in *Wapl* depleted cells. However, I cannot exclude the possibility that small amounts of cohesin that I could not detect by IFM are present on these chromosomes. In the future, I will therefore further test this possibility by expressing tagged versions of cohesin subunits which can be detected with higher sensitivity. Alternatively, *Wapl* inactivation could also result in the formation of chromosome bridges by preventing DNA-decatenation reactions catalyzed by topoisomerase II enzymes. These enzymes can catalyze both catenation and decatenation reactions, and the release of cohesin from chromosome arms in early mitosis and the resulting resolution of the sisters might therefore favor topoisomerase II decatenation activity. *Wapl* depletion could thus delay the decatenation of sister chromatids by maintaining them in too close proximity. Localization experiments showed that topoisomerase II α does still associate with chromosomes after *Wapl* inactivation (unpublished results), although I cannot exclude the possibility that cohesin inhibits topoisomerase II directly. Remarkably, topoisomerase II α knockout blocks mouse embryo development at the eight-cell stage, with one chromosome bridge connecting each pair of daughter cells (Akimitsu et al., 2003). This phenotype is similar to the binucleated interphase pMEFs observed after *Wapl* knockout. It would therefore be important to show if the chromosome bridges in *Wapl*-

depleted cells represent catenated sister chromatids, but there are currently no assays to directly test this idea. However, it might be possible in the future to test whether catalytically-active topoisomerase II can be detected on chromosome bridges by using an assay described by Agostinho et al (Agostinho et al., 2004), and whether topoisomerase II over expression might mitigate the segregation abnormalities in *Wapl* knockout anaphases.

Finally, I cannot exclude the possibility that the prophase pathway of cohesin dissociation has additional functions. As discussed in the introduction, the prophase pathway could preserve the bulk of cohesin from separase cleavage (Peters et al., 2008; Wendt et al., 2008). One prediction of this hypothesis is that in the absence of *Wapl* less cohesin can be re-loaded onto DNA in telophase, and this abnormality could cause defects in gene expression in G1 phase. In the future I am therefore planning to analyze cohesin binding to chromatin in telophase and gene expression in G1-phase in cells depleted of *Wapl*.

Are cohesin vermicelli the axes of interphase chromosomes?

It was very surprising to observe that in interphase *Wapl* knockout pMEFs the cohesin immunofluorescence signal was strongly enriched in elongated structures. These so-called cohesin vermicelli were not the consequence of incorrect mitoses because *Wapl* inactivation in G0 led to their formation long before the first mitosis. In interphase the cohesin vermicelli were embedded in chromatin, whereas in mitosis a continuous cohesin signal was observed from one end to the other of each chromosome. These observations strongly suggest that one interphase vermicello corresponds to one chromosome, although further

experiments, such as the combination of cohesin immunostaining with chromosome painting, will be required to formally demonstrate this point.

Consistent with previous results (Kueng et al., 2006), I also found an increase of chromatin-bound cohesin in *Wapl* knockout interphase cells. However, RNAi experiments revealed only a modest increase of chromatin-bound cohesin (1.25 fold increase) compared to the more dramatic one (2 fold increase) after *Wapl* inactivation in pMEFs. The other striking observation in *Wapl* knockout interphase cells was the more compact chromatin state which could be seen by Giemsa staining and to some extent by DAPI staining. Could the excess of chromatin-bound cohesin after *Wapl* inactivation cause this condensation? A role for the cohesin complex in chromosome condensation, independent of its function in sister chromatid cohesion, was already suggested by FISH experiments at the rDNA locus during mitosis of budding yeast (Guacci et al., 1997; Lavoie et al., 2002a). Lavoie et al. suggested that “cohesin could then act in a manner reminiscent of boundary elements, restricting condensin activity to defined domains and consequently imposing a regular array of loops” (Lavoie et al., 2002b). In future experiments it will therefore be interesting to address whether condensin is required for the partial condensation observed in *Wapl* knockout cells. However, several observations also indicate a direct role for cohesin in regulating higher-order chromatin conformation during interphase (see below).

DNA has to be packaged with proteins to be accommodated in the nucleus, but at the same time chromatin structure must be dynamic to allow proteins involved in gene expression, DNA repair and replication to access DNA. The basic unit of chromatin organization is the nucleosome, in which DNA is wrapped around a

histone octamer. Interactions between histone-tails of adjacent nucleosomes are thought to generate a more compact chromatin structure known as 30 nm fiber. Histone-tails are targets of covalent modifications such as acetylation, methylation and phosphorylation, that influence chromatin compaction (reviewed in Jenuwein and Allis, 2001). During mitosis, the compaction of chromatin increases, possibly through the folding of chromatin fibers into loops. It has been proposed that this process is mediated by proteins in the chromosome scaffold, such as condensins and topoisomerase II, and by cis-acting DNA sequences called SARs (reviewed in Swedlow and Hirano, 2003). It is intriguing that the cohesin vermicelli are similar to the axial condensin-containing structures of mitotic chromosomes. It is therefore tempting to speculate that cohesin might provide a scaffolding function in interphase chromosomes, like condensin complexes are believed to do in mitotic chromosomes.

How does cohesin structure the DNA and what might be the relationship between chromatin structure and cohesin vermicelli? There could be three possible explanations for the more compact chromatin structure observed after *Wapl* inactivation in pMEFs. First, *Wapl* inactivation could induce DNA damage or other stress signals which trigger cell death by apoptosis, because DNA condensation is one of the hallmarks of apoptosis. However, I would exclude this possibility because I could not detect DNA damage after *Wapl* inactivation as judged by formation of foci of DNA damage markers by immunofluorescence microscopy experiments (data not shown), and *Wapl* knockout cultures never contained floating apoptotic cells even after five weeks in culture. Second, *Wapl* depletion could have direct or indirect effects on gene expression. This could affect the

levels of important regulators of chromatin structure as histone acetyltransferases and nucleosome-remodeling complexes, which in turn would affect chromatin structure. Currently I cannot exclude such an indirect effect, and further experiments have to be carried out to explore this possibility.

Finally, Wapl inactivation could stabilize transient interactions between cohesin binding sites on an unreplicated chromosome, i.e. in cis, resulting in a more compact chromatin structure. Interestingly, recent experiments using Conformation Capture (3C) technique showed that cohesin was required for the formation of chromatin loops at three different chromosomal loci (Hadjur et al., 2009; Mishiro et al., 2009; Nativio et al., 2009). At these three particular loci cohesin is required for the insulator transcriptional function of CTCF, possibly by mediating the formation of chromatin loops. It is plausible, although not tested so far, that such long-range interactions between cohesin/CTCF binding sites take place more widely, defining functional domains in the genome. This hypothesis is consistent with my finding that the number of cohesin binding sites increases from approximately 11,000 in control interphase pMEFs to approximately 27,000 in *Wapl* knockout interphase pMEFs. FRAP experiments after *Wapl*-RNAi depletion showed that *Wapl* is required during G2 phase for the dynamic association of cohesin with chromatin, and that *Wapl* depletion increased the levels of chromatin-bound cohesin, possibly due to the increased residence time of cohesin on DNA (Kueng et al., 2006). However, the function of this dynamic cohesin pool during interphase is still unknown. I speculate that this dynamic cohesin pool is required during interphase for transient interactions between

cohesin binding sites in *cis*, possibly required for the regulation of gene expression or other unknown functions.

Based on the above consideration, I envisage a model where cohesin provides a scaffolding function in interphase chromosomes organizing the genome in functional domains through the formation of chromatin loops. These chromatin loops must be dynamic to allow genome regulation at different levels, and their formations might be regulated at least in part by Wapl. One prediction of this model is that more chromatin loops should be entrapped in a stable association after Wapl inactivation. One challenge for the future will therefore be to reveal the existence of these loops, for example by 3C and 4C techniques and more directly by FISH experiments. The partial condensation of interphase chromatin in Wapl-depleted cells could then be explained with the formation of stable chromatin loops that would in turn make the DNA more compact. Future FRAP experiments will also address whether cohesin stably associates with chromatin in interphase Wapl knockout pMEFs.

Wapl is required for G1/S progression

In addition to proper chromosome segregation, Wapl is also required for progression from G0/G1 phase to S phase. This requirement was not an indirect effect of mitotic defects, because in these experiments Wapl inactivation occurred during G0 phase. I reasoned that there could be three different explanations for this observation. First, we cannot exclude the possibility that Wapl might have an unknown function in interphase, unrelated to the cohesin complex. Second, it could be that Wapl inactivation triggers DNA damage and or senescence.

However, as already mentioned I could not observe accumulation of DNA damage, and *Wapl* knockout cells did not show the typical enlarged shape of senescent cells. A more detailed analysis, using additional markers for DNA damage and cell senescence, will be required to further clarify these points. A third possibility is that the excess of chromatin-bound cohesin could be the cause of cell cycle arrest. As a result of too much chromatin-bound cohesin, the chromatin structure could be so compact that protein complexes involved in transcription as well as in DNA replication could not properly associate or travel along the DNA. Alternatively, cohesin itself could be a barrier for the progression of the RNA and DNA polymerases. A recent publication showed that *Wapl* depletion by RNAi does not affect the velocity of replication forks (Terret et al., 2009). These data are not consistent with my finding that most of *Wapl* knockout cells do not progress in S phase at all and the few that reach S phase showed very low BrdU incorporation. It is therefore possible that *Wapl* was not completely depleted by RNAi in the study by Terret et al. (2009). Future experiments will be required to understand the causes of cell cycle arrest after *Wapl* inactivation in pMEFs.

5. References

- Agostinho, M., Rino, J., Braga, J., Ferreira, F., Steffensen, S., and Ferreira, J. (2004). Human topoisomerase IIalpha: targeting to subchromosomal sites of activity during interphase and mitosis. *Mol Biol Cell* 15, 2388-2400. Epub 2004 Feb 2320.
- Akimitsu, N., Adachi, N., Hirai, H., Hossain, M.S., Hamamoto, H., Kobayashi, M., Aratani, Y., Koyama, H., and Sekimizu, K. (2003). Enforced cytokinesis without complete nuclear division in embryonic cells depleting the activity of DNA topoisomerase IIalpha. *Genes Cells* 8, 393-402.
- Anderson, D.E., Losada, A., Erickson, H.P., and Hirano, T. (2002). Condensin and cohesin display different arm conformations with characteristic hinge angles. *J Cell Biol* 156, 419-424.
- Ben-Shahar, T.R., Heeger, S., Lehane, C., East, P., Flynn, H., Skehel, M., and Uhlmann, F. (2008). Eco1-dependent cohesin acetylation during establishment of sister chromatid cohesion. *Science* 321, 563-566.
- Bernard, P., Drogat, J., Maure, J.F., Dheur, S., Vaur, S., Genier, S., and Javerzat, J.P. (2006). A screen for cohesion mutants uncovers Ssl3, the fission yeast counterpart of the cohesin loading factor Scc4. *Curr Biol* 16, 875-881.
- Bernard, P., Schmidt, C.K., Vaur, S., Dheur, S., Drogat, J., Genier, S., Ekwall, K., Uhlmann, F., and Javerzat, J.P. (2008). Cell-cycle regulation of cohesin stability along fission yeast chromosomes. *Embo J* 27, 111-121.
- Blat, Y., and Kleckner, N. (1999). Cohesins bind to preferential sites along yeast chromosome III, with differential regulation along arms versus the centric region. *Cell* 98, 249-259.
- Canudas, S., and Smith, S. (2009). Differential regulation of telomere and centromere cohesion by the Scc3 homologues SA1 and SA2, respectively, in human cells. *J Cell Biol* 187, 165-173.
- Cardozo, T., and Pagano, M. (2004). The SCF ubiquitin ligase: insights into a molecular machine. *Nat Rev Mol Cell Biol* 5, 739-751.
- Ciosk, R., Shirayama, M., Shevchenko, A., Tanaka, T., Toth, A., and Nasmyth, K. (2000). Cohesin's binding to chromosomes depends on a separate complex consisting of Scc2 and Scc4 proteins. *Mol Cell* 5, 243-254.
- Darwiche, N., Freeman, L.A., and Strunnikov, A. (1999). Characterization of the components of the putative mammalian sister chromatid cohesion complex. *Gene* 233, 39-47.
- Dobie, K.W., Kennedy, C.D., Velasco, V.M., McGrath, T.L., Weko, J., Patterson, R.W., and Karpen, G.H. (2001). Identification of chromosome inheritance modifiers in *Drosophila melanogaster*. *Genetics* 157, 1623-1637.
- Dorsett, D., Eissenberg, J.C., Misulovin, Z., Martens, A., Redding, B., and McKim, K. (2005). Effects of sister chromatid cohesion proteins on cut gene expression during wing development in *Drosophila*. *Development* 132, 4743-4753.
- Furuya, K., Takahashi, K., and Yanagida, M. (1998). Faithful anaphase is ensured by Mis4, a sister chromatid cohesion molecule required in S phase and not destroyed in G1 phase. *Genes Dev* 12, 3408-3418.
- Gandhi, R., Gillespie, P.J., and Hirano, T. (2006). Human Wapl is a cohesin-binding protein that promotes sister-chromatid resolution in mitotic prophase. *Curr Biol* 16, 2406-2417.
- Gerlich, D., Koch, B., Dupeux, F., Peters, J.M., and Ellenberg, J. (2006). Live-Cell Imaging Reveals a Stable Cohesin-Chromatin Interaction after but Not before DNA Replication. *Curr Biol* 16, 1571-1578.

Gillespie, P.J., and Hirano, T. (2004). Scc2 couples replication licensing to sister chromatid cohesion in *Xenopus* egg extracts. *Curr Biol* *14*, 1598-1603.

Gimenez-Abian, J.F., Sumara, I., Hirota, T., Hauf, S., Gerlich, D., de la Torre, C., Ellenberg, J., and Peters, J.M. (2004). Regulation of sister chromatid cohesion between chromosome arms. *Curr Biol* *14*, 1187-1193.

Glynn, E.F., Megee, P.C., Yu, H.G., Mistrot, C., Unal, E., Koshland, D.E., DeRisi, J.L., and Gerton, J.L. (2004). Genome-wide mapping of the cohesin complex in the yeast *Saccharomyces cerevisiae*. *PLoS Biol* *2*, E259. Epub 2004 Jul 2027.

Gorr, I.H., Boos, D., and Stemmann, O. (2005). Mutual inhibition of separase and Cdk1 by two-step complex formation. *Mol Cell* *19*, 135-141.

Gruber, S., Haering, C.H., and Nasmyth, K. (2003). Chromosomal cohesin forms a ring. *Cell* *112*, 765-777.

Guacci, V., Hogan, E., and Koshland, D. (1994). Chromosome condensation and sister chromatid pairing in budding yeast. *J Cell Biol* *125*, 517-530.

Guacci, V., Koshland, D., and Strunnikov, A. (1997). A direct link between sister chromatid cohesion and chromosome condensation revealed through the analysis of MCD1 in *S. cerevisiae*. *Cell* *91*, 47-57.

Hadjur, S., Williams, L.M., Ryan, N.K., Cobb, B.S., Sexton, T., Fraser, P., Fisher, A.G., and Merckenschlager, M. (2009). Cohesins form chromosomal cis-interactions at the developmentally regulated IFNG locus. *Nature* *460*, 410-413.

Haering, C.H., Farcas, A.M., Arumugam, P., Metson, J., and Nasmyth, K. (2008). The cohesin ring concatenates sister DNA molecules. *Nature* *454*, 297-301.

Haering, C.H., Lowe, J., Hochwagen, A., and Nasmyth, K. (2002). Molecular architecture of SMC proteins and the yeast cohesin complex. *Mol Cell* *9*, 773-788.

Haering, C.H., Schoffnegger, D., Nishino, T., Helmhart, W., Nasmyth, K., and Lowe, J. (2004). Structure and stability of cohesin's Smc1-kleisin interaction. *Mol Cell* *15*, 951-964.

Hartman, T., Stead, K., Koshland, D., and Guacci, V. (2000). Pds5p is an essential chromosomal protein required for both sister chromatid cohesion and condensation in *Saccharomyces cerevisiae*. *J Cell Biol* *151*, 613-626.

Hauf, S., Roitinger, E., Koch, B., Dittrich, C.M., Mechtler, K., and Peters, J.M. (2005). Dissociation of cohesin from chromosome arms and loss of arm cohesion during early mitosis depends on phosphorylation of SA2. *Plos Biology* *3*, 419-432.

Hauf, S., Waizenegger, I.C., and Peters, J.M. (2001). Cohesin cleavage by separase required for anaphase and cytokinesis in human cells. *Science* *293*, 1320-1323.

Hauf, S., Waizenegger, I.C., and Peters, J.-M. (2001). Cohesin cleavage by separase required for anaphase and cytokinesis in human cells. *Science*, in press.

Hirano, M., and Hirano, T. (2002). Hinge-mediated dimerization of SMC protein is essential for its dynamic interaction with DNA. *Embo J* *21*, 5733-5744.

Hirano, T. (2006). At the heart of the chromosome: SMC proteins in action. *Nat Rev Mol Cell Biol* *7*, 311-322.

Hirota, T., Gerlich, D., Koch, B., Ellenberg, J., and Peters, J.M. (2004). Distinct functions of condensin I and II in mitotic chromosome assembly. *J Cell Sci* *117*, 6435-6445.

Hornig, N.C., Knowles, P.P., McDonald, N.Q., and Uhlmann, F. (2002). The dual mechanism of separase regulation by securin. *Curr Biol* *12*, 973-982.

Hou, F., and Zou, H. (2005). Two human orthologues of Eco1/Ctf7 acetyltransferases are both required for proper sister-chromatid cohesion. *Mol Biol Cell* *16*, 3908-3918.

Huang, X., Andreu-Vieyra, C.V., York, J.P., Hatcher, R., Lu, T., Matzuk, M.M., and Zhang, P. (2008). Inhibitory phosphorylation of separase is essential for genome stability and viability of murine embryonic germ cells. *PLoS Biol* 6, e15.

Huang, X., Hatcher, R., York, J.P., and Zhang, P. (2005). Securin and separase phosphorylation act redundantly to maintain sister chromatid cohesion in mammalian cells. *Mol Biol Cell* 16, 4725-4732.

Ivanov, D., and Nasmyth, K. (2005). A topological interaction between cohesin rings and a circular minichromosome. *Cell* 122, 849-860.

Ivanov, D., and Nasmyth, K. (2007). A physical assay for sister chromatid cohesion in vitro. *Mol Cell* 27, 300-310.

Ivanov, D., Schleiffer, A., Eisenhaber, F., Mechtler, K., Haering, C.H., and Nasmyth, K. (2002). Eco1 is a novel acetyltransferase that can acetylate proteins involved in cohesion. *Curr Biol* 12, 323-328.

Jenuwein, T., and Allis, C.D. (2001). Translating the histone code. *Science* 293, 1074-1080.

Kitajima, T.S., Hauf, S., Ohsugi, M., Yamamoto, T., and Watanabe, Y. (2005). Human Bub1 defines the persistent cohesion site along the mitotic chromosome by affecting Shugoshin localization. *Curr Biol* 15, 353-359.

Kitajima, T.S., Sakuno, T., Ishiguro, K., Iemura, S., Natsume, T., Kawashima, S.A., and Watanabe, Y. (2006). Shugoshin collaborates with protein phosphatase 2A to protect cohesin. *Nature* 441, 46-52.

Kueng, S., Hegemann, B., Peters, B.H., Lipp, J.J., Schleiffer, A., Mechtler, K., and Peters, J.M. (2006). Wapl controls the dynamic association of cohesin with chromatin. *Cell* 127, 955-967.

Kumada, K., Yao, R., Kawaguchi, T., Karasawa, M., Hoshikawa, Y., Ichikawa, K., Sugitani, Y., Imoto, I., Inazawa, J., Sugawara, M., *et al.* (2006). The selective continued linkage of centromeres from mitosis to interphase in the absence of mammalian separase. *J Cell Biol* 172, 835-846.

Lavoie, B.D., Hogan, E., and Koshland, D. (2002a). In vivo dissection of the chromosome condensation machinery: reversibility of condensation distinguishes contributions of condensin and cohesin. *J Cell Biol* 156, 805-815.

Lavoie, B.D., Hogan, E., and Koshland, D. (2002b). In vivo dissection of the chromosome condensation machinery: reversibility of condensation distinguishes contributions of condensin and cohesin. *J Cell Biol* 156, 805-815.

Lenart, P., Petronczki, M., Steegmaier, M., Di Fiore, B., Lipp, J.J., Hoffmann, M., Rettig, W.J., Kraut, N., and Peters, J.M. (2007). The small-molecule inhibitor BI 2536 reveals novel insights into mitotic roles of polo-like kinase 1. *Curr Biol* 17, 304-315.

Lengronne, A., Katou, Y., Mori, S., Yokobayashi, S., Kelly, G.P., Itoh, T., Watanabe, Y., Shirahige, K., and Uhlmann, F. (2004). Cohesin relocation from sites of chromosomal loading to places of convergent transcription. *Nature* 430, 573-578.

Lengronne, A., McIntyre, J., Katou, Y., Kanoh, Y., Hopfner, K.P., Shirahige, K., and Uhlmann, F. (2006). Establishment of Sister Chromatid Cohesion at the *S. cerevisiae* Replication Fork. *Mol Cell* 23, 787-799.

Lipp, J.J., Hirota, T., Poser, I., and Peters, J.M. (2007). Aurora B controls the association of condensin I but not condensin II with mitotic chromosomes. *J Cell Sci* 120, 1245-1255.

Liu, P., Jenkins, N.A., and Copeland, N.G. (2003). A highly efficient recombineering-based method for generating conditional knockout mutations. *Genome Res* 13, 476-484.

Losada, A., Hirano, M., and Hirano, T. (1998). Identification of *Xenopus* SMC protein complexes required for sister chromatid cohesion. *Genes Dev* 12, 1986-1997.

Losada, A., Hirano, M., and Hirano, T. (2002). Cohesin release is required for sister chromatid resolution, but not for condensin-mediated compaction, at the onset of mitosis. *Genes Dev* 16, 3004-3016.

Losada, A., Yokochi, T., and Hirano, T. (2005). Functional contribution of Pds5 to cohesin-mediated cohesion in human cells and *Xenopus* egg extracts. *J Cell Sci* 118, 2133-2141.

Losada, A., Yokochi, T., Kobayashi, R., and Hirano, T. (2000). Identification and Characterization of SA/Scp3p Subunits in the *Xenopus* and Human Cohesin Complexes. *J Cell Biol* 150, 405-416.

McGuinness, B.E., Hirota, T., Kudo, N.R., Peters, J.M., and Nasmyth, K. (2005). Shugoshin prevents dissociation of cohesin from centromeres during mitosis in vertebrate cells. *Plos Biology* 3, 433-449.

Melby, T.E., Ciampaglio, C.N., Briscoe, G., and Erickson, H.P. (1998). The symmetrical structure of structural maintenance of chromosomes (SMC) and MukB proteins: Long, antiparallel coiled coils, folded at a flexible hinge. *J Cell Biol* 142, 1595-1604.

Michaelis, C., Ciosk, R., and Nasmyth, K. (1997). Cohesins: chromosomal proteins that prevent premature separation of sister chromatids. *Cell* 91, 35-45.

Mishiro, T., Ishihara, K., Hino, S., Tsutsumi, S., Aburatani, H., Shirahige, K., Kinoshita, Y., and Nakao, M. (2009). Architectural roles of multiple chromatin insulators at the human apolipoprotein gene cluster. *Embo J* 28, 1234-1245.

Moldovan, G.L., Pfander, B., and Jentsch, S. (2006). PCNA Controls Establishment of Sister Chromatid Cohesion during S Phase. *Mol Cell* 23, 723-732.

Morgan, D.O. (1997). Cyclin-dependent kinases: engines, clocks, and microprocessors. *Annu Rev Cell Dev Biol* 13, 261-291.

Morgan, D.O. (2007). *The Cell Cycle: Principles of Control* (London, New Science Press).

Murray, A.W. (2004). Recycling the cell cycle: cyclins revisited. *Cell* 116, 221-234.

Murray, A.W., and Szostak, J.W. (1985). Chromosome segregation in mitosis and meiosis. *Ann Rev Cell Biol* 1, 289-315.

Musacchio, A., and Salmon, E.D. (2007). The spindle-assembly checkpoint in space and time. *Nat Rev Mol Cell Biol* 8, 379-393.

Nasmyth, K., and Haering, C.H. (2005). The structure and function of SMC and kleisin complexes. *Annu Rev Biochem* 74, 595-648.

Nasmyth, K., and Haering, C.H. (2009). Cohesin: its roles and mechanisms. *Annu Rev Genet* 43, 525-558.

Nativio, R., Wendt, K.S., Ito, Y., Huddleston, J.E., Uribe-Lewis, S., Woodfine, K., Krueger, C., Reik, W., Peters, J.M., and Murrell, A. (2009). Cohesin is required for higher-order chromatin conformation at the imprinted IGF2-H19 locus. *PLoS Genet* 5, e1000739.

Oikawa, K., Ohbayashi, T., Kiyono, T., Nishi, H., Isaka, K., Umezawa, A., Kuroda, M., and Mukai, K. (2004). Expression of a novel human gene, human wings apart-like (hWAPL), is associated with cervical carcinogenesis and tumor progression. *Cancer Res* 64, 3545-3549.

Panizza, S., Tanaka, T., Hochwagen, A., Eisenhaber, F., and Nasmyth, K. (2000). Pds5 cooperates with cohesin in maintaining sister chromatid cohesion. *Curr Biol* 10, 1557-1564.

Parelho, V., Hadjur, S., Spivakov, M., Leleu, M., Sauer, S., Gregson, H.C., Jarmuz, A., Canzonetta, C., Webster, Z., Nesterova, T., *et al.* (2008). Cohesins functionally associate with CTCF on mammalian chromosome arms. *Cell* *132*, 422-433.

Perrimon, N., Engstrom, L., and Mahowald, A.P. (1985). Developmental genetics of the 2C-D region of the *Drosophila* X chromosome. *Genetics* *111*, 23-41.

Peters, J.M. (2006). The anaphase promoting complex/cyclosome: a machine designed to destroy. *Nat Rev Mol Cell Biol* *7*, 644-656.

Peters, J.M., and Bhaskara, V. (2009). Cohesin acetylation: from antiestablishment to establishment. *Mol Cell* *34*, 1-2.

Peters, J.M., Tedeschi, A., and Schmitz, J. (2008). The cohesin complex and its roles in chromosome biology. *Genes Dev* *22*, 3089-3114.

Pinsky, B.A., and Biggins, S. (2005). The spindle checkpoint: tension versus attachment. *Trends Cell Biol* *15*, 486-493.

Porter, A.C., and Farr, C.J. (2004). Topoisomerase II: untangling its contribution at the centromere. *Chromosome Res* *12*, 569-583.

Rankin, S., Ayad, N.G., and Kirschner, M.W. (2005). Sororin, a substrate of the anaphase-promoting complex, is required for sister chromatid cohesion in vertebrates. *Mol Cell* *18*, 185-200.

Riedel, C.G., Katis, V.L., Katou, Y., Mori, S., Itoh, T., Helmhart, W., Galova, M., Petronczki, M., Gregan, J., Cetin, B., *et al.* (2006). Protein phosphatase 2A protects centromeric sister chromatid cohesion during meiosis I. *Nature* *441*, 53-61.

Rollins, R.A., Korom, M., Aulner, N., Martens, A., and Dorsett, D. (2004). *Drosophila* nipped-B protein supports sister chromatid cohesion and opposes the stromalin/Scc3 cohesion factor to facilitate long-range activation of the cut gene. *Mol Cell Biol* *24*, 3100-3111.

Rowland, B.D., Roig, M.B., Nishino, T., Kurze, A., Uluocak, P., Mishra, A., Beckouet, F., Underwood, P., Metson, J., Imre, R., *et al.* (2009). Building sister chromatid cohesion: smc3 acetylation counteracts an antiestablishment activity. *Mol Cell* *33*, 763-774.

Rubio, E.D., Reiss, D.J., Welcsh, P.L., Disteche, C.M., Filippova, G.N., Baliga, N.S., Aebersold, R., Ranish, J.A., and Krumm, A. (2008). CTCF physically links cohesin to chromatin. *Proc Natl Acad Sci U S A*.

Salic, A., Waters, J.C., and Mitchison, T.J. (2004). Vertebrate shugoshin links sister centromere cohesion and kinetochore microtubule stability in mitosis. *Cell* *118*, 567-578.

Schleiffer, A., Kaitna, S., Maurer-Stroh, S., Glotzer, M., Nasmyth, K., and Eisenhaber, F. (2003). Kleisins: a superfamily of bacterial and eukaryotic SMC protein partners. *Mol Cell* *11*, 571-575.

Schmidt-Suppran, M., and Rajewsky, K. (2007). Vagaries of conditional gene targeting. *Nat Immunol* *8*, 665-668.

Schmitz, J., Watrin, E., Lenart, P., Mechtler, K., and Peters, J.M. (2007). Sororin is required for stable binding of cohesin to chromatin and for sister chromatid cohesion in interphase. *Curr Biol* *17*, 630-636.

Seibler, J., Zevnik, B., Kuter-Luks, B., Andreas, S., Kern, H., Hennek, T., Rode, A., Heimann, C., Faust, N., Kauselmann, G., *et al.* (2003). Rapid generation of inducible mouse mutants. *Nucleic Acids Res* *31*, e12.

Shintomi, K., and Hirano, T. (2009). Releasing cohesin from chromosome arms in early mitosis: opposing actions of Wapl-Pds5 and Sgo1. *Genes Dev* *23*, 2224-2236.

Skibbens, R.V., Corson, L.B., Koshland, D., and Hieter, P. (1999). Ctf7p is essential for sister chromatid cohesion and links mitotic chromosome structure to the DNA replication machinery. *Genes Dev* 13, 307-319.

Stead, K., Aguilar, C., Hartman, T., Drexel, M., Meluh, P., and Guacci, V. (2003). Pds5p regulates the maintenance of sister chromatid cohesion and is sumoylated to promote the dissolution of cohesion. *J Cell Biol* 163, 729-741.

Stedman, W., Kang, H., Lin, S., Kissil, J.L., Bartolomei, M.S., and Lieberman, P.M. (2008). Cohesins localize with CTCF at the KSHV latency control region and at cellular c-myc and H19/Igf2 insulators. *Embo J* 27, 654-666.

Stemmann, O., Zou, H., Gerber, S.A., Gygi, S.P., and Kirschner, M.W. (2001). Dual Inhibition of Sister Chromatid Separation at Metaphase. *Cell* 107, 715-726.

Strunnikov, A.V., Larionov, V.L., and Koshland, D. (1993). SMC1: an essential yeast gene encoding a putative head-rod-tail protein is required for nuclear division and defines a new ubiquitous protein family. *J Cell Biol* 123, 1635-1648.

Sumara, I., Vorlaufer, E., Gieffers, C., Peters, B.H., and Peters, J.M. (2000). Characterization of vertebrate cohesin complexes and their regulation in prophase. *Journal of Cell Biology* 151, 749-761.

Sumara, I., Vorlaufer, E., Stukenberg, P.T., Kelm, O., Redemann, N., Nigg, E.A., and Peters, J.M. (2002). The dissociation of cohesin from chromosomes in prophase is regulated by polo-like kinase. *Molecular Cell* 9, 515-525.

Sutani, T., Kawaguchi, T., Kanno, R., Itoh, T., and Shirahige, K. (2009). Budding yeast Wpl1(Rad61)-Pds5 complex counteracts sister chromatid cohesion-establishing reaction. *Curr Biol* 19, 492-497.

Swedlow, J.R., and Hirano, T. (2003). The making of the mitotic chromosome. Modern insights into classical questions. *Mol Cell* 11, 557-569.

Takahashi, T.S., Basu, A., Bermudez, V., Hurwitz, J., and Walter, J.C. (2008). Cdc7-Drf1 kinase links chromosome cohesion to the initiation of DNA replication in *Xenopus* egg extracts. *Genes Dev* 22, 1894-1905.

Takahashi, T.S., Yiu, P., Chou, M.F., Gygi, S., and Walter, J.C. (2004). Recruitment of *Xenopus* Scc2 and cohesin to chromatin requires the pre-replication complex. *Nat Cell Biol* 6, 991-996.

Tanaka, K., Hao, Z., Kai, M., and Okayama, H. (2001). Establishment and maintenance of sister chromatid cohesion in fission yeast by a unique mechanism. *Embo J* 20, 5779-5790.

Tang, Z., Shu, H., Qi, W., Mahmood, N.A., Mumby, M.C., and Yu, H. (2006). PP2A is required for centromeric localization of Sgo1 and proper chromosome segregation. *Dev Cell* 10, 575-585.

Tang, Z., Sun, Y., Harley, S.E., Zou, H., and Yu, H. (2004). Human Bub1 protects centromeric sister-chromatid cohesion through Shugoshin during mitosis. *Proc Natl Acad Sci U S A* 101, 18012-18017.

Terret, M.E., Sherwood, R., Rahman, S., Qin, J., and Jallepalli, P.V. (2009). Cohesin acetylation speeds the replication fork. *Nature* 462, 231-234.

Toth, A., Ciosk, R., Uhlmann, F., Galova, M., Schleiffer, A., and Nasmyth, K. (1999). Yeast cohesin complex requires a conserved protein, Eco1p(Ctf7), to establish cohesion between sister chromatids during DNA replication. *Genes Dev* 13, 320-333.

Uhlmann, F. (2009). A matter of choice: the establishment of sister chromatid cohesion. *EMBO Rep* 10, 1095-1102.

Uhlmann, F., Lottspeich, F., and Nasmyth, K. (1999). Sister-chromatid separation at anaphase onset is promoted by cleavage of the cohesin subunit Scc1. *Nature* *400*, 37-42.

Uhlmann, F., Wernic, D., Poupart, M.A., Koonin, E.V., and Nasmyth, K. (2000). Cleavage of cohesin by the CD clan protease separin triggers anaphase in yeast. *Cell* *103*, 375-386.

Unal, E., Heidinger-Pauli, J.M., Kim, W., Guacci, V., Onn, I., Gygi, S.P., and Koshland, D.E. (2008). A molecular determinant for the establishment of sister chromatid cohesion. *Science* *321*, 566-569.

Verni, F., Gandhi, R., Goldberg, M.L., and Gatti, M. (2000). Genetic and molecular analysis of wings apart-like (*wapl*), a gene controlling heterochromatin organization in *Drosophila melanogaster*. *Genetics* *154*, 1693-1710.

Waizenegger, I., Gimenez-Abian, J.F., Wernic, D., and Peters, J.M. (2002). Regulation of human separase by securin binding and autocleavage. *Curr Biol* *12*, 1368-1378.

Waizenegger, I.C., Hauf, S., Meinke, A., and Peters, J.M. (2000). Two distinct pathways remove mammalian cohesin from chromosome arms in prophase and from centromeres in anaphase. *Cell* *103*, 399-410.

Wang, S.W., Read, R.L., and Norbury, C.J. (2002). Fission yeast Pds5 is required for accurate chromosome segregation and for survival after DNA damage or metaphase arrest. *J Cell Sci* *115*, 587-598.

Warren, C.D., Eckley, D.M., Lee, M.S., Hanna, J.S., Hughes, A., Peyser, B., Jie, C., Irizarry, R., and Spencer, F.A. (2004). S-phase checkpoint genes safeguard high-fidelity sister chromatid cohesion. *Mol Biol Cell* *15*, 1724-1735.

Watrln, E., and Peters, J.M. (2006). Cohesin and DNA damage repair. *Exp Cell Res* *312*, 2687-2693.

Watrln, E., Schleiffer, A., Tanaka, K., Eisenhaber, F., Nasmyth, K., and Peters, J.M. (2006). Human *scc4* is required for cohesin binding to chromatin, sister-chromatid cohesion, and mitotic progression. *Curr Biol* *16*, 863-874.

Weaver, B.A., and Cleveland, D.W. (2006). Does aneuploidy cause cancer? *Curr Opin Cell Biol* *18*, 658-667.

Wendt, K.S., and Peters, J.M. (2009). How cohesin and CTCF cooperate in regulating gene expression. *Chromosome Res* *17*, 201-214.

Wendt, K.S., Yoshida, K., Itoh, T., Bando, M., Koch, B., Schirghuber, E., Tsutsumi, S., Nagae, G., Ishihara, K., Mishiro, T., *et al.* (2008). Cohesin mediates transcriptional insulation by CCCTC-binding factor. *Nature* *451*, 796-801.

Wirth, K.G., Wutz, G., Kudo, N.R., Desdouets, C., Zetterberg, A., Taghybeeglu, S., Seznec, J., Ducos, G.M., Ricci, R., Firnberg, N., *et al.* (2006). Separase: a universal trigger for sister chromatid disjunction but not chromosome cycle progression. *J Cell Biol* *172*, 847-860.

Zhang, B., Jain, S., Song, H., Fu, M., Heuckeroth, R.O., Erlich, J.M., Jay, P.Y., and Milbrandt, J. (2007). Mice lacking sister chromatid cohesion protein PDS5B exhibit developmental abnormalities reminiscent of Cornelia de Lange syndrome. *Development* *134*, 3191-3201.

Zhang, J., Shi, X., Li, Y., Kim, B.J., Jia, J., Huang, Z., Yang, T., Fu, X., Jung, S.Y., Wang, Y., *et al.* (2008). Acetylation of Smc3 by Eco1 is required for s phase sister chromatid cohesion in both human and yeast. *Mol Cell* *31*, 143-151.

Materials and Methods

Antibodies

Commercial antibodies: alpha-tubulin (SIGMA, 1:5000 for Western blotting); Aurora B antibody (Becton Dickinson, 611083; 1:500 for immunofluorescence); BrdU antibody (Becton Dickinson, 347580, for immunofluorescence); PCNA antibody (Santa cruz, sc-56, 1:1000 for immunofluorescence); Scc1 antibody (Upstate, 05-908, 1:50 for immunofluorescence); Smc1 antibody (Bethyl, #A300-055A, 1:1000 for Western blotting); H3S10pH antibody (Upstate, #05-499, 1:500 for immunofluorescence); anti-rabbit HRP (SIGMA, #A 4914); anti-mouse HRP (Jackson ImmunoResearch, #115-035-068); secondary antibodies for immunofluorescence: alexa488, 568 and 633 conjugated antibodies from Molecular Probes.

Non-commercial antibodies: the antibodies against Smc3 (727), Scc1 (575) Scc1 (623) SA1/2 (447), Wapl (986) has been described (Sumara et al., 2000; Waizenegger et al. 2000; Kueng at al. 2006)

PCR primer sequences

Targeting vector

Pair 1-2 CTGACTCGAGATATGCCACAAACTCTCC; ATAAGCGGCCGGCTACAAACCCATTAECTAC;
Pair 3-4 GTCGTCGACACAGTCCTATTTTCAGGTAAG; GTCGAATTCAATAGCAGGGCTATCTGAAC;
Pair 5-6 ATAGGATCCTGTTAATTTGCATAGTGATGAC; ATAAGCGGCCGCGACTGGGAGTTCCAAGTATC;
Pair 7-8 GTCGAATTCGGGTTGAGCCCTCTAATG;GTCGTCGACACTTGAACACTGGAAAGC;
Pair 9-10 ATAAGCGGCCGCGCCATATTTAGACATATGATTAC; ATAGGATCCTTAECTTTTTATTGGGAAGTTACC

Southern blotting

Probe a: GATAAGATGGTGATAACCTTTC; GCCCTCATTTCTCCTATGTG
Probe b: AAGTGCATCTAAACAGCT; GTGCTATAACGTGGTGATTG

Mice genotyping

Wapl floxed allele: ACTGTTTCAGATAGCCCTGC; CCACTGCGGTTTCTGCATTG

Wapl null allele: ACTGTTTCAGATAGCCCTGC; AACAGTTGTGAGCCACTACC

Targeting strategy for the Wapl allele

BAC clone RP23-478G5 (CHORI, <http://bacpac.choru.org>) was used for construction of the *Wapl* targeting vector. A 4.9kb fragment containing *Wapl* exons 3 and 4 was cloned into a pBluescript II KS (-) vector (Stratagene) by a recombineering-based method (Liu et al., 2003). A *LoxP* site was engineered upstream of exon 3, and an *Frt-neo-tk-Frt* cassette and a second *LoxP* site was then inserted downstream of exon 4. Gene targeting was performed in A9 ES cells by electroporating 50 µg of *NotI*-linearized targeting construct. For selection, 300 µg/mL G418 was used, and clones were screened by Southern blot analysis of *EcoRI*-digested ES cell DNA by using an external probe (probe a). The targeting frequency for correct integration of the targeting vector at the *Wapl* genomic locus was ~ 3%. The presence of the second *loxP* site was confirmed by using a *SacI* digest and a second C-terminal external probe (probe b).

Chimeric mice were created by injection of three independent targeted ES cell clones into C57Bl/6 blastocysts. Chimeric mice were crossed to C57Bl/6 wild-type animals and maintained on a mixed genetic background of C57Bl/6 and 129/Sv. The *Frt-neo-tk-Frt* cassette was removed crossing *Wapl*^{+/*F*(*Frt-neo-tk-Frt*)} mice with *Flpe* transgenic mice. The resulting *Wapl*^{+/*F*} mice were crossed to transgenic *More-Cre* mice to generate *Wapl*^{+/*Δ*} mice. *Wapl*^{+/*F*} and *Wapl*^{+/*Δ*} mice were then crossed with transgenic *R26cre-ER^{T2}* mice and *Separase*^{+/*F*} and *Separase*^{+/*Δ*} mice. To distinguish between the different alleles, tail snip DNA was PCR genotyped. *Flpe*, *More-Cre* and *R26cre-ER^{T2}* mice were obtained from Jackson

Laboratories (Bar Harbor, USA); the Separase mice have been described (Wirth et al., 2006).

Culture of mouse embryonic fibroblasts

pMEFs were prepared from 13.5 dpc embryos then cultured in gelatin-coated flasks in DMEM supplemented with 10% FCS, 0.2 mM L-glutamine, 100 U/ml penicillin, 100 µg/ml streptomycin, 1 mM sodium pyruvate, 0.1 mM 2-mercaptoethanol, and nonessential amino acids.

Virus infection was performed as previously described (Wirth et al., 2006). To induce ER-Cre^{T2}, pMEFs were cultured in optiMEM media (Invitrogen) plus 2% charcoal/dextran-treated serum (Hyclone); 4-hydroxy-tamoxifen (Sigma, 10 mg/ml stock in ethanol) was added at 0.5 µM. Nocodazole was used at a final concentration of 300 ng/ml.

Scc1 RNA-interference was performed with Lipofectamine RNAi MAX reagent (Invitrogen) according to the manufactory. The Scc1 siRNA was described in a previous study (Wendt et al., 2008).

Immunofluorescence microscopy

Cells were grown on 18 mm coverslips and fixed with 4% formaldehyde in PBS for 10 min. In experiments where BrdU antibody was used, cells were labeled by addition of 50 µM BrdU to the medium for 30 min before fixation. In experiments where PCNA antibody was used, cells were treated with icecold methanol for 5 min following formaldehyde fixation. After fixation, cells were permeabilized with 0.1% Triton X-100 in PBS for 10 min and then blocked with 3% FBS in PBS containing 0.01% Triton X-100. Cells were then incubated with primary and

secondary antibodies as previously described (Kueng et al., 2006). Images were taken using Zeiss axioplan 2 microscope with a Coolsnap HQ camera.

In order to quantify the level of chromatin-bound cohesin, cells were preextracted with 0.1% Triton X-100 for 2 min prior to fixation with 4% formaldehyde in PBS for 10 min and stained with antibodies against Aurora B and Scc1. DNA was visualized by DAPI (4',6-diamidino-2-phenylindole). G1- early S cells (Aurora B negative) were used to quantify chromatin-bound cohesin. DAPI staining was used to define outlines of interphase nuclei. Scc1 fluorescence intensities were measured in the nuclear outlines and background-corrected. Quantification of Scc1 levels was performed using Image J (<http://rsb.info.nih.gov/ij/>).

Giemsa spreads: mitotic pMEFs were collected by shake off after 5 hour of nocodazole treatment (300 ng/ml). Hypotonic spreading and Giemsa staining was performed as described (Kueng et al. 2006).

ChIP sequencing

Crosslinked cell lysates and Smc3 ChIP were obtained as previously described (Wendt et al., 2008). In brief, pMEFs at 70–80% confluency were crosslinked with 1% formaldehyde for 10 min and, after quenching with 125 mM glycine, were prepared for ChIP. ChIP was performed using SMC3 (Bethyl) and control antibodies. In brief, crosslinked cell lysates were incubated with the antibodies for 14 h at 4 °C. After this, the lysates were incubated for 2 h at 4 °C with pre-absorbed protein A Affiprep beads (Bio-Rad). The beads were washed several times and eluted with elution buffer (50 mM Tris, 10 mM EDTA, 1% SDS) for 20 min at 65 °C. The eluates were treated with proteinase K for 1 h at 37 °C and

then incubated at 65 °C overnight to reverse the crosslinks. Contaminating RNA was removed by RNase treatment. The samples were further purified by phenol-chloroform extraction and one additional purification step using a PCR purification kit (Qiagen). The samples were eluted from the columns with 80 µl water.

Sequencing libraries were obtained from 10 ng of ChIP DNA by adaptor ligation, gel purification and 18 cycles of PCR. Sequencing was carried out using the Illumina Genome Analyzer (GA) I system according to the manufacturer's protocol. 3711,833 uniquely alignable sequence tags were mapped to the mouse genome (NCBI build 36) using the GA-Pipeline V0.3. Tags passing the standard GA-Pipeline quality threshold and mapping uniquely with not more than two mismatches were used for data analyses.

High density map: A theoretical fragment density for each 25 bp window was calculated. Uniquely aligned tags within 200 bp and oriented toward it, were counted as 1 for each 25 bp window and as 0.25 if they were within 200 bp and 300 bp. Low-density map: For each 200 bp window the uniquely aligned tags were counted. Peaks of significant enrichment were identified using the USeq toolkit (<http://useq.sourceforge.net/>): A sliding window of 1 kb was used to calculate smoothed window scores (ScanSeqs). For each window a Bonferroni corrected P-value was estimated using a global Poisson distribution and windows with a minimum score of 10 (low cut off) or 60 (high cut off) and a maximum distance of 500 bp were combined to enriched regions (EnrichedRegionMaker).

Curriculum Vitae

Name: Antonio Tedeschi
Date of Birth: 01 July 1978
Nationality: Italian
Email: tedeschi@imp.univie.ac.at

Education

Undergraduate studies: Faculty of Biology, University "La Sapienza" of Rome, Italy Graduation Degree ("Laurea") with highest honours (110/110 cum Laude).
September 1997 to March 2005

Graduate studies: CNR-Institute of Molecular Biology and Pathology, c/o Department of Genetics and Molecular Biology, University "La Sapienza" of Rome, Italy
March 2005 to December 2005

PhD student (Vienna Biocenter International PhD programme in Molecular Life Science, Vienna University) at IMP-Research Institute of Molecular Pathology, Vienna, Austria
January 2006 to present

Research Experience

October 2002 to February 2005: Undergraduate student with Dr. Patrizia Lavia
CNR-Institute of Molecular Biology and Pathology, c/o Department of Genetics and Molecular Biology, University "La Sapienza" of Rome, Italy

Topic: Investigating the function of the human RanBP1 gene through RNA interference

March 2005 to December 2005: Research fellow with Dr. Patrizia Lavia
CNR-Institute of Molecular Biology and Pathology,
c/o Department of Genetics and Molecular Biology,
University "La Sapienza" of Rome, Italy

Topic: Investigating genomic instability in breast cancer: molecular mechanisms; prognostic and diagnostic value; and predictive significance for the outcome of chemotherapeutic treatment.

January 2006-present: Graduate research in the Laboratory of Jan-Michael Peters at IMP-Research Institute of Molecular Pathology, Vienna, Austria

Topic: Role of Wapl in cell cycle and chromosome segregation

Publications

Peters, J.M., **Tedeschi, A.**, and Schmitz, J. (2008). The cohesin complex and its roles in chromosome biology. *Genes Dev* 22, 3089-3114.

Rensen, WM., Roscioli, E., **Tedeschi, A.**, Mangiacasale, R., Ciciarello, M., Di Gioia, S.A., and Lavia, P (2009). RanBP1 downregulation sensitizes cancer cells to taxol in a caspase-3-dependent manner. *Oncogene* 28(15):1748-58.

Tedeschi A., Ciciarello, M., Mangiacasale, R., Roscioli, E., Rensen, WM., and Lavia, P (2007). RANBP1 localizes a subset of mitotic regulatory factors on spindle microtubules and regulates chromosome segregation in human cells. *J Cell Sci.* 120(Pt 21):3748-61.

Acknowledgments

First of all, I would like to thank Jan-Michael Peters for the possibility to work on this project, and for his constant support and encouragement. I would like to thank all former and current members of the Peters lab for their support and help, in particular Gordana, Julia, Jim, Peter, Rene, Stephanie and Venu.